Partial Response Advanced Modulation Formats for Bandwidth Limited Optical Links

Madsen, Peter

Publication date:
2019

Document Version
Publisher's PDF, also known as Version of record

Ph.D. Thesis
Doctor of Philosophy

DTU Fotonik
Department of Photonics Engineering

Partial Response Advanced Modulation Formats for Bandwidth Limited Optical Links

Peter Madsen

Kongens Lyngby 2018

DTU

DTU Fotonik
Department of Photonics Engineering
Technical University of Denmark

Ørsteds Plads
Building 343
2800 Kongens Lyngby, Denmark
Phone +45 4525 6352
www.fotonik.dtu.dk

Abstract

The ever increasing Internet traffic, poses a need for more Bandwidth (BW) of the optical network systems. The required specifications of the optical systems, needed to carry the expected increment in traffic, does not comply with the well known Non-Return to Zero (NRZ) modulation format. Therefore, other modulation formats are considered, among these are Pulse Amplitude Modulation (PAM) and partial response modulation. The most considered modulation format for future Intensity Modulated/Direct Detection (IM/DD) optical systems, is the sub-modulation format, PAM4. As a contester to this modulation format, duobinary modulation is proposed. Duobinary is the lowest level of sub-modulation formats from the partial response modulation format family.
The focus on partial response stems from the rapid development of Digital Signal Processing (DSP). Normally DSP is used in long haul applications, but the gained advantages slowly outweighs the increased cost. Partial response has become a viable solution because DSP is moving into short reach IM/DD systems.
This thesis analyses the implementation of duobinary and PAM4 in various optical systems, with a focus on solving the band limitations that resides within the systems. Where it is possible, PAM4 and duobinary are compared to each other, and to NRZ, based on Bit Error Ratio (BER) performance.
The comparison of NRZ, duobinary and PAM4 is done through theoretical calculations, and followed by experimental validations in the setups presented in the work. The targeted optical systems include; point-to-point connections, data center interconnections and Passive Optical Network (PON) connections. These optical connections are the expected bottlenecks of the Internet. These optical connections are based on IM/DD technology where NRZ is typically used. The state of the art within Dense Wavelength Division Multiplexing (DWDM) PONs includes port agnostics. The inclusion of a Pilot Tone (PT) to control tunable laser sources in new DWDM PONs, means an extension of the theoretical base to include PT modulation.
The results presented in this thesis, shows that duobinary is, in most cases, a better suited candidate for modulation format than PAM4.

Resumé

Den stadigt stigende internettrafik udgør et behov for mere båndbredde i de optiske netværkssystemer. De påkrævede specifikationer for de optiske systemer, der er nødvendige for at bære den forventede stigning i datatrafikken, overholdes ikke det velkendte NRZ modulationsformat. Derfor overvejes andre moduleringsformater, såsom Pulse Amplitude Modulation (PAM) og partielle respons modulation.
Det mest betragtede modulationsformat for fremtidige Intensitets Modulerede og Direkte Detekterede (IM/DD) optiske systemer er submoduleringsformatet, PAM4. Som alternativ for dette modulationsformat foreslås duobinary modulation. Duobinary er det laveste niveau af submodulationsformater fra familien af partielle respons modulationsformat.
Fokus på partiel respons stammer fra den hurtige udvikling af Digital Signal Processering (DSP). Normalt anvendes DSP i langdistanceapplikationer, men de opnåede fordele overstiger langsomt de øgede omkostninger. partiel respons er blevet en mulig løsning, fordi DSP bevæger sig mere og mere ind i IM/DD systemer med kortere rækkevidde.
Denne afhandling analyserer implementeringen af duobinary og PAM4 i forskellige optiske systemer, der fokuseres på at løse de båndbredde begrænsninger der eksisterende i systemerne. Hvor end det er muligt, sammenlignes præstationerne for PAM4 og duobinary, både med hinanden og med NRZ. Alt sammen baseret på Bit-Fejl-Rate (BER).
Sammenligningen af NRZ, duobinary og PAM4 sker gennem teoretiske beregninger og efterfulgt af eksperimentelle valideringer i de opsætninger, der præsenteres i arbejdet. De målrettede optiske systemer omfatter; punkt-til-punkt-forbindelser, data center forbindelser og Passive Optiske Netværks (PON) forbindelser. Disse optiske forbindelser, er de forventede flaskehalse i internettet. Disse optiske forbindelser er baseret på IM/DD-teknologi, hvor NRZ typisk anvendes. Den nyeste teknologi inden for Komprimerede Bølgelængde Divisions Sammenkobling (DWDM) PON'er omfatter port agnostikere. Inkluderingen af en Pilot Tone (PT) til styring af justerbare laserkilder i nye DWDM PON'er betyder en udvidelse af den teoretiske base, til at inkludere PT-modulation.
Resultaterne, som bliver fremlagt i denne afhandling viser, at duobinary i de fleste tilfælde er en bedre egnet kandidat som modulationsformat end PAM4.

Preface

This PhD thesis presents the resulting work of my PhD project during the period from June 2015 till November 2018. The work was carried out at DTU Fotonik, the department of Photonics Engineering at the Technical University of Denmark in fulfillment of the requirements for acquiring the PhD degree. Part of the PhD project was completed during an internship at ADVA Optical Networking SE in Meningen, Germany, in the period from January 2018 till May 2018.

This PhD project was funded by the Villums Fonden through the SEES-project. The work that was done during the internship at ADVA received funding from the European Union's Horizon 2020 research and innovation program under grant agreement No 762055 (project BlueSpace).

This PhD project was supervised by:

- Anders Clausen,(main supervisor), Associate Professor, DTU Fotonik, Technical University of Denmark, Kgs. Lyngby, Denmark.
- Lars Dittmann, (Co-supervisor), Professor, DTU Fotonik, Technical University of Denmark, Kgs. Lyngby, Denmark.

Kongens Lyngby, December 6, 2018

Peter Madsen

List of Publications

Journal papers

[**J1**] **P. Madsen**, A. T. Clausen, A. Dochhan, & M. Eiselt, *"Pilot Tone Assisted Intensity Modulation Formats"*. Journal of Lightwave Technology, **To be submitted**, 2018.

[**J2**] **P. Madsen**, L. F. Suhr, & I. Tafur Monroy, *"Inter-data center 28 Gbaud 4-PAM transmission over 240 km standard single mode fiber"*. Optical Fiber Technology, vol. 44, pp. 86–88., 2018.

[**J3**] J. J. Vegas Olmos, I. Tafur Monroy, **P. Madsen**, L. F. Suhr, B. Cimoli, T. K. Johansen, & V. Zhurbenko, *"Challenges in Polybinary Modulation for Bandwidth Limited Optical Links"*. Journal of Lasers, Optics and Photonics, vol. 3, no. 2, 2016.

[**J4**] L. F. Suhr, **P. Madsen**, I. Tafur Monroy„ & J. J. Vegas Olmos, *"Analog-based duobinary-4-PAM for electrical bandwidth limited optical fiber links"*. Optica Applicata (Online), vol. 46, no. 1, pp. 71–78., 2016.

[**J5**] **P. Madsen**, L. F. Suhr, J. S. Rodríguez Páez, I. Tafur Monroy, & J. J. Vegas Olmos, *"Performance Evaluation of mMltilevel Modulation Formats Using Partial Response for Capacity Upgrade in Access Network With Limited Electronic Bandwidth"*. Optical Fiber Technology, vol. 31, pp. 168–171., 2016.

Conference papers

[**C1**] **P. Madsen**, A. T. Clausen, A. Dochhan, & M. Eiselt *"Experimental Investigation of Effects of Pilot Tone Modulation on Partial Response Modulation Formats"*. Proc. European Conference on Optical Communication, Rome, 2018, paper Th2.70.

[**C2**] **P. Madsen**, L. F. Suhr, A. T. Clausen, & I. Tafur Monroy. *"Experimental Demonstration of 32 Gbaud 4-PAM for Data Center Interconnections of up to 320 km"*. Proc. Asia Communications and Photonics Conference, 2017, paper M2G.3.

[**C3**] L. F. Suhr, **P. Madsen**, A. T. Clausen, & I. Tafur Monroy. *"Experimental Validation of Duobinary Modulation at 60 Gbaud for Data Center Interconnects of up to 300 km"*. Proc. Asia Communications and Photonics Conference, 2017, paper S4B.3.

[**C4**] S. Rodriguez, **P. Madsen**, I. T. Monroy, & J. J. V. Olmos. *"Dynamic Optical Fiber Delivery of Ka-Band Packet Transmissions for Wireless Access Networks"*. 2017 International Conference on Optical Network Design and Modeling (ONDM), 2017.

Abbreviations

ASE Amplified Spontaneous Emission

AWG Arbitary Waveform Generator

$\mathbf{AWG_r}$ Arrayed Waveguide Grating

B2B Back to Back

BER Bit Error Ratio

BW Bandwidth

CW Continous Wave

DAC Digital to Analog Converter

DC Direct Current

DCF Dispersion Compensating Fiber

DCM Dispersion Compensating Module

DD-LMS Decision-Directed Least-Mean-Square

DFB Distributed Feedback Laser

DFE Decision Feedback Equalizer

DMT Discrete Multi Tone

DSF Dispersion Shifted Fiber

DSO Digital Storage Ocilloscope

DSP Digital Signal Processing

DWDM Dense Wavelength Division Multiplexing

EAM Electro Absorbtion Modulator

EDFA Erbium Doped Fiber Amplifier

EM External Modulator

ER Extinction Ratio

FEC Forward Error Correction

HD High Definition

HEE Head-End Equipment

IM/DD Intensity Modulated/Direct Detection

IOE Internet of Everything

ITU-T International Telecommunication Union - Telecommunication Standadization Sector

LD Laser Diode

LIV Light Current Voltage

LO Local Oscillator

M2M Machine to Machine

MZM March Zehnder Modulator

NRZ Non-Return to Zero

NZDSF Non-Zero Dispersion Shifted Fiber

OBF Optical Bandpass Filter

OFDM Othogonal Frequency Division Multiplexing

OH Overhead

OPEX Operational Expenditure

OSA Optical Spectrum Analyzer

OSNR Optical Signal to Noise Ratio

P2P Peak to Peak

PAM Pulse Amplitude Modulation

PD Photodetector

PON Passive Optical Network

PPG Pulse Patteren Generator

PRBS Pesudo Random Bit Sequence

PT Pilot Tone

SMF Single Mode Fiber

SNR Signal to Noise Ratio

SSMF Standard Single Mode Fiber

TEE Tail-End Equipment

UHD Ultra High Definition

VOA Variable Optical Attenuator

WDM Wavelength Division Multiplexing

Contents

CHAPTER 1

Introduction

The growth of the Internet is clear from the global Internet analysis by Cisco[1]. In 1992 the global internet traffic was approximately 100 GB per day. This number has since increased to 26.600 GB per second in 2016 and is predicted to further increase to 105.800 GB per second in 2021. The increase in global Internet traffic takes rise in three major parts. The first part is the massive amount of entertainment that is based on data streaming, such as TV on demand and streaming services, such as YouTube, Netflix and HBO [2]. The second part is cloud computing and storage, which is mainly used by companies to secure large amounts of data via online storage with global availability [3]. The third part is based on the concept of everything is connected and online, also known as the Internet of Everything (IOE). IOE is mentioned in Ciscos analysis as Machine to Machine (M2M) communication. M2M is not the most traffic heavy communication, with only 3% of the global Internet traffic in 2016 and an expected increase to 6% in 2021. But the growth of devices that make up the M2M network is expected to grow from 34% of the total sum of Internet connected devices in 2016, to 51% in 2021. Comparing this to the number of Smartphones, tablets, PCs and TVs, it is seen that the number of tablet does not grow from 2016 till 2021, remaining at 3%. Smartphones make up the second largest percentages, and will increase from 21% to 23% between 2016 and 2021. PCs will see a decrease from 8% to 5% from 2016 to 2021 and TVs will stay at 12% from 2016 to 2021.
When looking at the global Internet traffic by device type, a clear trend of entertainment on the go is seen, as smartphone traffic is expected to surpass that of PC traffic with 39% versus 28% in 2021. Also the expectancy of more TVs getting upgraded from High Definition (HD) to Ultra High Definition (UHD) or 4K, almost doubling the bandwidth usage from 7.2 Mbps to 18 Mbps, is seen as a 3% increase in global Internet traffic by TVs from 2016 till 2021.

From the early days of the World Wide Web till todays vast and constant connectivity, the Internet it self, and the way it is used, has evolved and developed faster than many other man-made things. The evolution of the Internet is needed to keep up with our ever increasing user needs. People demand constant connectivity and access, faster data rates, and low latency of their services. This puts a pressure on the technology that makes up the access network. This part of the network connects users with data centers, and data centers with other closely located data centers. With the ever increasing traffic trends that is stated in the Cisco analysis, a bottleneck in the access network will be expected. To combat this, more bandwidth is needed both in the access network and in

the data center interconnections.

Looking at current trends for data center interconnections, newly build Facebook facilities implement 100G and 200G connections [4]. With the Cisco analysis stating that 75% of the future global IP data traffic increase will remain inside the data centers, the connections need to be upgraded to 400G connections soon. To reach 400G and beyond, the options are; to aggregate multiple links into a single link, (using more fiber and multiple laser sources) or use advanced modulation formats with more bits per symbol or a combination of the two. From a financial, technical and scalable point of view, some of the options are not feasible. In conclusion, for data center interconnections, upgrade solutions with a lower number of laser sources and higher baud rate offers an advantage in terms of scaling, cost and power consumption.[5]

A similar problem must be faced in the access network. Scalability, cost and power consumption need to be reasonable. The access network of today is mostly based on 10G DWDM PONs [6]. Future networks will need increased capacity beyond 25G, which makes access and metro networks a very popular research area. One of the key challenges for access networks, is to increase data rates while coexisting with legacy networks in a cost effective manner. One very discussed option to overcome this problem is the use of advanced modulation formats and detections techniques that is enabled by DSP. This would allow for high speed transmission with digital compensation for fiber dispersion and nonlinearities [7]. It is safe to assume that the viable upgrade solutions, that will move 10G connections towards 25G ones, have an advantage if these also include a lower number of lasers and offers higher baud rate [8]. Long haul coherent optics provides the necessary capacity and scalability, with transmission over several thousand of kilometers, and very high baud rates [9]. But because of the current component cost and power consumption, not many of the long haul coherent technologies are feasible. Bringing the expenses of these technologies down and implementing them into access networks is a whole research field on its own. Will coherent optics ever become cost efficiently enough [10], or is the component cost, heat dissipation and power consumption a killer for DSP in access networks?

Power consumption is closely related to running expenses of any network. It has always been a goal for any network operator to keep Operational Expenditure (OPEX) low [11], [12]. That is one of the reasons why IM/DD technologies are still being used in access and data center networks. The components are cheap, the chip footprints are small and the power consumption is minimal [13]. But IM/DD systems have limitations, and a new network evolution is needed [14], to either improve and keep IM/DD systems, or switch to cost effective coherent optics.

1.1 Motivation and Outline of Contributions

The goal of this Ph.D. project have been to study, propose and implement partial response into existing system, as means of pushing the capacity passed what the optical systems was originally designed towards. During the study, technological advances forced the implementation of DSP into relative simple optical systems. This in-turn introduced an immense field of possible systems to implement partial response modulation into. A wide variety of optical systems have been tested, some more successful than others. The systems presented in this thesis are PONs, access and metro networks including data center interconnections.

1.2 Structure of the Thesis

The thesis is structured as follows: chapter 2 presents the theoretical material that the concept of partial response is base upon, with a strong focus on implementability. chapter 3 presents the initial work of the study. A proof of concept that shows the capacity enhancement ability of partial response modulation. chapter 4 presents the extended possibilities for partial response modulation, when combined with equalizers implemented in DSP. chapter 5 presents the exploit of the key features for partial response modulation, which is the bandwidth reduction capabilities. Here it is used in an industrial collaboration for future PON development.

CHAPTER 2

Fundamentals

This chapter presents the basic theory for the modulation formats that this thesis evolves around. It serves as a knowledge base for the topics addressed throughout the following chapters.

2.1 Modulation formats

The most important part of an optical transmission system, is the data that it carries from point A to point B. The way the data bits are represented in the system is determined by a modulation format. The modulation format can alter the performance and efficiency of an optical transmission system, therefore it is important to determine the modulation format when designing an optical system. Many different kinds of modulation formats have been developed through time, some which are more suitable for optical communication than others.
Presented in this section is the two most used modulation formats of this thesis.

2.1.1 Pulse Amplitude Modulation

The general term PAM covers a wide verity of intensity modulations, all following the same principle, which is the combination of bits into a multi-level signal consisting of symbols. Depending on the number of amplitude levels M, one symbols consists of N bits, which can be found by Equation 2.1.

$$N = log_2(M) \tag{2.1}$$

From Equation 2.1 is it clear that a NRZ is considered a PAM2 where each symbol consist of 1 bit. The goal of PAM is to reduce the required bandwidth for a certain bit rate. This is easily gathered from the natural development from PAM2 to PAM4 where each symbol consist of 2 bits. Theoretically there is no limit to the number of bits per symbol used in PAM, thus the creation of very high levels of PAM have been done [15]. But more intensity levels makes the signal more susceptible to limitations due to noise and transmission impairments. As such, the experimental work that is the base of this thesis is limited to PAM4.

2.1.1.1 PAM4 Symbol mapping

As mentioned before, one PAM4 symbol consists of 2 bits. The performance of the resulting PAM4 signal, is heavily dependent on which bit combination corresponds to which symbol. Therefore gray coding is used when mapping bits to PAM4 symbols, as in Table 2.1.

Table 2.1: Gray coded bit mapping of PAM4 symbols

gray coded symbols	**bit 1**	**bit 2**
0	0	0
1	1	0
2	1	1
3	0	1

The benefits of gray codes, is that an erroneous received symbol creates a minimum amount of bit errors, because they are equidistant. That is the adjacent symbols only differ by one bit change.

2.1.1.2 Analog PAM4

PAM4 can be implemented by analog solutions using a Digital to Analog Converter (DAC) and 2 uncorrelated bit streams. In experimental work this is often done as seen from Figure 2.1. Two similar electrical signal representation of a NRZ is often used. The two signals are uncorrelated using a delay line and one signal is attenuated to half power with a 6 dB attenuator before the signals are combined in a DAC.

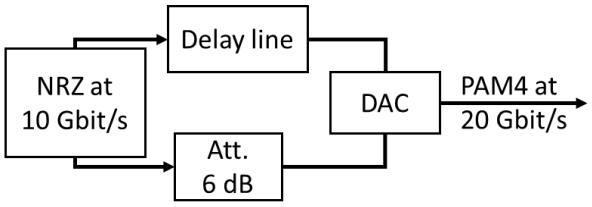

Figure 2.1: General creation of analog PAM4

It is clear that when PAM4 is created in this fashion, the bandwidth of the resulting PAM4 will be the same as the NRZ from which it was created, but the effective bit rate will be doubled.

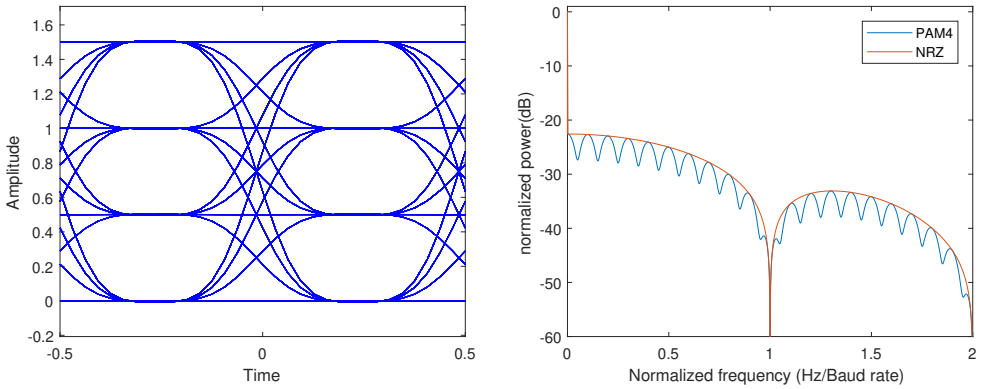

(a) Example of PAM4 eyediagram.

(b) PAM4 spectrum compared to NRZ spectrum.

Figure 2.2: Eyediagram and spectrum of PAM4 generated from the combination of 2 NRZ streams.

The eyediagram and spectrum of a very ideal PAM4 signal is observed in Figure 2.2. The 4 signal levels are 0, 0.5, 1 and 1.5 corresponding to a half a bit stream add to it self. From the spectrum in Figure 2.2b it is seen that the PAM4 spectrum follows and fills the spectrum of NRZ. which means that the PAM4 and NRZ is operating at the same baud rate. This corresponds to an effective bit rate of the PAM4 which is twice that of the NRZ.

2.1.2 Partial Response Modulation

Partial response modulation format was first introduced in 1963 by A. Lender [16]. The goal of partial response modulation is to reduce the required bandwidth for a certain bit rate, initially intended for wireless communication. The principle of partial response modulation in general is to introduce a controlled amount of Intersymbol Interference (ISI) into the system. The ISI helps shape the signal spectrum, and because it is controlled, it can be easily removed. The ISI can be introduced either by coding or by low pass filtering. With partial response modulation, an M level signal is transformed into a Y level signal following Equation 2.2.

$$Y = A \cdot M - 1 \tag{2.2}$$

Where A is the level of partial response. When $A = 2$ the modulation is called duobinary and results in a 3 leveled signal. When $A > 2$ is called Y level polybinary.

2.1.2.1 Duobinary filtering

When partial response is coded it introduces a special transfer function into the system based on the level of Y. For a basic duobinary the transfer function is seen from

Equation 2.3.

$$2T \cdot cos(\frac{\omega}{2}T) \quad \text{for} \quad |\omega| \leq \frac{\pi}{T} \tag{2.3}$$

When digitally creating duobinary it is possible to take the Fast Fourier Transform (FFT) of the signal and multiply the spectrum with the transfer function of Equation 2.3. Then applying the Inverse Fast Fourier Transform (IFFT) to get the time domain duobinary signal. Another way to digitally create duobinary would be to implement a delay and add filter. Simply delay one symbol and add it to the previous symbol.
Implementing a digital filter creates the ideal partial response, but in a transmission system, with dispersion and noise, the ideal partial response might not prove optimal in terms of performance. Therefore partial response is often best created using a low pass filter or applying an additional low pass filter to the coded partial response. The low pass filter can be either a discrete filter or it can be a system component such as a bandwidth limited Directly Modulated Laser (DML) or another type of modulator. Generally the filtering must have a suitable roll-off, maintain as flat a phase response as possible, and have a 3 dB cutoff that matches the desired level of partial response. For a duobinary signal, the filter should have a 3 dB cutoff at approximately 25 % of the baud rate [17].

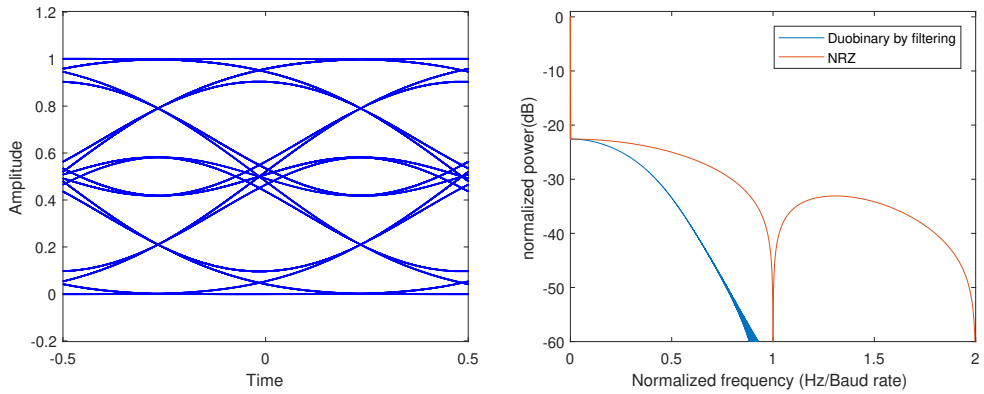

(a) Eyediagram of low pass filtered duobinary

(b) Spectrum of low pass filtered duobinary compared to the spectrum of NRZ

Figure 2.3: Eyediagram and spectrum of duobinary created by filtering an NRZ with a low pass Bessel filter

An example of a duobinary signal created from low pass Bessel filtering an NRZ signal is observed in Figure 2.3. Compared to the coded duobinary, the eyediagram of the filtered duobinary in Figure 2.3a, looks quite different. The 3 levels of the filtered duobinary signal is obtained by sampling at Time = 0. Inspecting the spectrum of the filtered duobinary in Figure 2.3b, it is evident that the low pass Bessel filter have removed the high frequency components of the NRZ signal. The spectral width of the filtered duobinary is 50% to that of the spectral width of the NRZ from which it was

created.

In theory the M level base signal in Equation 2.2 can take any shape or form before being transformed into a partial response format. In one experiment presented in chapter 3, a 4 leveled PAM is used, as base for a duobinary partial response, resulting in a 7 leveled duobinary PAM4. A simulated example of this is seen from Figure 2.4.

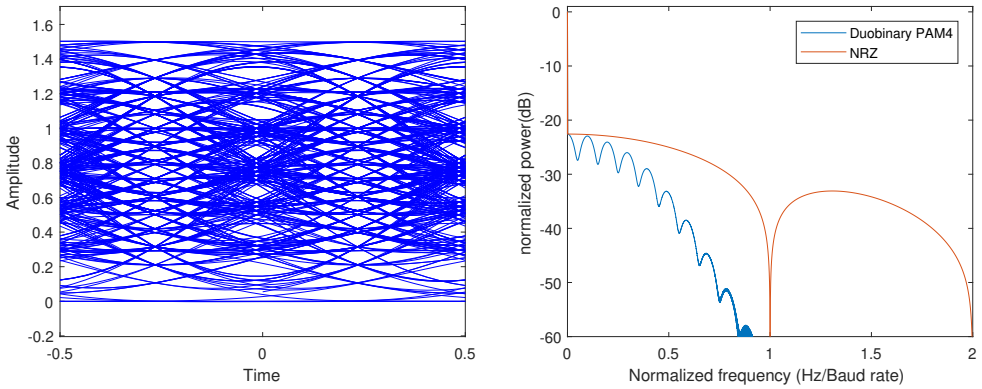

(a) Example of 7 level duobinary PAM4 eyediagram

(b) Duobinary PAM4 spectrum compared to NRZ spectrum

Figure 2.4: Eyediagram and spectrum of a 7 level duobinary PAM4, generated by filtering a PAM4

In the eyediagram, in Figure 2.4a, the 7 signal levels of duobinary PAM4 appears at Time = 0. It is clear that this many levels imposes a very low noise tolerance at the receiver. Already from this somewhat ideal duobinary PAM4 signal, the eye openings are very small. This is of course a trade-off between system performance versus increased spectral efficiency. As observed from the spectrum in Figure 2.4b, the original PAM4 which operates at the same baud rate, has a spectral width which is 50% of the NRZ spectrum. As illustrated in Figure 2.4, high levels of partial response suffers from the same system impairments as high level PAMs. Being; low noise tolerance and intensity level skewing as a result of fiber chromatic dispersion [18]. These impairments increases the receiver complexity of the system in order to work sufficiently.
Therefore not many optical transmission systems can implement these increased intensity levels. As such, the work done during the thesis, is limited to duobinary partial response, but partial response with as much as 15 intensity levels have been reported [19].

2.1.2.2 Duobinary Coding

Duobinary partial response can be created by the use of coding [20]. The 3 level partial response symbol stream (c) follows Equation 2.4.

$$c_k = b_k + b_{k-1} \tag{2.4}$$

Where b_k is a correlated precoding bit stream created using Equation 2.5.

$$b_k = a_k \oplus b_{k-1} \tag{2.5}$$

In Equation 2.5, a_k is the original M level signal. The precoding step b_k is needed in order to avoid error propagation at the receiver [21] . Often in a test system a Pesudo Random Bit Sequence (PRBS) of a certain length is used to simulate random data. Such a sequence will in practical manner be time shifted by Equation 2.5. In a test system transmitting a PRBS based partial response code, where the received sequence is processed offline by DSP, the retiming is often corrected by a similar shift and therefore the precoding can be omitted in PRBS based test systems.
To recover a_k from the transmitted c_k the receiver needs only to implement the modulo 2 operation as in Equation 2.6.

$$a_k = c_k \ mod 2 \tag{2.6}$$

An example of duobinary encoding is seen from Table 2.2. It is clear form the table that a direct transition from minimal to maximal signal value is not possible. There will always be an intermediate transition value between, hence the name partial response.

Table 2.2: Example of duobinary coding

a_k		1	0	1	1	0	0	1	0	1	0	1	0
b_k	0	1	1	0	1	1	1	0	0	1	1	0	0
c_k		1	2	1	1	2	2	1	0	1	2	1	0
$c_k mod(2)$		1	0	1	1	0	0	1	0	1	0	1	0

A simulated ideal duobinary signal, made by coding a PRBS15, is seen in Figure 2.5. The 3 levels of the coded duobinary signal is seen from the eyediagram in Figure 2.5a. There is no direct transition from 0 to 2 and vise versa in the eyediagram, not like in the PAM4 eyediagram of Figure 2.2a. The eyediagram looks as if two NRZs signals were layered. When the spectrum of the coded duobinary is compared to the spectrum of NRZ in Figure 2.5b, it is seen that there is an intermediate attenuation notch in the spectrum of the coded duobinary. This notch appears at 50% of the spectral width of the NRZ. This indicates that the duobinary signal contains higher frequencies components, but just as with NRZ these are low pass filterable at the first notch, of appropriate spectrum, without losing information.

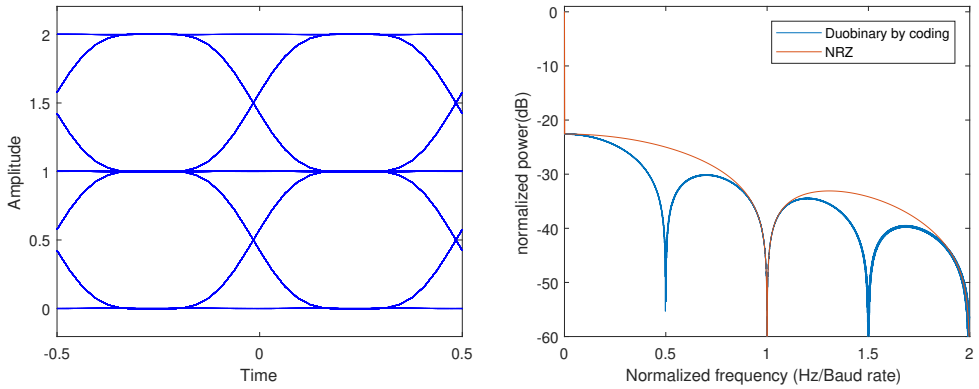

(a) Eyediagram of coded duobinary

(b) Spectrum of the coded duobinary compared to the spectrum of NRZ

Figure 2.5: Eyediagram and spectrum of duobinary created by coding a PRBS

2.2 BER Theory

One of the most common performance measures for transmission systems and modulation formats is BER. It is used extensively through the work of this thesis. As such this section presents the theoretical background for the BER measurement for each of the base modulations; NRZ, duobinary and PAM4.
The BER for these modulation formats have been analyzed before, but in order to keep the theory to the same format, this section will start off with a NRZ derivation based on [22]. The BER theory of duobinary and PAM4 will build on the NRZ derivation. To ease this extension of the theory, NRZ is denoted as working with symbols, even though only one bit is transmitted per symbol. The explicit calculations can be found in Appendix A.

2.2.1 BER Theory for NRZ

A sampled signal value I fluctuates from symbol to symbol around two average values for s_1 and s_0 denoted I_1 and I_0. As seen from the reference figure in Figure 2.6, the decision threshold value I_{1th} is compared to the sampled value I, if $I > I_{1th}$ then s_1 is detected and if $I < I_{1th}$ then a s_0 is detected. An error occurs if s_1 is detected for $I < I_{1th}$, and is s_0 is detected for $I > I_{1th}$.

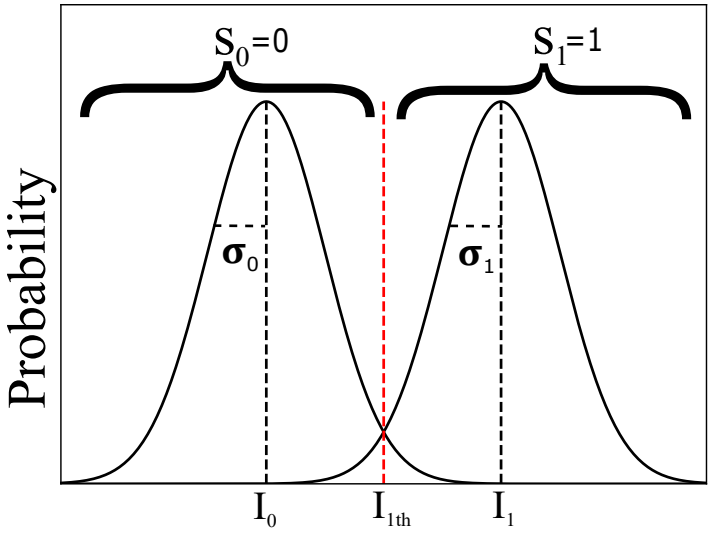

Figure 2.6: Reference figure for NRZ, displaying the symbol ranges, average signal values, threshold and the according Gaussian distributions.

The error probability of NRZ can be written as in Equation 2.7:

$$BER_{NRZ} = p(s_1)P(s_0|s_1) + p(s_0)P(s_1|s_0) \tag{2.7}$$

In Equation 2.7, $p(s_1)$ and $p(s_0)$ are the probabilities of receiving 1 and 0. $P(s_0|s_1)$ is the probability of deciding a 0 when a 1 is received and $P(s_1|s_0)$ is vice versa. Since 1 and 0 is equally likely to occur then $p(s_0) = p(s_1) = \frac{1}{2}$. Equation 2.7 can now be written as in Equation 2.8

$$BER_{NRZ} = \frac{1}{2}[P(s_0|s_1) + P(s_1|s_0)] \tag{2.8}$$

It is assumed that the noise affecting I can be described as a Gussian probability density function with the variance as in Equation 2.9:

$$\sigma^2 = \sigma_s^2 + \sigma_T^2 \tag{2.9}$$

In Equation 2.9, σ_s^2 is the shot noise contribution and σ_T^2 is the thermal noise contribution. Defined as in Equation 2.10 and Equation 2.11 respectively.

$$\sigma_s^2 = 2q(I_p + I_d)\Delta f \tag{2.10}$$

$$\sigma_T^2 = \frac{4k_BT}{R_L}F_n\Delta f \tag{2.11}$$

Where F_n represents a factor, by which the thermal noise is enhanced by different amplifiers in the system, via their internal resistors. k_B is the Boltzmann constant. T is

the absolute temperature (kelvin). Δf is the effective noise bandwidth of the receiver. q is the electron charge of a photon (constant). I_d is the dark current of the photo diode. I_p is the average current denoted as in Equation 2.12:

$$I_p = R_d P_{in} \tag{2.12}$$

In Equation 2.12, R_d is the responsivity of the Photodetector (PD). P_{in} is the incident optical power.
Since the noise affecting I is assumed Gaussian in nature, the probability $P(s_1|s_0)$ and $P(s_0|s_1)$ can be described by a Gaussian distribution, but since both the average current and noise variance is different for s_0 and s_1 the probabilities are described as follows:

$$P(s_0|s_1) = \frac{1}{2}\, erfc\left(\frac{I_1 - I_{1th}}{\sigma_1\sqrt{2}}\right) \tag{2.13}$$

$$P(s_1|s_0) = \frac{1}{2}\, erfc\left(\frac{I_{1th} - I_0}{\sigma_0\sqrt{2}}\right) \tag{2.14}$$

In Equation 2.13 and 2.14 $erfc$ denotes the complementary error function defined as in [23]. By substituting Equation 2.13 and 2.14 into Equation 2.8 the general BER expression for NRZ is obtained as:

$$BER_{NRZ} = \frac{1}{4}\left[erfc\left(\frac{I_1 - I_{1th}}{\sigma_1\sqrt{2}}\right) + erfc\left(\frac{I_{1th} - I_0}{\sigma_0\sqrt{2}}\right)\right] \tag{2.15}$$

2.2.2 BER Theory for Duobinary

As described in subsubsection 2.1.2.2 duobinary modulation transmit one bit per symbol and consists of three different symbols. Therefore the BER of duobinary can be derived based on the symbol levels, even though there are some intermediate steps in the coding and precoding.
As seen from the reference figure in Figure 2.7, for duobinary, a sampled signal value I fluctuates over the symbols s_0,s_1 and s_2 with the average signal values I_0, I_1 and I_2 respectively. For duobinary two thresholds are defined as I_{1th} and I_{2th}. If $I < I_{1th}$ a s_0 is detected, if $I_{1th} < I < I_{2th}$ a s_1 is detected and if $I > I_2th$, a s_2 is detected. Due to demodulation then $s_0 = s_2$ this is an important notice when the BER probabilities are defined. An error occurs if s_1 is detected for $I < I_{1th}$ or $I > I_{2th}$ and if s_0 or s_2 is detected for $I_{1th} < I < I_{2th}$.

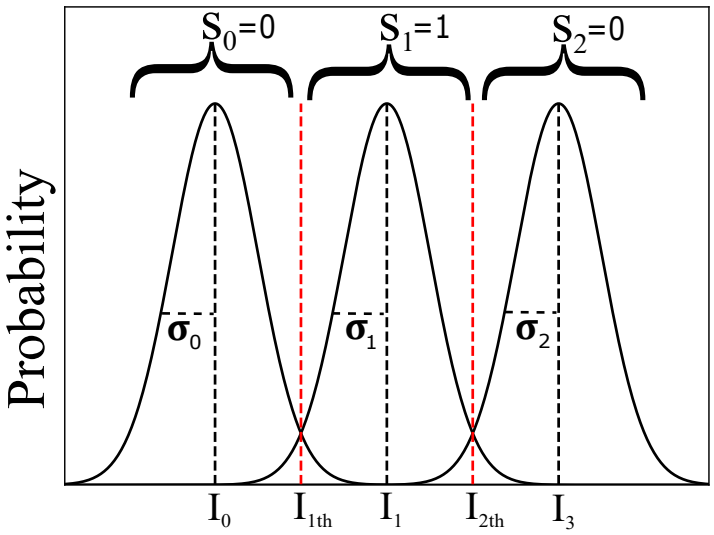

Figure 2.7: Reference figure for duobinary, displaying the symbol ranges, average signal values, thresholds and the according Gaussian distributions.

The error probability for duobinary is given by Equation 2.16:

$$\begin{aligned} BER_{duobinary} = {} & p(s_2)P(s_1|s_2) + p(s_1)[P(s_0|s_1) + P(s_2|s_1)] \\ & + p(s_0)P(s_1|s_0) \end{aligned} \tag{2.16}$$

From the coding and decoding process it is seen that both symbol s_0 and s_2 is received as a 0 bit, therefore $P(s_0|s_2)$ and $P(s_2|s_0)$ both falls into a false positive, that is why these probabilities are subtracted later in this section, from $P(s_1|s_0)$ and $P(s_1|s_2)$, as these are incorrect but will be detected correctly. The symbol probabilities are also concluded from the coding and decoding as $p(s_0) = p(s_2) = \frac{1}{4}$ and $p(s_1) = \frac{1}{2}$. Inserting the error probabilities into Equation 2.16 results in:

$$BER_{duobinary} = \frac{1}{4}P(s_1|s_2) + \frac{1}{2}P(s_0|s_1) + \frac{1}{2}P(s_2|s_1) + \frac{1}{4}P(s_1|s_0) \tag{2.17}$$

Again, the affecting noise is assumed Gaussian of nature, and the probabilities can be described by Gaussian distributions which are different for each signal level in terms of shot noise and intensity. As such the probability distributions of the duobinary symbols are defined as:

$$P(s_0|s_1) = \frac{1}{2}\, erfc\left(\frac{I_1 - I_{1th}}{\sigma_1\sqrt{2}}\right) \tag{2.18}$$

$$P(s_1|s_0) = \frac{1}{2}\left[erfc\left(\frac{I_{1th} - I_0}{\sigma_0\sqrt{2}}\right) - erfc\left(\frac{I_{2th} - I_0}{\sigma_0\sqrt{2}}\right)\right] \tag{2.19}$$

$$P(s_1|s_2) = \frac{1}{2}\left[erfc\left(\frac{I_2 - I_{2th}}{\sigma_2\sqrt{2}}\right) - erfc\left(\frac{I_2 - I_{1th}}{\sigma_2\sqrt{2}}\right)\right] \tag{2.20}$$

$$P(s_2|s_1) = \frac{1}{2}erfc\left(\frac{I_{2th} - I_1}{\sigma_1\sqrt{2}}\right) \tag{2.21}$$

Again the complementary error function is used to simplify the expressions. With the probability distributions defined, they can be substituted into Equation 2.17 and through some algebraic operations Equation 2.22 is obtained.

$$\begin{aligned} BER_{duobinary} = &\frac{1}{4}\left[erfc\left(\frac{I_1 - I_{1th}}{\sigma_1\sqrt{2}}\right) + erfc\left(\frac{I_{2th} - I_1}{\sigma_1\sqrt{2}}\right)\right] \\ &+ \frac{1}{8}\left[erfc\left(\frac{I_{1th} - I_0}{\sigma_0\sqrt{2}}\right) + erfc\left(\frac{I_2 - I_{2th}}{\sigma_2\sqrt{2}}\right)\right. \\ &\left.-erfc\left(\frac{I_{2th} - I_0}{\sigma_0\sqrt{2}}\right) - erfc\left(\frac{I_2 - I_{1th}}{\sigma_2\sqrt{2}}\right)\right] \end{aligned} \tag{2.22}$$

2.2.3 BER Theory for PAM4

As mentioned in subsection 2.1.1 the symbols of PAM4 consists of 2 bits each. This needs to be taken into account in the BER expression otherwise the result will refer to the Symbol Error Rate (SER) and not the BER. A sampled signal value I fluctuates over the symbols s_0, s_1, s_2 and s_3 with the average signal values I_0, I_1, I_2 and I_3 respectively. The thresholds for PAM4 are defined as I_{1th}, I_{2th} and I_{3th}. If gray coding is assumed as in subsubsection 2.1.1.1 the following statements are obtained: If $I < I_{1th}$ then s_0 is received, corresponding to bits 00. If $I_{1th} < I < I_{2th}$, then s_1 is received corresponding to bits 01. From the reference figure in Figure 2.8 is it seen that, if $I_{2th} < I < I_{3th}$ then s_2 is received corresponding to bits 11. And if $I_3 > I_{3th}$ then s_3 is received corresponding to bits 10. An error occurs on the first bit of symbol s_0 if s_2 or s_3 is detected for $I < I_{1th}$. An error occur on the first bit of symbol s_1 if s_2 or s_3 is detected for $I_{1th} < I < I_{2th}$. An error occur on the first bit of symbol s_2 if s_0 or s_1 is detected for $I_{2th} < I < I_{3th}$. Finally an error occur on the first bit of symbol s_3 if s_0 or s_1 is detected for $I > I_{3th}$. These errors are defined as class 1 errors. Class 2 errors are errors on the second bit of the symbol, that is: An error occur on the second bit of symbol s_0 if s_1 or s_2 is detected for $I < I_{1th}$. An error occur on the second bit of symbol s_1 if s_0 or s_3 is detected for $I_{1th} < I < I_{2th}$. An error occur on the second bit of symbol s_2 if s_0 or s_3 is detected for $I_{2th} < I < I_{3th}$. Finally an error occur on the second bit of symbol s_3 if s_1 or s_2 is detected for $I > I_{3th}$. The error probability can now still be describes in terms of symbols while still referring to the BER and not the SER.

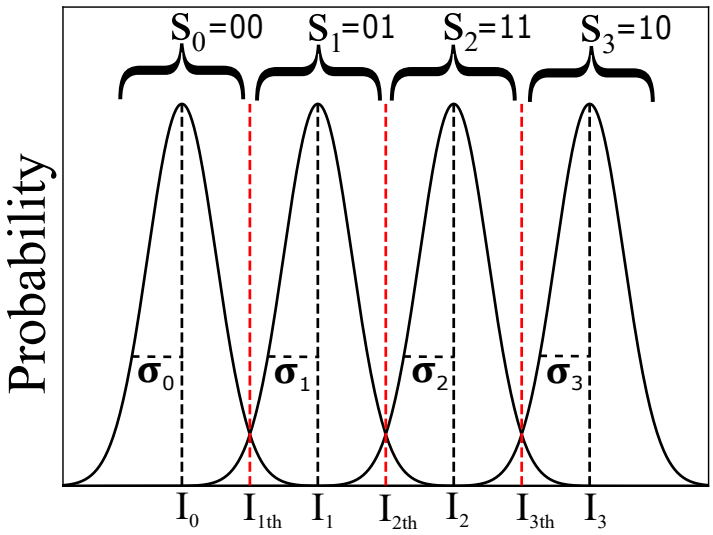

Figure 2.8: Reference figure for PAM4, displaying the symbol ranges, average signal values, thresholds and the according Gaussian distributions.

$$\begin{aligned} BER_{PAM4} = {} & p(s_0)[P(s_2, s_3|s_0) + P(s_1, s_2|s_0)] \\ & + p(s_1)[P(s_2, s_3|s_1) + P(s_0, s_3|s_1)] \\ & + p(s_2)[P(s_0, s_1|s_2) + P(s_0, s_3|s_2)] \\ & + p(s_3)[P(s_0, s_1|s_3) + P(s_1, s_2|s_3)] \end{aligned} \tag{2.23}$$

The symbol probability is obtained from the PAM4 symbol mapping as $\frac{1}{4}$ for each symbol. But using the symbol probability alone would result in calculation of the SER. Therefore the probability of each bit the the symbol must be included. The bit probability in this case $\frac{1}{2}$, the total probability is then $p(s_0) = p(s_1) = p(s_2) = p(s_3) = \frac{1}{4} * \frac{1}{2} = \frac{1}{8}$. These can be substituted into Equation 2.23

$$\begin{aligned} BER_{PAM4} = {} & \frac{1}{8}[P(s_2, s_3|s_0) + P(s_1, s_2|s_0)] \\ & + \frac{1}{8}[P(s_2, s_3|s_1) + P(s_0, s_3|s_1)] \\ & + \frac{1}{8}[P(s_0, s_1|s_2) + P(s_0, s_3|s_2)] \\ & + \frac{1}{8}[P(s_0, s_1|s_3) + P(s_1, s_2|s_3)] \end{aligned} \tag{2.24}$$

Once again the probabilities are assumed to be describable through Gaussian distributions, as such the probability distributions are found by integrating across the combined

symbol space that appear within each probability.

$$P(s_2, s_3|s_0) = \frac{1}{2}\, erfc\left(\frac{I_0 - I_{2th}}{\sigma_0\sqrt{2}}\right) \tag{2.25}$$

$$P(s_1, s_2|s_0) = \frac{1}{2}\left[erfc\left(\frac{I_0 - I_{1th}}{\sigma_0\sqrt{2}}\right) - erfc\left(\frac{I_0 - I_{3th}}{\sigma_0\sqrt{2}}\right)\right] \tag{2.26}$$

$$P(s_0, s_3|s_1) = \frac{1}{2}\left[erfc\left(\frac{I_{1th} - I_1}{\sigma_1\sqrt{2}}\right) + erfc\left(\frac{I_1 - I_{3th}}{\sigma_1\sqrt{2}}\right)\right] \tag{2.27}$$

$$P(s_2, s_3|s_1) = \frac{1}{2}erfc\left(\frac{I_1 - I_{2th}}{\sigma_1\sqrt{2}}\right) \tag{2.28}$$

$$P(s_0, s_1|s_2) = \frac{1}{2}erfc\left(\frac{I_{2th} - I_2}{\sigma_2\sqrt{2}}\right) \tag{2.29}$$

$$P(s_0, s_3|s_2) = \frac{1}{2}\left[erfc\left(\frac{I_{1th} - I_2}{\sigma_2\sqrt{2}}\right) + erfc\left(\frac{I_2 - I_{3th}}{\sigma_2\sqrt{2}}\right)\right] \tag{2.30}$$

$$P(s_0, s_1|s_3) = \frac{1}{2}erfc\left(\frac{I_{2th} - I_3}{\sigma_3\sqrt{2}}\right) \tag{2.31}$$

$$P(s_1, s_2|s_3) = \frac{1}{2}\left[erfc\left(\frac{I_{3th} - I_3}{\sigma_3\sqrt{2}}\right) - erfc\left(\frac{I_{1th} - I_3}{\sigma_3\sqrt{2}}\right)\right] \tag{2.32}$$

Once again the complementary error function is used to simplify the resulting expressions. The probabilities are substituted into Equation 2.24 and after some algebraic operations Equation 2.33 is obtained.

$$\begin{aligned} BER_{PAM4} = \frac{1}{16}\Bigg[&erfc\left(\frac{I_0 - I_{2th}}{\sigma_0\sqrt{2}}\right) + erfc\left(\frac{I_0 - I_{1th}}{\sigma_0\sqrt{2}}\right) + erfc\left(\frac{I_1 - I_{2th}}{\sigma_1\sqrt{2}}\right) \\ &+erfc\left(\frac{I_{1th} - I_1}{\sigma_1\sqrt{2}}\right) + erfc\left(\frac{I_1 - I_{3th}}{\sigma_1\sqrt{2}}\right) + erfc\left(\frac{I_{2th} - I_2}{\sigma_2\sqrt{2}}\right) \\ &+erfc\left(\frac{I_{1th} - I_2}{\sigma_2\sqrt{2}}\right) + erfc\left(\frac{I_2 - I_{3th}}{\sigma_2\sqrt{2}}\right) + erfc\left(\frac{I_{2th} - I_3}{\sigma_3\sqrt{2}}\right) \\ &+erfc\left(\frac{I_{3th} - I_3}{\sigma_3\sqrt{2}}\right) - erfc\left(\frac{I_{3th} - I_0}{\sigma_0\sqrt{2}}\right) - erfc\left(\frac{I_{1th} - I_3}{\sigma_3\sqrt{2}}\right)\Bigg] \end{aligned} \tag{2.33}$$

2.2.4 Theoretical BER Comparison

In order to make a theoretical comparison of Equation 2.15, 2.22 and 2.33 assumptions on the noise and signal power are needed.
It is assumed that the affecting noise has the same variance for each signal level, enabling the following condition

$$2\sigma_0^2 = 2\sigma_1^2 = 2\sigma_2^2 = 2\sigma_3^2 = N_0 \tag{2.34}$$

Also it is assumed, that the signal levels hold an equal amount of power and are symmetrical around 0 such that following condition apply.

$$\int_{-\infty}^{a} exp(-u^2)du = \int_{a}^{\infty} exp(-u^2)du \tag{2.35}$$

Hamming distances also need to be applied to each average intensity value of the symbols and the decision thresholds. These can be read from Table 2.3

Table 2.3: Distances of average intensity value and thresholds from 0.

I **signal value**	I_0	I_{1th}	I_1	I_{2th}	I_2	I_{3th}	I_3
NRZ	-d	0	d				
duobinary	-2d	-d	0	d	2d		
PAM4	-3d	-2d	-d	0	d	2d	3d

The the energy per bit E_b can be related to the hamming distances through Equation 2.36 [24]:

$$d = \sqrt{\frac{3 \cdot log_2(M) \cdot E_b}{(M^2 - 1)}} = a\sqrt{E_b} \tag{2.36}$$

In Equation 2.36 a is a constant determined by the signal symbols M. For NRZ $M = 2$, for duobinary $M = 3$ and for PAM4 $M = 4$. From Equation 2.36 the Signal to Noise Ratio (SNR) per bit can be found by describing d as $a\sqrt{E_b}$.

$$n\frac{d}{\sqrt{N_0}} = n\frac{a\sqrt{E_b}}{\sqrt{N_0}} = na\sqrt{SNR} \tag{2.37}$$

In Equation 2.37, $n \in \{1, 3, 5\}$ is the appropriate hamming distance.
Continuing the theoretical BER comparison requires specific SNR calculation for the individual modulation format. These calculations are done in the following sections.

2.2.4.1 Calculations of SNR per Bit for NRZ

With the noise condition in Equation 2.34 together with the hamming distances for NRZ from Table 2.3, Equation 2.15 can be written as:

$$\begin{aligned} BER_{NRZ} &= \frac{1}{2}\left[\frac{1}{\sigma_1\sqrt{2\pi}}\int_{-\infty}^{0} exp(-\frac{(x-d)^2}{N_0})dx + \frac{1}{\sigma_0\sqrt{2\pi}}\int_{0}^{\infty} exp(-\frac{(x-(-d))^2}{N_0})dx\right] \\ &= \frac{1}{4}\left[erfc\left(\frac{-d}{\sqrt{N_0}}\right) + erfc\left(\frac{d}{\sqrt{N_0}}\right)\right] \end{aligned} \tag{2.38}$$

Utilizing the assumption of symmetry from Equation 2.35 the above equation can be rewritten into:

$$BER_{NRZ} = \frac{1}{2}erfc\left(\frac{d}{\sqrt{N_0}}\right) \tag{2.39}$$

By substituting Equation 2.36 and 2.37 where $M = 2$ and $n = 1$ into Equation 2.39 the BER for NRZ can now be expressed in terms of SNR per bit as in:

$$BER_{NRZ} = \frac{1}{2}\, erfc\left(\sqrt{\frac{3 \cdot log_2(2)}{2^2 - 1}}\sqrt{SNR}\right) \tag{2.40}$$

2.2.4.2 Calculations of SNR per Bit for Duobinary

Using the assumptions in the same manner as in the calculations for NRZ together with the hamming distances from Table 2.3 and by substitution of Equation 2.36 into the BER for duobinary, Equation 2.22 can be expressed as function of hamming distances by:

$$BER_{duobinary} = \frac{3}{4}\, erfc\left(\frac{d}{\sqrt{N_0}}\right) - \frac{1}{4}\, erfc\left(\frac{3d}{\sqrt{N_0}}\right) \tag{2.41}$$

Equation 2.37 can now be utilized with $M = 3$ and $n \in \{1, 3\}$ to describe the BER of duobinary as function of SNR per bit.

$$\begin{aligned} BER_{duobinary} = {} & \frac{3}{4}\, erfc\left(\sqrt{\frac{3 \cdot log_2(3)}{3^2 - 1}}\sqrt{SNR}\right) \\ & - \frac{1}{4}\, erfc\left(3\sqrt{\frac{3 \cdot log_2(3)}{3^2 - 1}}\sqrt{SNR}\right) \end{aligned} \tag{2.42}$$

2.2.4.3 Calculations of SNR per Bit for PAM4

Substituting the hamming distances for PAM4 form Table 2.3 into Equation 2.33 and applying the same noise and power assumptions once again, an expression of the BER as function of hamming distances can be obtained for PAM4.

$$BER_{PAM4} = \frac{3}{8} erfc\left(\frac{d}{\sqrt{N_0}}\right) + \frac{1}{4} erfc\left(\frac{3d}{\sqrt{N_0}}\right) - \frac{1}{8} erfc\left(\frac{d5}{\sqrt{N_0}}\right) \tag{2.43}$$

Applying Equation 2.37 as argument to the complementary error function, with $M = 4$ and $n \in \{1, 3, 5\}$, an expression of the BER for PAM4 as function of SNR per bit is

obtained.

$$BER_{PAM4} = \frac{3}{8}\, erfc\left(\sqrt{\frac{3 \cdot log_2(4)}{4^2-1}}\sqrt{SNR}\right) + \frac{1}{4}\, erfc\left(3\sqrt{\frac{3 \cdot log_2(4)}{4^2-1}}\sqrt{SNR}\right) - \frac{1}{8}\, erfc\left(5\sqrt{\frac{3 \cdot log_2(4)}{4^2-1}}\sqrt{SNR}\right) \tag{2.44}$$

The three modulation formats can now be evaluated as function of SNR per bit.

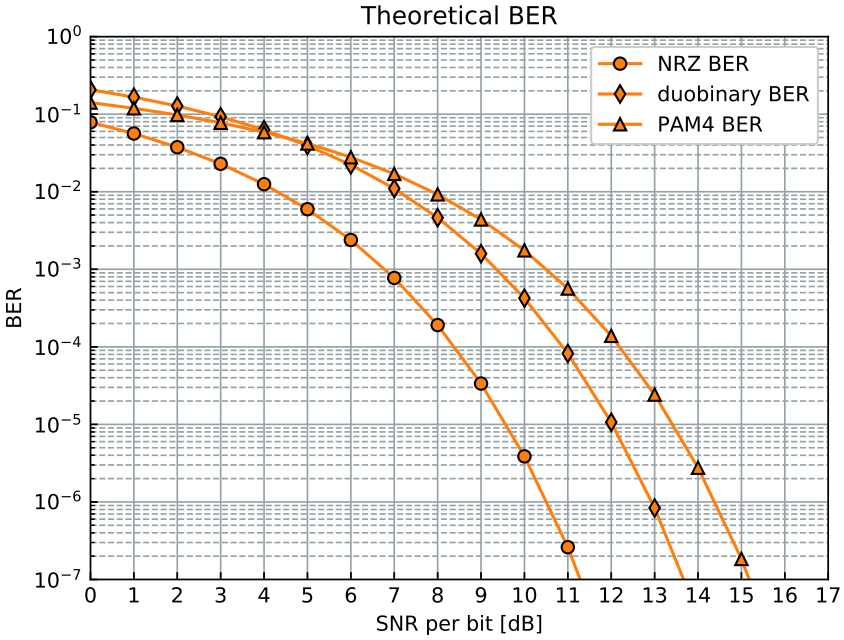

Figure 2.9: Theoretical BER comparison of NRZ, duobinary and PAM4 as function of SNR per bit.

From Figure 2.9 the general BER performance of NRZ, duobinary and PAM4 as function of SNR per bit is observed. The performance of each modulation format is decreasing as the SNR gets smaller. At low SNR values, PAM4 outperforms duobinary. At higher SNR values (above 7 dB), duobinary shows better performance then PAM4. At a BER of 10^{-9}, duobinary is 1.5 dB better than PAM4. The lowered noise tolerance of the multi level signals is observed, as performance for duobinary and PAM4 is worse than that of NRZ for the same amount of SNR.

CHAPTER 3

Capacity Upgrading Optical Access Systems

This chapter is based the work published in **[J5]** and **[C1]**. Presented are the experiments corresponding to the implementation of duobinary and PAM4 into short range optical systems. These systems fit well into the 10G class DWDM PON standard [25], with the intention of upgrading the capacity from 10 Gbit/s to 25 Gbit/s.

3.1 Introduction

Already back in 2014 it was confirmed that metro network only traffic had surpassed that of long haul networks[26]. This puts a stress on the capacity in optical access systems. The main limitation in these systems is the limited electronic BW of the access equipment. To reach higher capacity, the implementation of advanced modulation formats have been adopted by most equipment manufactures. Advanced modulation formats has a downside in that they often require complex DSP, which increases power consumption of the processing [10], [11]. This is why formats such as Discrete Multi Tone (DMT) and Othogonal Frequency Division Multiplexing (OFDM), which can provide large BW utilization, are assessed to be too costly to implement for access networks [27], [28]. Multilevel modulation formats such as PAM4 and duobinary can be handled by analog options such as DACs and electrical filters. the main advantage of duobinary and PAM4 is that they require a reduced amount of DSP to function well, but performance can be increased with increased amount of DSP [29]. Furthermore, the principles of duobinary can be combined with PAM4, as showed in chapter 2, to create an optical signal with seven intensity levels. Duobinary PAM4 has a lower noise tolerance compared to pure duobinary, NRZ and PAM4, but offers a reduced signal BW. Which means that the system BW can be better utilized.

3.1.1 Access Network Scenario

The scenario for the experimental work is a PON network with a 20 km optical link between the central office and the split point as seen in Figure 3.1.

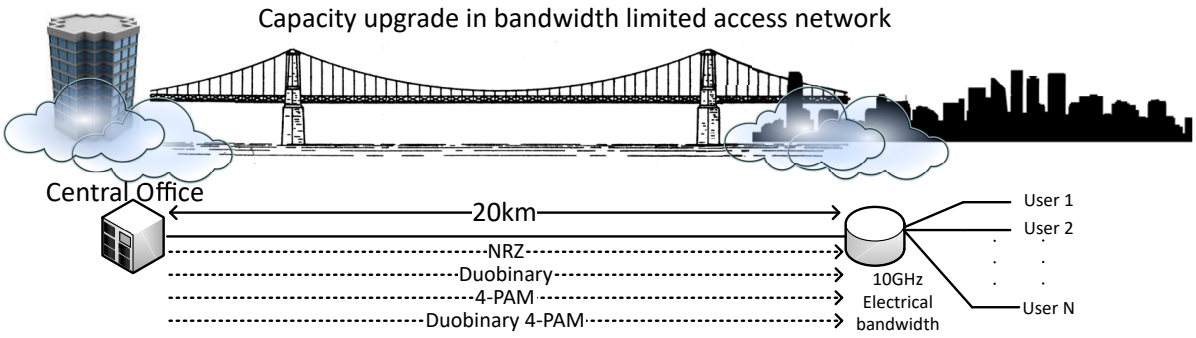

Figure 3.1: PON network scenario for the experimental work

The optical link can consist of any single type of fiber from Standard Single Mode Fiber (SSMF), Dispersion Shifted Fiber (DSF) or Non-Zero Dispersion Shifted Fiber (NZDSF). The different Single Mode Fiber (SMF) types have different dispersion effects, which may prove an advantage when combined with a multilevel modulation format. The symbol rate of the transmitter is set to 10 Gbaud such that it fits with the electronic BW limit of the receiver circuit at 10 GHz. This enables the transmission of NRZ at speed of 10 Gbit/s. The distance of 20 km is possible without optical amplification, thus this scenario is a 10G class PON.

3.2 Experimental Work

Experimental work has been carried out in the optical laboratory. A setup that represent the scenario described in subsection 3.1.1 was constructed. The experimental setup varies very little between the different modulation formats. The base experimental setup transmit a NRZ signal and the analog generation of the other modulation formats adds one or two extra system elements. This underlines the simple evolution that a potential system needs to undergo, in order to implement the advanced multilevel modulation formats. The following sections describes the experimental setups.

3.2.1 NRZ Transmission

The simplest setup in this experiment, is when NRZ is being transmitted as seen in Figure 3.2.

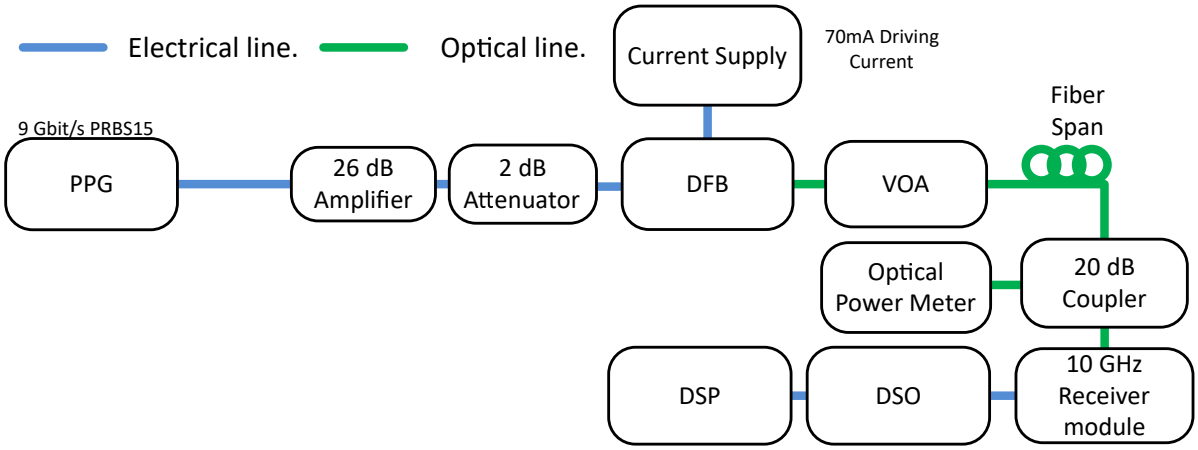

Figure 3.2: Experimental setup for transmitting 9 Gbit/s NRZ

To generate a 9 Gbaud NRZ, corresponding to 9 Gbit/s , a Pulse Patteren Generator (PPG) is set to output a PRBS with length 15 (PRBS15). The frequency of the PPG is set to 9 GHz due to the PPG being faulty and generating a noisy signal in the frequency range 9.5 GHz to 11.1 GHz. The output from the PPG is amplified to 2 V Peak to Peak (P2P), so to match the optimum driving voltage of the Distributed Feedback Laser (DFB) laser. The DFB is biased with a 70 mA driving current. This is where the Light Current Voltage (LIV) curve is linear. This is an important feature when modulating the DFB with multilevel signals, as this creates equal distance between the levels of the optical output and insures maximum Extinction Ratio (ER) The optical output from the DFB is power controlled with a Variable Optical Attenuator (VOA) then launched into the transmission fiber. The VOA allows for an adjustable optical power and enables the measurement of BER curves. As mentioned in subsection 3.1.1, the transmission is done over SSMF, DSF and NZDSF. The transmission span lengths are 0 km, also called optical Back to Back (B2B), 5 km and 20 km. After the transmission span, a 20 dB optical coupler is used to monitor the optical power received by the PD. The PD used, is a receiver module with an electronic BW of 10 GHz. The electrical signal is then recorded with a 40 GSa/sDigital Storage Ocilloscope (DSO). This allows for offline DSP where the signal is re-synchronized, demodulated and the BER was calculated bit by bit using a matched reference PRBS.

3.2.2 Duobinary Transmission

By modifying the setup for NRZ transmission in Figure 3.2, to include an electrical 4 GHz low pass Bessel filter, then a 9 Gbaud duobinary signal is generated as seen in Figure 3.3.

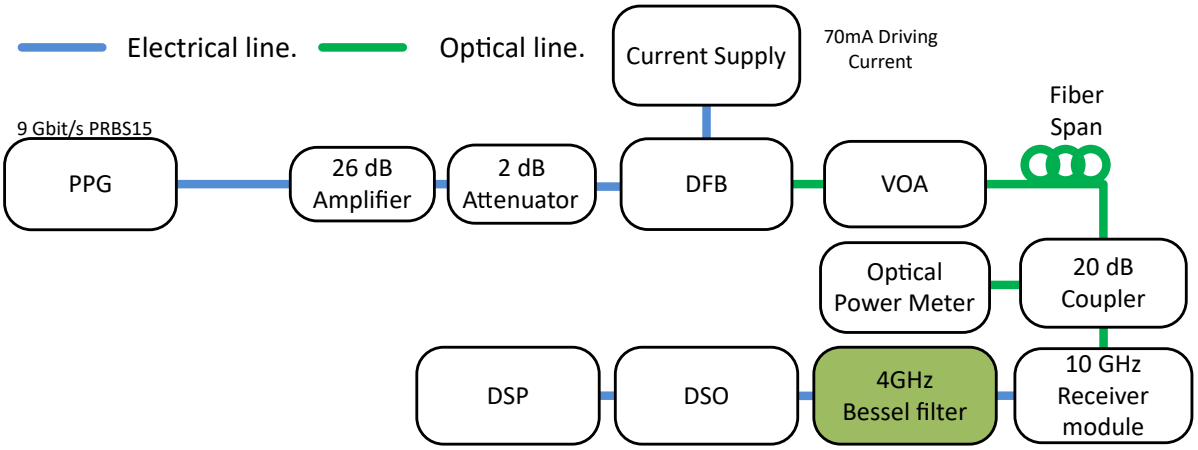

Figure 3.3: Experimental setup for transmitting 9 Gbit/s duobinary

In this setup, the Bessel filter is included after the optical receiver. This is done, to remove some of the high frequency noise that might stem from the PD. The filter could also be added digitally using DSP. Othewise the setup remains unchanged from that of the NRZ transmission. The data rate of the duobinary modulation has not changed from that of the NRZ (9 Gbit/s) but since the signal BW is being limited by 4 GHz low pass Bessel filter and not the otherwise 10 GHz PD, this corresponds to about $> 50\%$ system BW utilization. Theoretically, if the PPG could be switched out for one able to work at a frequency of 18 GHz, producing a 18 Gbit/s NRZ. Then generate duobinary instead of NRZ at the receiver. This would be done by using a 9 GHz low pass Bessel filter. The otherwise unchanged 10 GHz transmission system would, in theory, have an effective data rate of 18 Gbit/s.

3.2.3 PAM4 Transmission

Generation of analog PAM4 requires the use of a DAC in the transmitter.

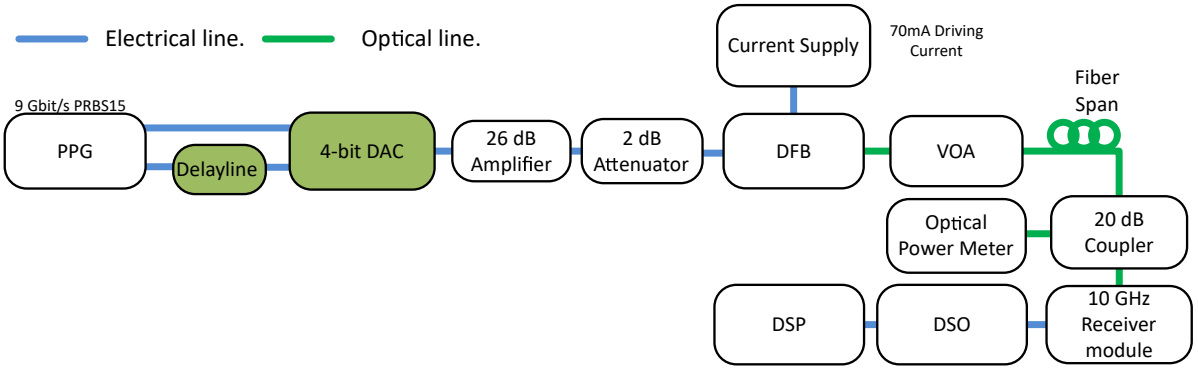

Figure 3.4: Experimental setup for transmitting 18 Gbit/s PAM4

In the setup seen in Figure 3.4, a high speed 4-bit DAC is used. The input to the DAC is supplied using two outputs from the PPG. An electrical delay line is used to set the timing between the two PPG outputs, thus they are uncorrelated. The combined PAM4 signal is then amplified to 2 V P2P before modulating the DFB. After this the signal is transmitted just as explained in the NRZ transmission subsection 3.2.1, using the same receiver setup. The data rate of PAM4 is doubled that of the original NRZ, because each cycle in the PPG generates a bit in each of the two output, these are then uncorrelated and combined into a PAM4 symbol. The effective data rate of the PAM4 transmission is then 18 Gbit/s.

3.2.4 Duobinary PAM4 Transmission

By modifying the PAM4 setup to include the 4 GHz low pass Bessel filter from the duobinary setup. It is possible to double the data rate and the BW utilization. This setup is seen in Figure 3.5.

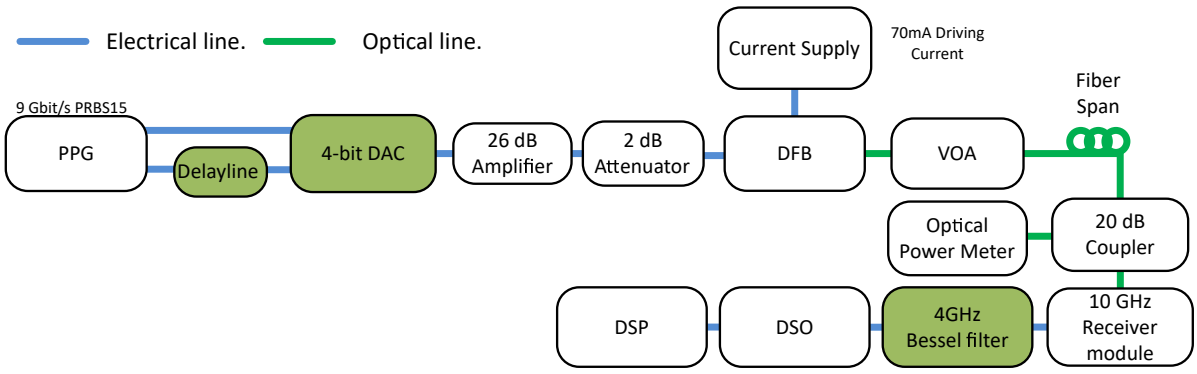

Figure 3.5: Experimental setup for transmitting 18 Gbit/s duobinary PAM4

By implementing duobinary PAM4, the system is able to transmit at a data rate of 18 Gbit/s being limited by the 4 GHz low pass Bessel filter. As in the case of duobinary transmission, if the PPG was able work at 18 GHz, and a 9 GHz low pass Bessel filter was implemented, this regular 10 GHz system could in theory transmit at a data rate of 36 Gbit/s by implementing duobinary PAM4.

3.2.5 Results

The results from the experiments on the four different setups are combined into one graph of BER curves for an easy comparison.

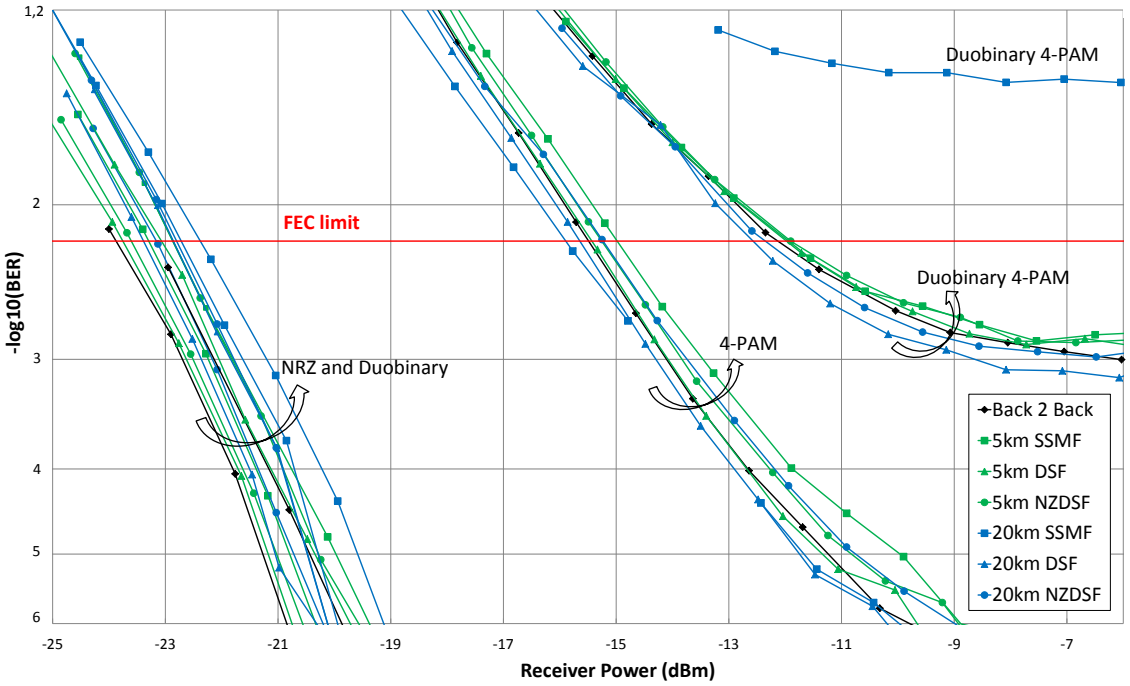

Figure 3.6: Resulting BER from transmitting NRZ, duobinary, PAM4 and duobinary PAM4 at 9 Gbaud on a 10 GHz limited PON system

The BER curves in Figure 3.6 are pre-Forward Error Correction (FEC) results. The FEC limit displayed corresponds to a Beyond Bound Decoding with 7% Overhead (OH) [30]. The results shows that each modulation format, under test, preforms below the displayed FEC limit for certain fibers. One immediate outlier is the duobinary PAM4 over 20 km of SSMF. Due to the heavy amount of dispersion in SSMF there is not a single measurement point below the FEC limit. Also noticeable is the y-axis not protruding below 6 on the $-log_{10}(BER)$. This it because the number of data points stored by the DSO theoretically only allows for a BER of 10^{-6} if one bit error is assumed.
Apart from the case of duobinary PAM4, the spreading from fiber type and length only varies very little in received power for the given modulation formats. NRZ and duobinary are indistinguishable, this could be due to an unfiltered high frequency component from the DFB laser, that causes NRZ a limited performance in this system. The maximum spread from best to worst performance for the two modulation formats is approximately 2 dB. For PAM4 the maximum spread is approximately 1.5 dB. The received power penalty from NRZ or duobinary to PAM4 is approximately 6 dB at the FEC limit. This penalty increases by approximately 2.5 dB to a total of 8.5 dB at the FEC limit, when duobinary PAM4 is implemented. Transmitting duobinary PAM4 leads to an error floor at a BER of 10^{-3}. This is still below the displayed FEC, but only just so. NRZ, duobinary and PAM4 shows a tendency to enable transmission at even lower BER than 10^{-6}. these modulation formats does not require a 7% overhead FEC but might make due with a lower OH percentage, or no OH at all, for this particular system.

3.3 Discussion

Based on these initial experiments in partial response modulation formats, it is found that implementing duobinary partial response is very easy. Especially when experimental validation is based on offline DSP, then including the modulo operation does not pose significant extra computational stress. Also combining the partial response with other higher order modulation formats is found easy and viable. The filter selection for creating the analog implementation of duobinay is considered a trail and error process. The electrical low pass Bessel filters comes in different frequencies, and a 4.5 GHz low pass Bessel filter would be assumed to provide best performance. Such a filter was not available during the experiment, so filters at 6 GHz and 4 GHz were tested. Best performance was concluded with the 4 GHz low pass Bessel filter. From the result one could argue that since the performance of duobinary and NRZ are equal there would be no reason to use duobinary. It is true for this system, where the speed is only 9 Gbit/s and fiber dispersion poses no penalty. But as seen later in chapter 5, when data rates are increased, there exist to much dispersion in SSMF for NRZ to be transmitted, but since duobinary takes up half the BW of NRZ it is more resilient to fiber dispersion. If the results from this experiment is compared to the theory in chapter 2, it is clearly observed that the SNR of the transmission system is effecting the performance of the modulation formats which has more intensity levels. Also it is clear that this system holds a limitation in minimum performance since NRZ and duobinary performs on pair, and very close to their B2B measurements.
Since it is a standard thing to utilize FEC in transmission systems now a days [31], it is clear that the best spectral efficiency is gained from combining duobinary and PAM4 together. Effectively doubling the net bit rate and halving the spectral width. But as seen from the experiments, it is only possible with the use of FEC and non standard single mode fiber that alters the dispersion factor.

CHAPTER 4

Partial Response and Pulse Amplitude Modulation Formats for Data Center Interconnections

This chapter is based on the work published in **[J2]**, **[C2]**, and **[C3]**. Presented in this chapter are the experiments in which partial response and PAM4 are being implemented in DWDM systems intended for data center interconnections.

4.1 Introduction

Optical links in and around data centers are a whole field of research on its own. But limited to the view of modern trends and developments, along with a sharp focus on partial response modulation formats, there is one scenario/type of links where partial modulation could be applied, namely data center interconnects. Stemming directly from the growth of data traffic described in chapter 1, new data centers are being build to handle the pressure of future demands, while older data centers will experience a potential bottleneck effect. Especially in the connection between data center sites [32]. But when it comes to data center interconnections there is a clear gap between the capabilities of clients-side and long-haul optics, caused by the scaling trends in the data center business [33]. As mentioned before, the capacity and reach that is offered by long-haul optics is very attractive to interconnections, but are still considered to be too expensive and with very high complexity [34]. This is also why the development of the IEEE P802.3bs 400GbE standard is adopting PAM4 as modulation format [35].
By lowering the analog implementation complexity, using IM/DD solutions, and turning up the DSP complexity, the gap between old and new data centers could be bridged by using PAM4 and duobinary modulation formats.

4.1.1 Data center interconnection scenario

In a scenario where two data centers are interconnected using a long distance, high bit rate link, it is desirable to generate a high speed duobinary or PAM4 signal in a rack in data center A and transmit this through a long range, uninterrupted link to a rack in data center B just as depicted in Figure 4.1.

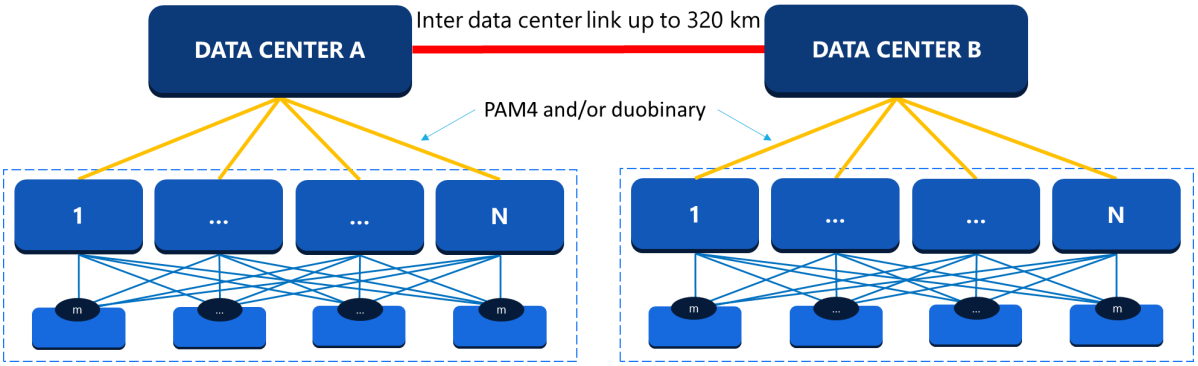

Figure 4.1: Scenario for 320 km inter data center link. Each data center contains N racks and m sub-racks.

4.2 Experimental Work

All the experimental work for data center interconnections are carried out on an old Tellabs 400 km DWDM transmission span system, with 32 channels in a 100 GHz grid spacing, originally designed for 10G communication. Because of this, the varying part of the setup is the signal generation, signal speed and, at which range the signal is tapped out of the transmission link.
The experiments never succeeded in going all 400 km. The maximum successful transmission is 320 km. Successful is considered as a pre-FEC BER below the typical FEC limit for such a type of transmission link [36].

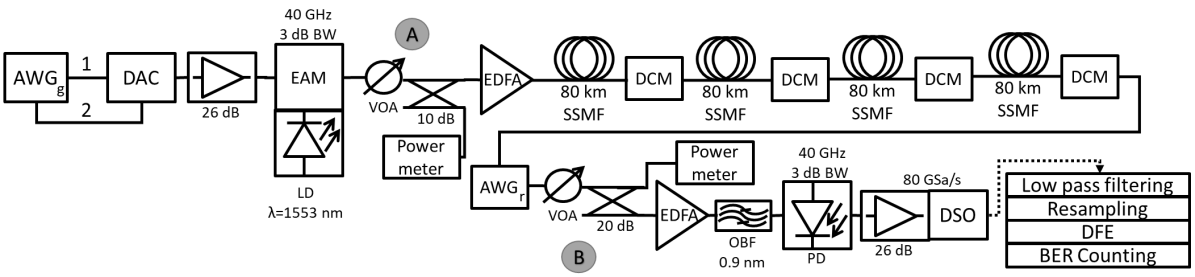

Figure 4.2: Experimental setup for transmitting high speed duobinary and PAM4 over 320 km SSMF

As seen from Figure 4.2 the transmission link consists of a series of 80 km SSMF attached to Dispersion Compensating Modules (DCMs) containing a two-step Erbium Doped Fiber Amplifier (EDFA) with Dispersion Compensating Fiber (DCF) in between. The EDFAs have a 6 dB noise figure and 20 dB gain. The DCM compensates for the fiber loss and dispersion of the respective 80 km SSMF. In total the complete 400 km transmission link is fully loss and dispersion compensated, but it is done in such a way that the link can be broken into parts of 80 km fully loss and dispersion compensated links.
Following the signal path of Figure 4.2 going from left to right. A 62 Gbaud Arbitary Waveform Generator $(AWG)_g$ is programmed to generate the test signals. Both duobinary and PAM4 starts with a MATLAB® programmed PRBS15. This is either encoded into douobinary as in subsubsection 2.1.2.2 then transmitted from the AWG_g using channel 1. Or the PRBS is transmitted on channel 1 and 2 where one channel is delayed, such that the two channels are uncorrelated. Then the two channels are used as input for a 32 Gbaud DAC where PAM4 is created.
The Laser used in the setup, is an Electro Absorbtion Modulator (EAM) with a 40 GHz 3 dB BW packaged together with a Continous Wave (CW) Laser Diode (LD), thermal controlled to emit at 1553 nm. The EAM performs best when the modulating electrical signal has a P2P power of 2 V. Therefore a 26 dB electrical amplifier is applied and gain controlled adjusted, to match the driving power of the EAM. The optical output of the EAM is launch power controlled using a VOA and launch power is measured with an optical power meter after a 10 dB optical coupler. After the VOA, the optical signal is boosted with a standalone EDFA before entering the transmission span. At the end of the transmission span, the system incorporates a 32 channel Arrayed Waveguide Grating (AWG_r) where one channel is used to tap out the transmitted signal. Another VOA is implemented to adjust received power, which is measured with yet another optical power meter after a 20 dB optical coupler. The optical receiver consists of a pre-amplifying EDFA with constant pump power, and a 0.9 nm Optical Bandpass Filter (OBF) which removes unwanted Amplified Spontaneous Emission (ASE). After the OBF a PD with 40 GHz 3 dB BW, does the optical to electrical conversion. The output signal from the PD is electrically amplified 26 dB before the signal is received and stored for offline DSP by a 80 GSa/s DSO with a BW of 33 GHz. The offline DSP consists of; additional low pass filtering, resampling and a Decision Feedback Equalizer (DFE) with 41 forward tabs and 21 feedback tabs. The DFE is controlled using a Decision-Directed Least-Mean-Square (DD-LMS) algorithm. Finally, the BER calculation is done through bit by bit comparison, using a reference PRBS.

4.2.1 28 Gbaud PAM4

The first experiment on the setup, is the transmission of 28 Gbaud PAM4 at a distance of 240 km. This demonstrates the reuse of conventional links for inter data center communication, without re-engineering the transmission link design.
To clarify on the signal generation. The AWG_g in the setup of Figure 4.2 is set to produce

two NRZ bit streams at 28 Gbit/s these are then uncorrelated with AWG_g channel delay. They traverse to the transmitter DAC through channel 1 and 2. They are combined in the DAC to create 28 Gbaud PAM4, corresponding to a 56 Gbit/s data transmission.

4.2.1.1 Results

To determine the optimal launch power into the transmission span, a measurement of BER versus optical output power of the transmitter is completed. The optical output power of the transmitter is measured, using the optical coupler and power meter in point A of Figure 4.2. The launch power is adjusted by using the VOA in same point A of Figure 4.2.

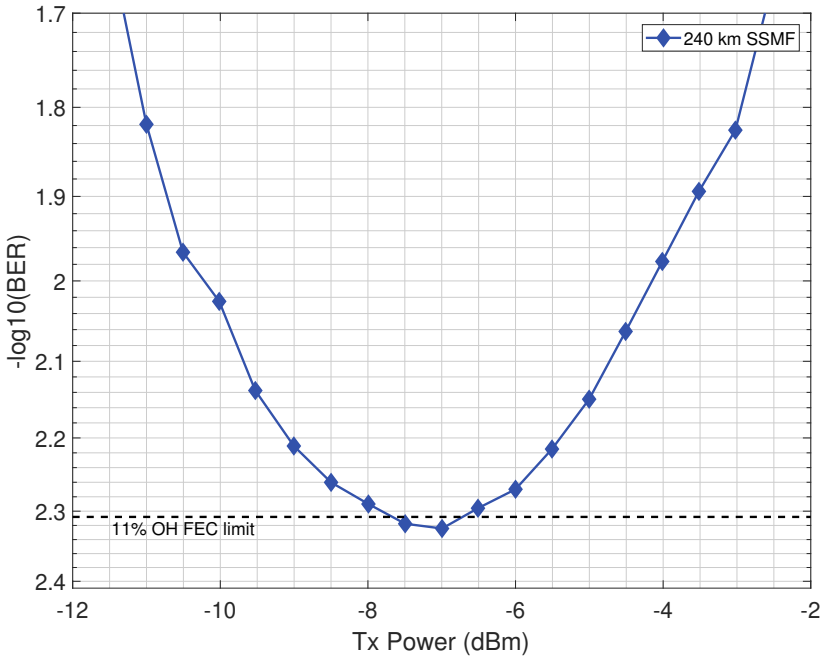

Figure 4.3: BER as function of transmitter power (Tx Power) for 28 Gbaud PAM4 over 320 km SSMF

The results from the transmitter power measurement in seen in Figure 4.3. From the 240 km SSMF curve it is observed that with a transmitter power of −7.5 dBm the BER goes below 2.32 on the $-log_{10}(\text{BER})$ scale, which is the 11% OH FEC code. Using this or a similar performing FEC code, the system is considered error free. The lowest BER is reached at a transmitter power of −7 dBm, which is the most optimal launch power for this setup.
The launch power is set to −7 dBm during the rest of the experimental measurements. At higher launch powers, worse BER is measured. This indicates that optical nonlinearities are the limiting factor for this system. This is caused by the high amplification of the first EDFA in the transmission span which is seen just after point A in Figure 4.2.

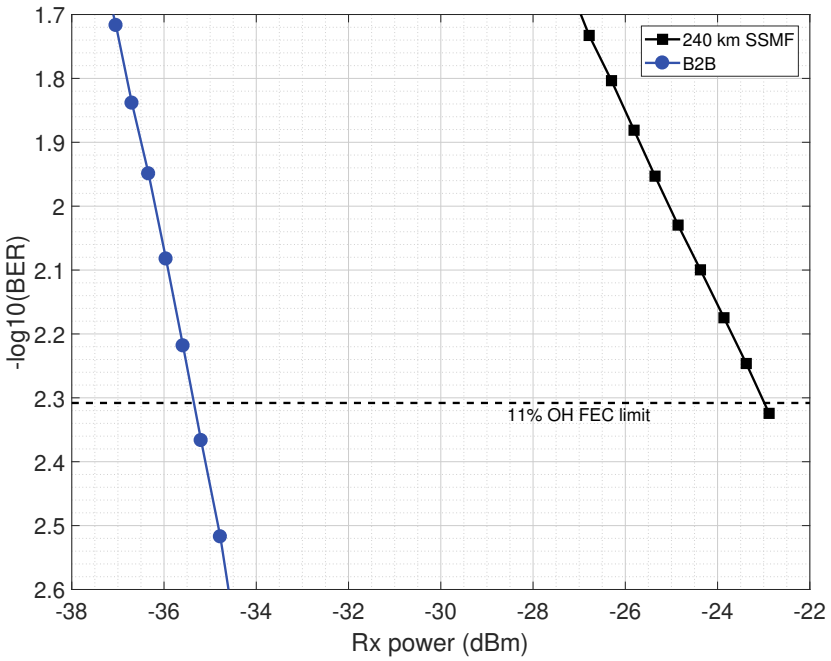

Figure 4.4: BER as function of receiver power (Rx power) for PAM4 over 320 km SSMF and in the B2B scenario

The results of the BER measurement is shown in Figure 4.4. The optical B2B measurement is done by connecting point A, with point B in Figure 4.2 using a ordinary optical patch cord. The B2B curve of Figure 4.4 shows that a received power, higher than -35.65 dBm results in a BER below the 11% FEC limit. The BER curve for transmitting over the 240 km transmission span, show that the same 11% OH FEC can be reached at a received power of -22.9 dBm. This corresponds to a power penalty of 12.75 dB compared to the B2B transmission.
Reaching a BER below 2.3 on the $-log_{10}(\text{BER})$, would not be possible at the distance of 240 km if not for the DFE implemented in the DSP as seen from Figure 4.5.

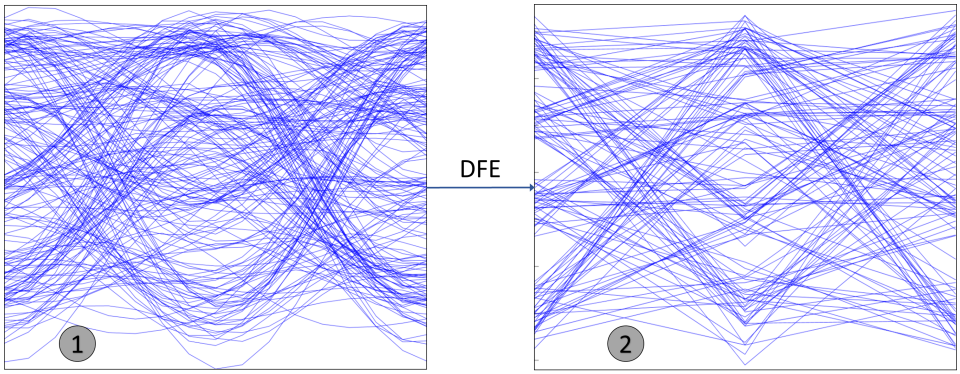

Figure 4.5: Signal clean-up by using an DFE via offline processing

The eyediagram in Figure 4.5 is based on the signal at the received power of −22.9 dBm for transmitting over 240 km. Eyediagram 1 shows the eye after lowpass filtering, again done in DSP. The middle eye of the PAM4 signal is closed due to noise impairments. Only the top and bottom levels are perceivable, but the eyes are not sufficiently open, to perform below the FEC limit. Eyediagram 2 shows the eye after the DFE. The DFE manages to remove some of the noise from the middle eyeopening and the lowest of the two middle levels now appear more clearly. The shape of the eye has changed as a result of having 1 sample per symbol as contrast to the, before, 16 samples per symbol. As observed, the signal in eyediagram 2 is just clear enough to perform below the FEC limit, while before the DFE, the signal contains too much noise to be received below the FEC limit.

4.2.2 32 Gbaud PAM4

After the success of transmitting 28 Gbaud PAM4, it was decided to optimize slightly on the DSP implementation, and enable Optical Signal to Noise Ratio (OSNR) measurements by implementing an Optical Spectrum Analyzer (OSA). Now, best performance BER versus OSNR can be obtained by sweeping transmission power and receiver power individually. This allows faster transmission speed over longer distances Sthen before. This results in the success full transmission of 32 Gbaud PAM4 over 320 km, corresponding to a data rate of 64 Gbit/s. During this experiment, the OSA is incorporated in the setup, just before the AWG_r in Figure 4.2. The noise power level of the DWDM spectrum is measured and compared to the power of the channel at 1553 nm. The reference optical bandwidth of the OSA is set to 0.1 nm, following standard OSNR measurements.

4.2.2.1 Results

The results for transmitting 32 Gbaud PAM4 over 320 km is observed from the BER curves in Figure 4.6

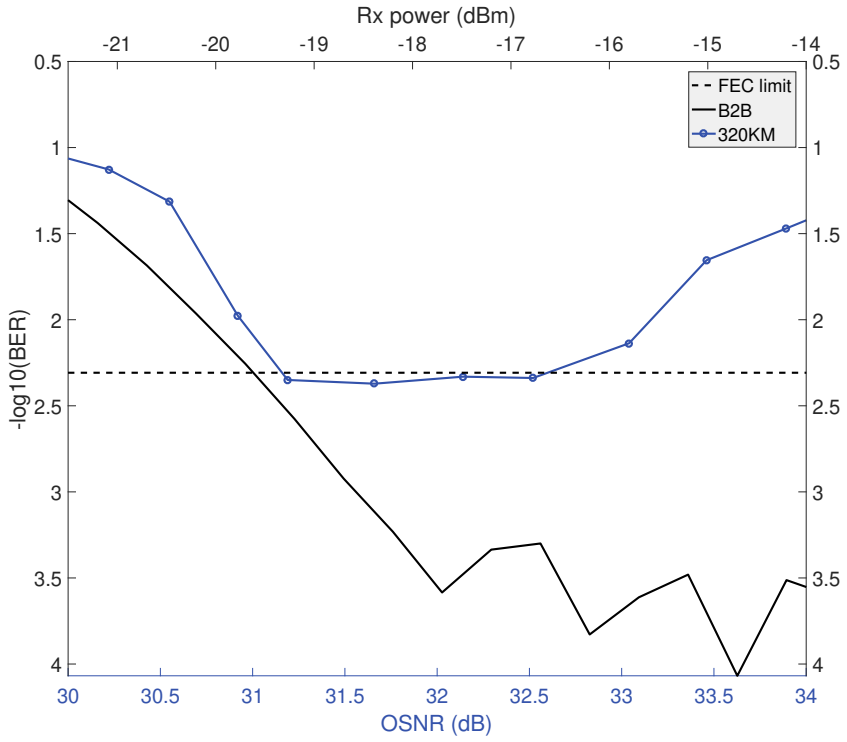

Figure 4.6: BER curves of 32 Gbaud PAM4 for B2B versus received power (Rx power) and for 320 km transmission versus OSNR

The black B2B curve is versus received power which is the corresponding top black x-axis in Figure 4.6. In this experiment, the B2B measurement was done by including the EDFAs of the transmitter and receiver. The error floor around a BER of 3.5 on the $-log_{10}(\text{BER})$ in the B2B case, is caused by these two EDFAs. After the transmission of 320 km it is observed, that a BER below the 11% OH FEC limit can be achieved at an OSNR between 31.2 dB to 32.5 dB. The difference in the error floor of the B2B case and the error floor 320 km transmission, is caused by the filtering effect of the AWG_r. The AWG_r has a 100 GHz channel grid, corresponding to a 3 dB cutoff of 50 GHz. This is a narrower filter than the OBF at 0.9 nm. Since the AWG_r is not included in the B2B case, more noise is present in the B2B case, causing the high error floor. The incline in BER of the 320 km transmission performance, is due to the sweeping of transmission power. This causes a limitation by fiber non-linearities as a result of having too high transmission power, similar to the case of Figure 4.3.

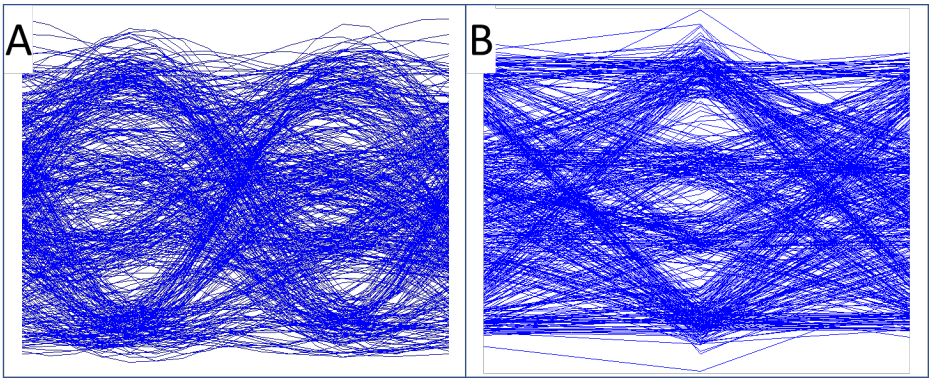

Figure 4.7: Eyediagrams for the BER corresponding to an OSNR of 31.66 dB. A is after lowpass filtering and resampling. B is after the DFE

Once again the effect of the DFE is clearly visible from the eyediagrams in Figure 4.7. The signal after lowpass filtering and resampling is seen in Figure 4.7 A. Here the four levels of the PAM4 signal are visible, but the eyeopenings are almost closed in top and middle. After the DFE seen in B, the top and middle eyeopenings are much more open, while the bottom eyeopning remains the same. The eyeshape is changed due to the lowered amounts of samples. Like in the case of the eyediagrams in Figure 4.5, the amount of samples per symbol drops from 16 to 1.

4.2.3 60 Gbaud Duobinary

The last experiment on the DWDM setup, is the transmission of 60 Gbaud duobinary modulation. This experiment follows the same optimization as in the previous 32 Gbaud PAM4 experiment. That is, a sweeping of the transmission power and receiver power is done separately, and best results are chosen. The duobinary encoding is done purely in DSP. Here a PRBS15 in the form of an NRZ sampled to match 60 Gbit/s when transmitted with the AWG_g. The NRZ is encoded to duobinary following the method described in subsubsection 2.1.2.2, then transmitted through the AWG_g using only channel 1. The final output is a duobinary signal at a symbol rate of 60 Gbaud.

4.2.3.1 Results

During this experiment, a BER measurement was done at every 80 km transmission segment, as seen in Figure 4.8.

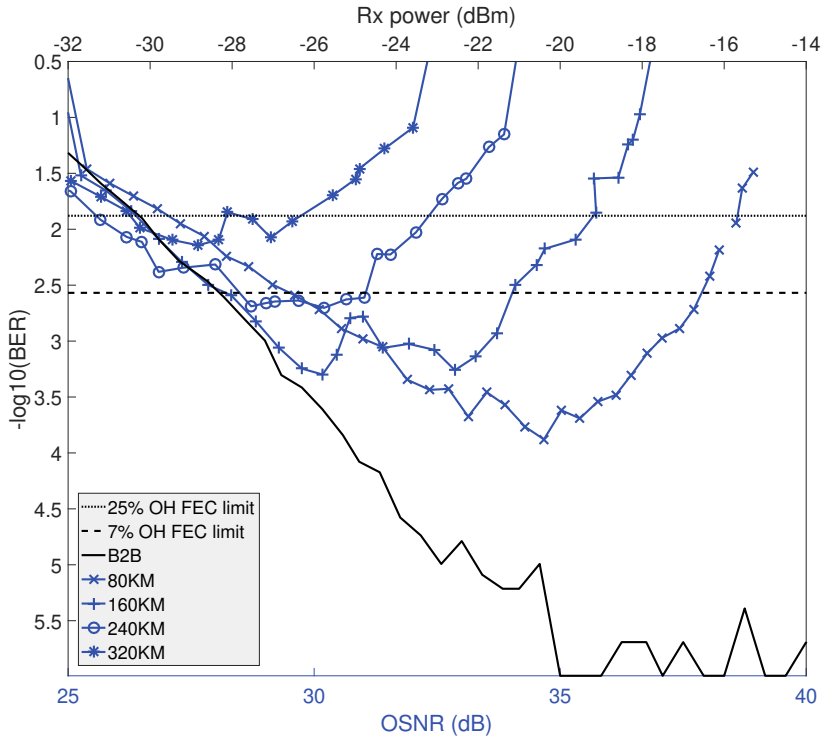

Figure 4.8: BER curves of 60 Gbaud duobinary modulation, transmitted from B2B to 320 km. The B2B curve is a function of received power (Rx power) and transmission from 80 km to 320 km is a function of OSNR

The BER is shown in Figure 4.8 once again as function of received power for the B2B case, and as function of OSNR for the transmission of 80 km to 320 km. The FEC limits marked in Figure 4.8 corresponds to 7% OH and 25% OH. As seen from the BER curves, BER performance below the 7% OH FEC limit is achieved for transmission up to 240 km. Transmission over 320 km SSMF is achievable with the use of the 25% OH FEC. Specifically, the lowest OSNR for 320 km transmission below the 25% OH FEC limit is approximately 26.5 dB.
For all the fiber transmission BER curves, an incline in BER performance is seen at higher levels of received power. This is again due to the sweeping of transmission power, that causes fiber non-linearities for high levels of transmission power.

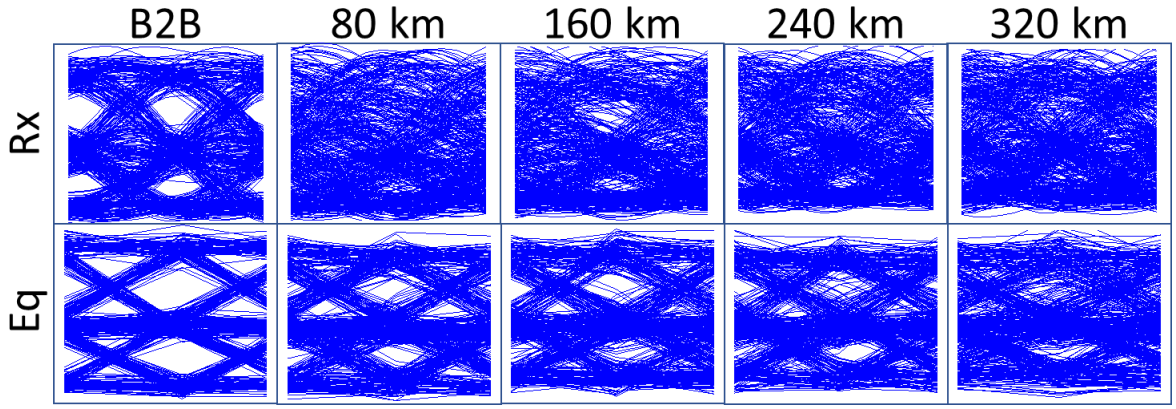

Figure 4.9: Evolution of eyediagrams of 60 Gbaud duobinary modulation, transmitted from B2B to 320 km. Eyediagrams are from the signal at best performance. Top row is after the low pass filtering done in DSP, The bottom row is after the DSP implemented DFE equalizer

As seen from the eyediagrams in Figure 4.9 without the DFE, only the B2B eyediagram looks as if it could be possible for reach a BER below the 7% FEC limit. Already after the transmission of 80 km of SSMF the DFE is needed in order to clean up the signal enough to get performance below the FEC limit. From the eyediagram after the DFE of the transmission over 320 km, it is clear that transmission of 400 km would not be possible without drastic system improvements.

4.3 Discussion

With the above experiments, the possibility of using PAM4 and duobinary for longer than access range communications have been opened up. It is clear that correct setting of the transmission power is needed for optimal system performance. Too much power will saturate the EDFAs in the system and nonlinearities will limit system performance. Also, transmitting more than 60 Gbit/s over these distances with an IM/DD system configuration, requires equalization. This poses the question; is it better to use coherent optics? or is the increased DSP complexity, from trying to use an IM/DD technique, still cost beneficial? The question is hard to answer for this particular system, because the planning for fiber dispersion and losses have already been done. It is possible that with coherent optics, the signal could transverse all 400 km without the use of EDFAs and DCMs. This is because of the improved OSNR gained from the Local Oscillator (LO) used in coherent optics. Also it is standard to include dispersion compensation in the receiver DSP for coherent optics [37], [38]. If the system was still in the design phase, coherent optics would be the technology to use. But since half of the features that coherent optics offers are already present in the system, it is a question of actual

performance, needed flexibility and future proofing [39].
For this particular system, it would have been interesting to see the performance of 32 Gbaud duobinary PAM4. The system should, in principal, be fully compensated from the most limiting factors in multi-level signals. It is seen from the PAM4 experiments, that transmission faster than 32 Gbaud will be hard to accomplish. From the duobinary experiments it is seen that, at 60 Gbaud, the transmission over 80 km is not possible without an equalizer. Therefore, a combination of the two formats (32 Gbaud duobinary PAM4), might prove more successful, in terms of performance without DSP equalization.

CHAPTER 5

Partial Response and Pulse Amplitude modulation for Next Generation PON Networks

At the end of 2017, a new PON standard was released by International Telecommunication Union - Telecommunication Standadization Sector (ITU-T) the G.698.4: Multichannel bi-directional DWDM applications with port agnostic single-channel optical interfaces(former G. Metro) [40]. The standard specifies optical interfaces, of a special type of 10G class DWDM PONs with transmitters that are wavelength tunable to match the selected DWDM grid. From the network traffic trends described in chapter 1 it is clear that the G.698.4 standard might already be outdated in terms of BW capabilities. This was realized early in 2018 by ADVA Optical Networking SE. A study on how duobinary and PAM4 preformed in a DWDM PON with port agnostic was preformed, to increase the BW of such a system. The results and conclusion of the study is presented in this chapter.

5.1 Next Generation PON Systems

An analysis of tuneability within Wavelength Division Multiplexing (WDM) PONs, done in 2000 [41], states that, a future WDM system must meet a certain combination of cost, scalability and flexibility. To be economically viable, user terminals in WDM systems need to be colorless and identical, otherwise inventory management cost and deployment issues will be excessive.
This led to numerous of tunable lasers solutions, along with algorithms and proposed systems, implementing central wavelength locking [42]–[45]. Earlier this year (2018) the G.698.4 standard was released. It describes the optical interfaces of a DWDM system where the Tail-End Equipment (TEE) contains tunable transmitters. The transmitters have the capability of automatically adapt to the channel frequency of the assigned DWDM channel.
The setup and tuning of the TEE is done via communication with the appropriate Head-

End Equipment (HEE). This communication is assisted by an amplitude modulated PT. The PT is used to make sure that the right transmitter is in the right DWDM channel. During the normal operation of the system, the PT is amplitude modulated on top of the systems data signal. This causes an impairment of the system performance. Early stage development of the standard shows that the modulation depth of the PT needs to be below 10% for NRZ modulation at 10 Gbit/s [46]. The standard for NRZ at 10 Gbit/s specifies the maximum modulation depth allowed to be 8% during operation. The scientific question asked is, how does a system of this standard hold up, if the data rate is increased to 25 Gbit/s as required by the data traffic trends? The following sections will present a theoretical BER analysis and experimental test that will tackle this question.

5.2 Pilot Tone Effect on System Performance

A first step consists in defining the PT, its terminology and measurements, to analyze its effects on the performance of the system.
The standard defines two different sets of parameters, depending on the systems state. During the message channel state, there is no transfer of data bits. This state is used during setup and turning. Data bits and PT is only transmitted together during the operation state. The specifications during operation state is shown in Table 5.1.

Table 5.1: Relevant specifications of the PT for the G.698.4 ITU-T Standard

Parameter	**Units**	**Value**
Maximum modulation depth of PT during operation	%	8
Minimum modulation depth of PT during operation	%	5
Maximum frequency of PT	kHz	52.5
Minimum frequency of PT	kHz	47.5

The modulation depth of the PT (m_{pt}) is specified by the standard as, the P2P power excursion of the signal at the PT frequency, divided by twice the average power.

$$m_{pt} = \frac{P_{max} - P_{min}}{P_{max} + P_{min}} \tag{5.1}$$

Measurement of the modulation depth, can be done by receiving the optical signal with a PD, then applying a low pass filter to the electrical signal, with a filter of appropriate cutoff frequency. To measure against the maximum modulation depth, the low pass filter needs a cutoff frequency of 280 kHz, as defined by the standard. To measure for minimum modulation depth, the low pass filter needs a cutoff frequency of 60 kHz. After the low pass filter, the minimum (P_{min}) and maximum (P_{max}) power of the resulting Direct Current (DC) coupled signal can be measured. Once maximum power and minimum power have been measured, Equation 5.1 can be used to find the modulation depth in percentage as $m_{pt} \cdot 100\%$.

5.2.1 Pilot Tone Modulation

The PT can be modulated on to the data signal in two different ways, referred to as multiplicative and additive modulation as in Equation 5.2 and 5.3 respectively.

$$P(t) = \hat{P}[1 + m_{pt} \cdot \cos(2\pi f_{tone} t)] \cdot d(t) \tag{5.2}$$

$$P(t) = \hat{P}[d(t) + m_{pt} \cdot \cos(2\pi f_{tone} t)] \tag{5.3}$$

The difference between the two methods is hinted in the names. In one method the PT gets multiplied to the data signal (Equation 5.2) and in the other method the PT gets added to the data signal (Equation 5.3). In Equation 5.2 and 5.3, $P(t)$ is the time dependent power variation. $\hat{P}$ is the unmodulated optical signal power. f_{tone} is the PT frequency in Hz. t is time and $d(t)$ is the data at time t.
From a receiver perspective there is a large difference between the two methods. In the additive modulation (Equation 5.3), the PT can be filtered away from the data signal using a high pass filter with a cutoff larger than f_{tone}. In the multiplicative modulation (Equation 5.2) the mixing by multiplication produces a data signal where the PT is present in the whole spectrum, thus it cannot be filter away.
The PT modulation method is dependent on how the data and PT are implemented physically in the transmitter.

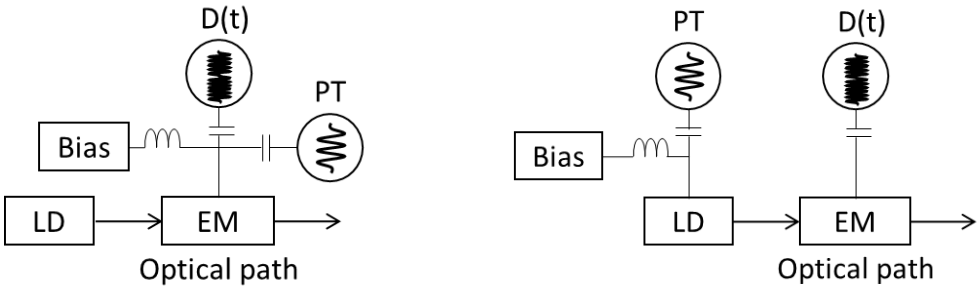

(a) Additive PT modulation, using a LD and an EM

(b) Multiplicative PT modulation, using a LD and an EM

Figure 5.1: Different PT modulation methods using the same system components

In Figure 5.1 the two main methods for additive and multiplicative PT modulation are shown, using an External Modulator (EM). In the additive PT modulation case (Figure 5.1a) the data signal, PT signal and signal bias are added electrically then fed to an EM that modulates of the LD CW output. In the multiplicative PT case (Figure 5.1b) the LD driving bias is combined with the slow moving PT signal such that the optical output is no long just a CW, but a signal. The data signal is still fed to the EM and as such the EM is optically modulating the PT with the data signal, creating a multiplication.
The PT modulation acts as extra added noise onto the transmitted signal. As such the BER theory form chapter 2 can be extended to include PT modulation.

Using Equation 5.3 or 5.2 directly by substituting for the $I'th$ signal level, the time resolved PT effected BER would be obtained. Now since the PT is a sinusoidal tone, each signal level will experience a high and a low point during a full period of the tone as seen from Figure 5.2.

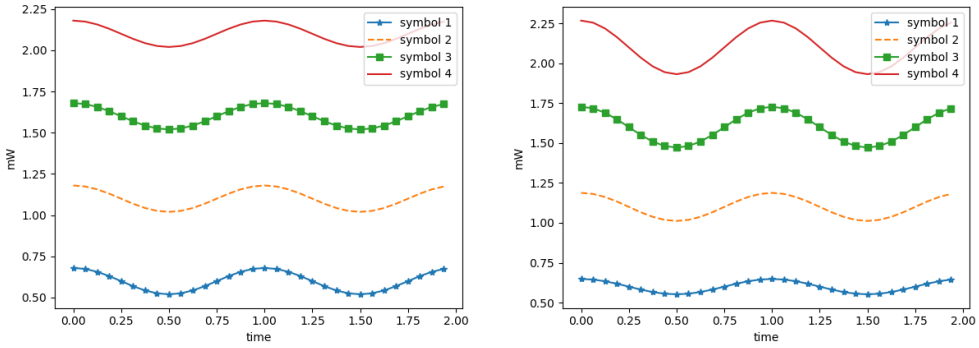

(a) Additive levels (b) Multiplicative levels

Figure 5.2: intensity levels effected by PT modulation

In Figure 5.2a the signal level affected by additive PT modulation are seen. For the additive PT modulation each signal level is affected by an equal amount, resulting in each signal level is showing the same swing in optical power. From Figure 5.2b the Multiplicative modulation are seen. It is clearly observed that the effect of the multiplicative PT on the signal levels is not equal. The swing is increasing with the increased optical power of the given signal level. From the power swing seen in Figure 5.2, it is clear that these fluctuations will show as an offset to the mean of the Gaussian distributions, used to describe the noise affected probability distributions in Equation 2.15, 2.22 and 2.33.

5.2.2 Theoretical BER Impairments

By inserting the power fluctuation from Equation 5.2 and 5.3 into the theoretical BERs in Equation 2.15, 2.22 and 2.33, the PT affected BERs for the different modulation formats can be obtained. The result is time resolved BER formulas that allow for BER to be calculated based on the PT time variation. To numerically evaluate the resulting BER expression, the time dependency needs to be removed. According to an analysis of subcarrier overmodulation [47], the exact error probability for the combined effects of the sinusoidal and the transmitted signal is found by convolving the Gaussian approximated probability distribution, for a given signal symbol, with the probability distribution for the sinusoidal. This results in a complex expression which can be approximated by applying stationary values for the sinusoids maximum and minimum value, whichever is closest to the threshold.

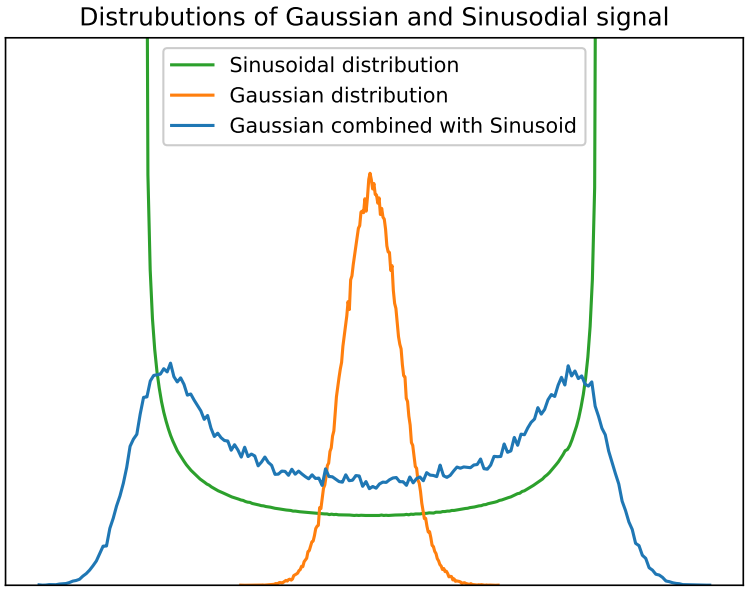

Figure 5.3: Probability distribution for a sinusoidal signal, a Gaussian signal and the combination of the two.

As seen from Figure 5.3, an estimation of the tail-ends to the combined Gaussian and sinusoid distribution, can be obtained from the Gaussian distributions tail-ends. This is done by moving the mean value of the Gaussian distribution, to the maximum and minimum value of the sinusoid function. This approximation is based on the Gaussian tendency of the tails on the combined Gaussian and sinusoid distribution. As explained in [47] the approximation is over estimating the BER, making it worse than it actual is. This is because, the peaks of the combined probability distributions are not located exactly at the minimum and maximum values of the sinusoid.
Using this approximation, it is possible to get rid of the time dependency of the PT variating average signal values. The exact calculation can be seen from Appendix A. It is seen from Equation 5.2 and 5.3 that $P(t)$ follows the same cosine function, which by definition has a maximum swing between -1 and 1. The worst case BER is given when the fluctuation of the signal level is closer to a threshold value. This happens at the peak value of the PT fluctuation. As such it is reasonable to set $cos(2\pi f_{tone}(t)) = -1$ in Equation 5.2 and 5.3. For ease of calculation $\hat{P}$ is also evaluated to 1. Equation 5.2 and 5.3 can be rewritten into:

$$P_k = I_k - m_{pt} * I_k \tag{5.4}$$

$$P_k = I_k - m_{pt} \tag{5.5}$$

In Equation 5.4 and 5.5, The data at time t $(d(t))$ has been replaced with the average signal value I for the k^{th} symbol where $k \in \{0, 1, 2, 3\}$. This allow calculation of the

average stationary signal value P_k for the k^{th} symbol influenced by multiplicative or additive PT modulation.

5.2.2.1 BER for NRZ affected by PT modulation

Equation 5.2 can be used in combination with Equation 2.15 to give a general expression for NRZ when combined with multiplicative PT modulation.

$$BER_{NRZ_M} = \frac{1}{4}\left[erfc\left(\frac{I_1 - m \cdot I_1 - I_{1th}}{\sigma_1\sqrt{2}}\right) + erfc\left(\frac{I_{1th} - I_0 - m \cdot I_0}{\sigma_0\sqrt{2}}\right)\right] \tag{5.6}$$

For additive PT modulation, Equation 5.3 is substituted for the average signal values in Equation 2.15.

$$BER_{NRZ_A} = \frac{1}{4}\left[erfc\left(\frac{I_1 - m - I_{1th}}{\sigma_1\sqrt{2}}\right) + erfc\left(\frac{I_{1th} - I_0 - m}{\sigma_0\sqrt{2}}\right)\right] \tag{5.7}$$

5.2.2.2 BER for duobinary affected by PT modulation

Using Equation 5.2 in combination with Equation 2.22 to give a general expression for duobinary when combined with multiplicative PT modulation.

$$\begin{aligned} BER_{duobinary_M} = {} & \frac{1}{4}\left[erfc\left(\frac{I_1 - m \cdot I_1 - I_{1th}}{\sigma_1\sqrt{2}}\right) + erfc\left(\frac{I_{2th} - I_1 - m \cdot I_1}{\sigma_1\sqrt{2}}\right)\right] \\ & + \frac{1}{8}\left[erfc\left(\frac{I_{1th} - I_0 - m \cdot I_0}{\sigma_0\sqrt{2}}\right) + erfc\left(\frac{I_2 - m \cdot I_2 - I_{2th}}{\sigma_2\sqrt{2}}\right)\right. \\ & \left. - erfc\left(\frac{I_{2th} - I_0 - m \cdot I_0}{\sigma_0\sqrt{2}}\right) - erfc\left(\frac{I_2 - m \cdot I_2 - I_{1th}}{\sigma_2\sqrt{2}}\right)\right] \end{aligned} \tag{5.8}$$

The BER affected by additive PT modulation can be expressed by substituting Equation 5.3 for the average signal values in Equation 2.22.

$$\begin{aligned} BER_{duobinary_A} = {} & \frac{1}{4}\left[erfc\left(\frac{I_1 - m - I_{1th}}{\sigma_1\sqrt{2}}\right) + erfc\left(\frac{I_{2th} - I_1 - m}{\sigma_1\sqrt{2}}\right)\right] \\ & + \frac{1}{8}\left[erfc\left(\frac{I_{1th} - I_0 - m}{\sigma_0\sqrt{2}}\right) + erfc\left(\frac{I_2 - m - I_{2th}}{\sigma_2\sqrt{2}}\right)\right. \\ & \left. - erfc\left(\frac{I_{2th} - I_0 - m}{\sigma_0\sqrt{2}}\right) - erfc\left(\frac{I_2 - m - I_{1th}}{\sigma_2\sqrt{2}}\right)\right] \end{aligned} \tag{5.9}$$

5.2.2.3 BER for PAM4 affected by PT modulation

Lastly Equation 5.2 can be used in combination with Equation 2.33 to give a general expression for duobinary when combined with multiplicative PT modulation.

$$\begin{aligned} BER_{PAM4_M} = \frac{1}{16}\Bigg[& erfc\left(\frac{I_0 - m\cdot I_0 - I_{2th}}{\sigma_0\sqrt{2}}\right) + erfc\left(\frac{I_0 - m\cdot I_0 - I_{1th}}{\sigma_0\sqrt{2}}\right) \\ & + erfc\left(\frac{I_1 - m\cdot I_1 - I_{2th}}{\sigma_1\sqrt{2}}\right) + erfc\left(\frac{I_{1th} - I_1 - m\cdot I_1}{\sigma_1\sqrt{2}}\right) \\ & + erfc\left(\frac{I_1 - m\cdot I_1 - I_{3th}}{\sigma_1\sqrt{2}}\right) + erfc\left(\frac{I_{2th} - I_2 - m\cdot I_2}{\sigma_2\sqrt{2}}\right) \\ & + erfc\left(\frac{I_{1th} - I_2 - m\cdot I_2}{\sigma_2\sqrt{2}}\right) + erfc\left(\frac{I_2 - m\cdot I_2 - I_{3th}}{\sigma_2\sqrt{2}}\right) \\ & + erfc\left(\frac{I_{2th} - I_3 - m\cdot I_3}{\sigma_3\sqrt{2}}\right) + erfc\left(\frac{I_{3th} - I_3 - m\cdot I_3}{\sigma_3\sqrt{2}}\right) \\ & - erfc\left(\frac{I_{3th} - I_0 - m\cdot I_0}{\sigma_0\sqrt{2}}\right) - erfc\left(\frac{I_{1th} - I_3 - m\cdot I_3}{\sigma_3\sqrt{2}}\right)\Bigg] \end{aligned} \tag{5.10}$$

By applying Equation 5.3 as substitute for the average signal values in Equation 2.33, an expression for the BER affected by additive PT modulation can be found.

$$\begin{aligned} BER_{PAM4_A} = \frac{1}{16}\Bigg[& erfc\left(\frac{I_0 - m - I_{2th}}{\sigma_0\sqrt{2}}\right) + erfc\left(\frac{I_0 - m - I_{1th}}{\sigma_0\sqrt{2}}\right) \\ & + erfc\left(\frac{I_1 - m - I_{2th}}{\sigma_1\sqrt{2}}\right) + erfc\left(\frac{I_{1th} - I_1 - m}{\sigma_1\sqrt{2}}\right) \\ & + erfc\left(\frac{I_1 - m - I_{3th}}{\sigma_1\sqrt{2}}\right) + erfc\left(\frac{I_{2th} - I_2 - m}{\sigma_2\sqrt{2}}\right) \\ & + erfc\left(\frac{I_{1th} - I_2 - m}{\sigma_2\sqrt{2}}\right) + erfc\left(\frac{I_2 - m - I_{3th}}{\sigma_2\sqrt{2}}\right) \\ & + erfc\left(\frac{I_{2th} - I_3 - m}{\sigma_3\sqrt{2}}\right) + erfc\left(\frac{I_{3th} - I_3 - m}{\sigma_3\sqrt{2}}\right) \\ & - erfc\left(\frac{I_{3th} - I_0 - m}{\sigma_0\sqrt{2}}\right) - erfc\left(\frac{I_{1th} - I_3 - m}{\sigma_3\sqrt{2}}\right)\Bigg] \end{aligned} \tag{5.11}$$

5.2.2.4 Theoretical PT affected BER Comparison

As in subsection 2.2.4 the above BER expressions, for multiplicative PT modulation, can be compared based on the SNR per bit, when the hamming distances from Table 2.3 are applied, along with the symmetry and noise assumption in Equation 2.35 and 2.34, to Equation 5.6, 5.8, and 5.10. At the same time Equation 2.36 and 2.37 are used to give an expression that can be numerically evaluated for the BER during multiplicative PT

modulation.

$$BER_{NRZ_M} = \frac{1}{2} erfc\left(\sqrt{\frac{3 \cdot log_2(2)}{2^2-1}}\sqrt{SNR} - m\sqrt{\frac{3 \cdot log_2(2)}{2^2-1}}\sqrt{SNR}\right) \tag{5.12}$$

$$\begin{aligned} BER_{duobinary_M} = {} & \frac{1}{2} erfc\left(\sqrt{\frac{3 \cdot log_2(3)}{3^2-1}}\sqrt{SNR}\right) \\ & + \frac{1}{4}\left[erfc\left(\sqrt{\frac{3 \cdot log_2(3)}{3^2-1}}\sqrt{SNR} - 2m\sqrt{\frac{3 \cdot log_2(2)}{2^2-1}}\sqrt{SNR}\right)\right. \\ & \left. -erfc\left(3\sqrt{\frac{3 \cdot log_2(3)}{3^2-1}}\sqrt{SNR} - 2m\sqrt{\frac{3 \cdot log_2(3)}{3^2-1}}\sqrt{SNR}\right)\right] \end{aligned} \tag{5.13}$$

$$\begin{aligned} BER_{PAM4_M} = {} & \frac{1}{8}\left[erfc\left(-3m\sqrt{\frac{3 \cdot log_2(4)}{4^2-1}}\sqrt{SNR} + 3\sqrt{\frac{3 \cdot log_2(4)}{4^2-1}}\sqrt{SNR}\right)\right. \\ & + erfc\left(-3m\sqrt{\frac{3 \cdot log_2(4)}{4^2-1}}\sqrt{SNR} + \sqrt{\frac{3 \cdot log_2(4)}{4^2-1}}\sqrt{SNR}\right) \\ & - erfc\left(-3m\sqrt{\frac{3 \cdot log_2(4)}{4^2-1}}\sqrt{SNR} + 5\sqrt{\frac{3 \cdot log_2(4)}{4^2-1}}\sqrt{SNR}\right) \\ & + erfc\left(-m\sqrt{\frac{3 \cdot log_2(4)}{4^2-1}}\sqrt{SNR} + \sqrt{\frac{3 \cdot log_2(4)}{4^2-1}}\sqrt{SNR}\right) \\ & \left. + erfc\left(-m\sqrt{\frac{3 \cdot log_2(4)}{4^2-1}}\sqrt{SNR} + 3\sqrt{\frac{3 \cdot log_2(4)}{4^2-1}}\sqrt{SNR}\right)\right] \\ & + \frac{1}{16}\left[erfc\left(m\sqrt{\frac{3 \cdot log_2(4)}{4^2-1}}\sqrt{SNR} + 3\sqrt{\frac{3 \cdot log_2(4)}{4^2-1}}\sqrt{SNR}\right)\right. \\ & \left. + erfc\left(m\sqrt{\frac{3 \cdot log_2(4)}{4^2-1}}\sqrt{SNR} + \sqrt{\frac{3 \cdot log_2(4)}{4^2-1}}\sqrt{SNR}\right)\right] \end{aligned} \tag{5.14}$$

The three modulation formats combined with multiplicative PT modulation is expressed as function of SNR per bit, and can be compared as such.

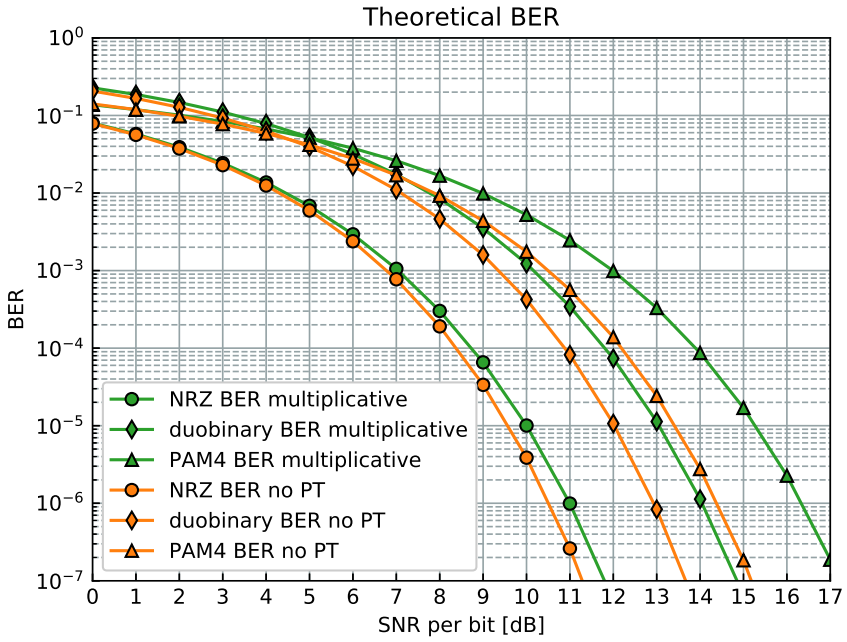

Figure 5.4: Comparison of theoretical BER as function of SNR per bit, between NRZ, duobinary and PAM4 with multiplicative PT modulation.

From Figure 5.4 it can be observed that there is an increase in the penalty from the multiplicative PT modulation with signal intensity levels. Also observed is, that at higher SNR per bit, the penalty increases. This effect stems from the multiplicative nature of the PT modulation, where the increase in signal power multiplies with the effect from the PT.

By substituting the hamming distances from Table 2.3, and the symmetry and noise assumption from Equation 2.35 and 2.34, into Equation 5.7, 5.9, and 5.11. By also utilizing Equation 2.36 and 2.37 an expression, which can be numerically evaluated, for the BER during additive PT modulation is found.

$$BER_{NRZ_A} = \frac{1}{4}\left[erfc\left(\sqrt{\frac{3\cdot log_2(2)}{2^2-1}}\sqrt{SNR} - \frac{m}{\sqrt{N_0}}\right) + erfc\left(\sqrt{\frac{3\cdot log_2(2)}{2^2-1}}\sqrt{SNR} + \frac{m}{\sqrt{N_0}}\right)\right] \tag{5.15}$$

$$
\begin{aligned}
BER_{duobinary_A} = \frac{3}{8}\Bigg[& erfc\left(\sqrt{\frac{3\cdot log_2(3)}{3^2-1}}\sqrt{SNR} - \frac{m}{\sqrt{N_0}}\right) \\
& + erfc\left(\sqrt{\frac{3\cdot log_2(3)}{3^2-1}}\sqrt{SNR} + \frac{m}{\sqrt{N_0}}\right)\Bigg] \\
& + \frac{1}{8}\Bigg[-erfc\left(3\sqrt{\frac{3\cdot log_2(3)}{3^2-1}}\sqrt{SNR} + \frac{m}{\sqrt{N_0}}\right) \\
& - erfc\left(3\sqrt{\frac{3\cdot log_2(3)}{3^2-1}}\sqrt{SNR} - \frac{m}{\sqrt{N_0}}\right)\Bigg]
\end{aligned}
\tag{5.16}
$$

$$
\begin{aligned}
BER_{PAM4_A} = \frac{1}{8}\Bigg[& erfc\left(-3\sqrt{\frac{3\cdot log_2(4)}{4^2-1}}\sqrt{SNR} - \frac{m}{\sqrt{N_0}}\right) \\
& + erfc\left(\frac{m}{\sqrt{N_0}} - 3\sqrt{\frac{3\cdot log_2(4)}{4^2-1}}\sqrt{SNR}\right)\Bigg] \\
& + \frac{3}{16}\Bigg[erfc\left(3\sqrt{\frac{3\cdot log_2(4)}{4^2-1}}\sqrt{SNR} - \frac{m}{\sqrt{N_0}}\right) \\
& + erfc\left(\frac{m}{\sqrt{N_0}} - \sqrt{\frac{3\cdot log_2(4)}{4^2-1}}\sqrt{SNR}\right)\Bigg] \\
& - \frac{1}{16}\Bigg[erfc\left(-5\sqrt{\frac{3\cdot log_2(4)}{4^2-1}}\sqrt{SNR} - \frac{m}{\sqrt{N_0}}\right) \\
& - erfc\left(\frac{m}{\sqrt{N_0}} - 5\sqrt{\frac{3\cdot log_2(4)}{4^2-1}}\sqrt{SNR}\right)\Bigg]
\end{aligned}
\tag{5.17}
$$

From the BER expressions for the additive PT modulation, it is clear that they depend on the noise N_0. This value has been fitted from the previous theoretical results to be $N_0 = -21\,\mathrm{dB}$. The three modulation formats can be evaluated as function of SNR per bit.

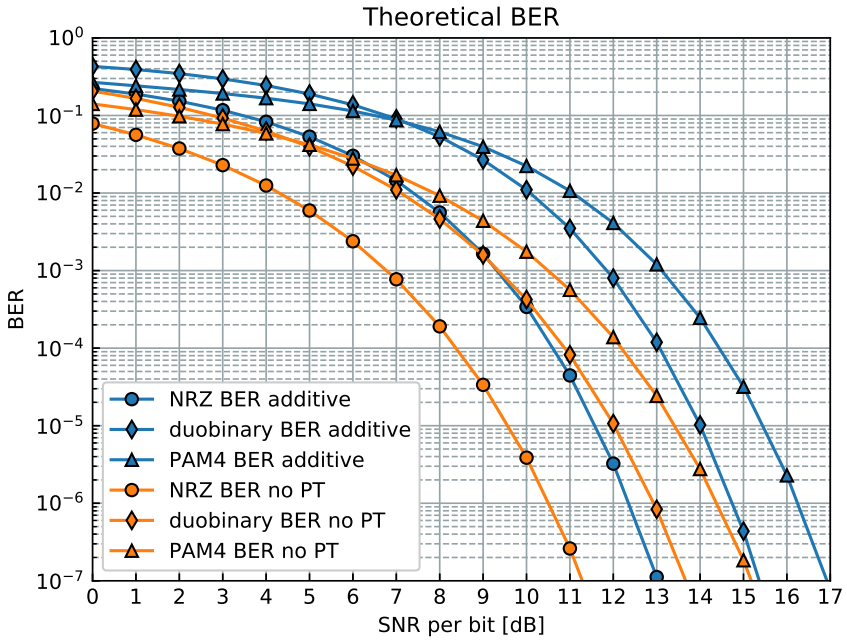

Figure 5.5: Comparison of theoretical BER as function of SNR per bit, between NRZ, duobinary and PAM4 with additive PT modulation.

From Figure 5.5 a complete shift of the BER curves can be observed. Adding the PT to the modulation formats induces a fixed penalty, which is in line with the addition of extra PT noise to all intensity levels of the signal. It might be an extreme penalty, due to the fitted value of N_0 or the over estimation of the Gaussian distributions mean value as mentioned before.

5.3 Experimental Work

The experiment presented is based on additive PT modulation only, due to a limit in available LDs sources. The bias current of the LD used in the experiments is not modifiable, because the LD is part of a larger rack mounted CW laser bank.

Just as in chapter 4 this section presents multiple transmissions of the different modulation formats on the same experimental setup.

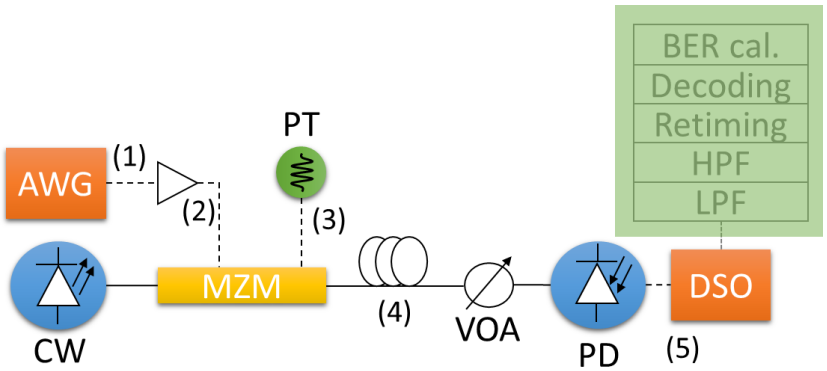

Figure 5.6: Experimental setup used for testing PT modulation together with multilevel signals.

The experimental setup is seen from Figure 5.6. The modulation formats; NRZ, duobinary and PAM4 are created in python code and transmitted with a 50 GSa/s AWG (1). The NRZ is created by transmitting a PRBS7 at 25 Gbaud. The same PRBS7 is coded as in Equation 2.4, creating the duobinary modulation to be transmitted. Finally PAM4 is created by gray code mapping pairs of bits from the PRBS7. The transmission speed in the case of PAM4 is decreased to 12.5 Gbaud. As such, each of the modulation formats produce a net bit rate of 25 Gbit/s. An electrical amplifier is used to fit the signals P2P power within the linear part of the power transfer function of the intensity March Zehnder Modulator (MZM) (2). The 48 kHz PT is created from a low frequency AWG acting as a tone generator. The PT is applied to the MZM bias port (3). In this configuration, the DC offset determines the MZM bias point and the combination of the bias and PT amplitude determines the modulation depth of the PT. This complicates setting the PT modulation depth at 8%. For this experiment the modulation was adjusted to 8% through a series of B2B transmission, each time measuring the depth as describes in Equation 5.1. As briefly mentioned the optical source for the MZM is a CW from a laser bank. The CW laser is equipped with a polarization maintaining connector. Connecting the CW to the MZM with a polarization maintaining fiber patch cord, eliminates the need for a polarization controller, and thus saves some intrinsic losses. The optical output of the MZM is launched into the transmission fiber (4). The fiber consists of SSMF with the lengths of B2B(0 km), and 20 km, following the specifications of G.698.4. A VOA resides inside an optical network coupler with monitoring and attenuation features. This enables the possibility of attenuating the signal, while also measuring the output power of the coupler, resulting in a measurement of the optical input power to the PD. The PD has a BW of 50 GHz and is very linear, because is does not contain a transimpedance amplifier. Therefore the PD requires quite high optical input power (−12 dBm to 2 dBm) and the equivalent electrical output power is very limited. The low electrical output is handled by connecting the PD directly to the DSO (5) used for storage and capturing of data. The DSO operates at 80 GSa/s and has a BW of 28 GHz. Important for this experiment, is the number of sample points stored with the DSO. Since the DSO also captures the slow varying PT, the number of

sample points dictates how many periods of the PT is captured. There is a trade-off between data processing speed and PT periods. A total of $4e^6$ sample points per data trace are stored. This results in $4e6/(80e^9/48e^3) = 2.4$ PT periods. The lowest BER that can be measured, assuming 1 bit error, is $1/(4e^6/(80e^9/25e^9)) = 8e^{-7}$. The DSP is done offline, and is kept as simple as possible; retiming, decoding and BER calculation based on bit by bit comparison.

5.3.1 Simulation of a Dynamic Receiver

As mentioned in the previous section, this experiment is limited to additive PT modulation, and therefore the PT can be filtered away from the received signal. In the case of multiplicative modulation, the PT cannot be filtered without causing a signal deformation [48]. As discussed from Figure 5.2b, the variations of PT is different for each intensity level. To eliminate the effect of the PT a dynamic receiver is proposed. The dynamics of the receiver lies in the ability to follow the PT and adjust the receiver thresholds accordingly. This is simulated in DSP by cutting up the stored signal traces, into smaller parts. Then the thresholds are calculated and the signal is evaluated against these thresholds for each part. This will make the receiver DSP act in a dynamic way. A requirement for the DSP demodulator is that each trace part must contain at least 3 full PRBS7 sequence.

PRBS7 is chosen because it is shorter and therefore the trace can be divided into very small parts. This increases the dynamics of the receiver. The dynamics of the receiver is defined as in Equation 5.18.

$$N_p = \left\lfloor \frac{N_{tp}}{(N_{ss} \cdot l_{PRBS}) \cdot 3} \right\rfloor \tag{5.18}$$

Where N_p is the number of parts that the trace should be split into. N_{tp} is the number of points in a stored trace ($4e^6$). N_{ss} is the number of samples per symbols, which is 3.2 for NRZ and duobinary and 6.4 for PAM4. Lastly l_{PRBS} is the length of transmitted PRBS, in this case $2^7 - 1 = 127$.
The maximum number of N_p is defined for PAM4 as 1640 parts. For NRZ and duobinary N_p is twice that of PAM4 equal to 3280 parts. This insures 3 PRBSs in each signal part demodulated. Of course the minimal number of parts is $N_p = 1$ but this represents a non-dynamic receiver. Instead $N_p = 10$ was selected to represent the minimal dynamic receiver.

5.3.2 Experimental Results

This section presents the results from transmitting NRZ, duobinary, and PAM4 with and without additive PT modulation. The results are divided into transmission lengths, and the result/test of the dynamic receiver is presented as minimal and maximal, which refers to the minimal and maximal value of N_p. It is important to emphasize that for

minimal and maximal results, the same traces are used, but the receiver DSP structure is different between the two.

5.3.2.1 B2B Results

The BER curves for NRZ, duobinary, and PAM4 when transmitted in the B2B case, is seen from Figure 5.7, 5.8, and 5.9.

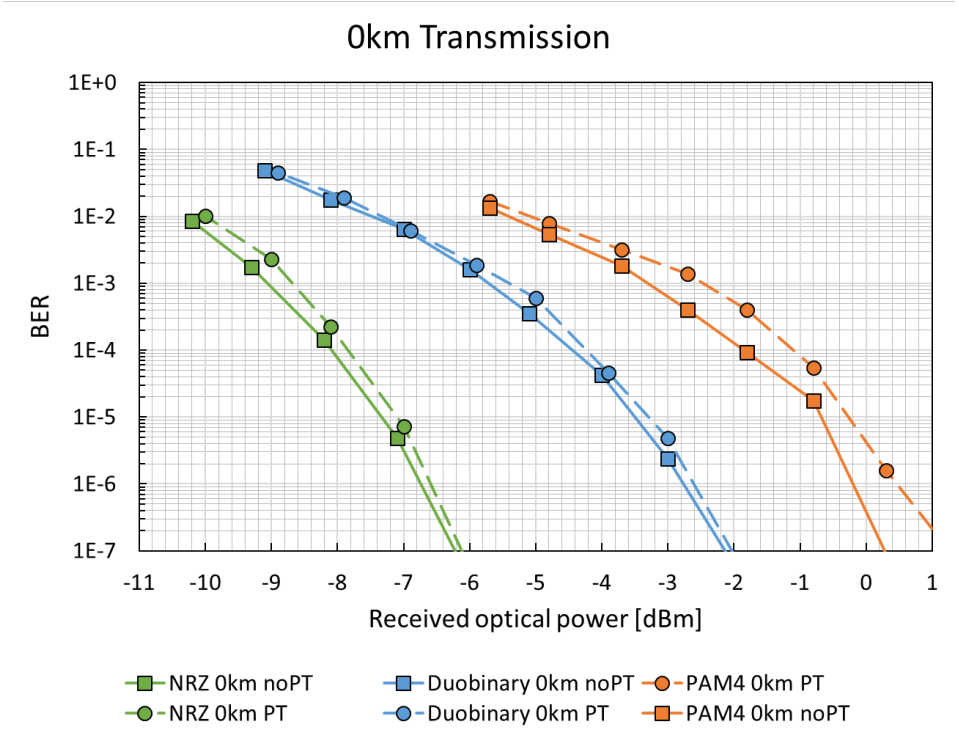

Figure 5.7: Resulting BER from transmitting NRZ, duobinary, PAM4 with and without PT in the B2B case with a standard receiver.

The BER curves seen in Figure 5.7 is the most basic of transmission on the system setup. Observed from the curves, is a clear distinction between the curves of NRZ, duobinary and PAM4. The performance for all modulation formats under test, reaches a BER below 10^{-5} in this B2B case. It is seen that the lowest received power measured is -10 dBm, which is duo to the PD, which does not include a transimpedance amplifier, and the PD requires high optical input power. In this simple B2B case the performance without the PT is seen superior for all modulations formats, but the difference from transmission with and without PT is very small. The difference is a maximum of 1 dB for PAM4 around $4 \cdot 10^{-4}$. Looking at the difference between with and without PT for NRZ and duobinary, the difference is less than 0.4 dB, which is hard to blame solely on the affecting PT.

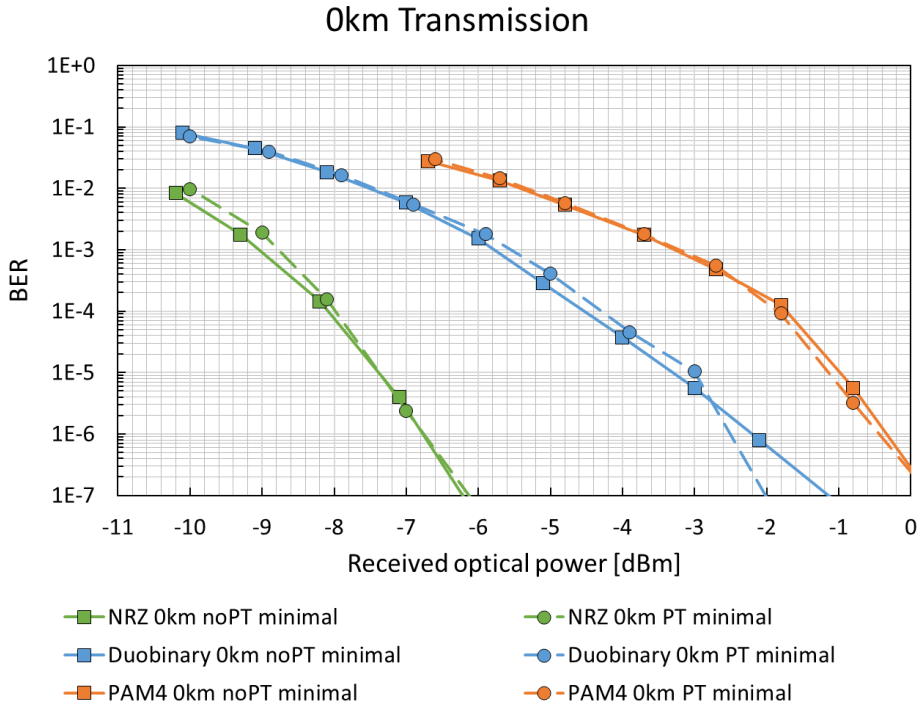

Figure 5.8: Resulting BER from transmitting NRZ, duobinary, PAM4 with and without PT in the B2B case using the minimal dynamic receiver DSP.

The results from demodulation the B2B traces with the minimal dynamic receiver are seen from Figure 5.8. At first glance, the difference between with and without PT, from the results in Figure 5.7 have been eliminated. Whether the difference is caused by the PT is still not clear. Both with and without PT perform almost identically. Most of the measurement points, shows a better performance then with the standard receiver DSP. The minimal receiver is able to reach at a BER of about $2.4 \cdot 10^{-6}$ at a received power of $-7\,\text{dBm}$ for NRZ. For duobinary it is able to reach a BER of about $8 \cdot 10^{-7}$ at a high received power of $-2\,\text{dBm}$. For PAM4 it is able to reach a BER at about $3.2 \cdot 10^{-6}$ for a received power of approximately $-1\,\text{dBm}$. These results shows slightly better performance from the minimal receiver than the ordinary receiver DSP, in the case of NRZ and PAM4. The performance is slightly worse for duobinary.

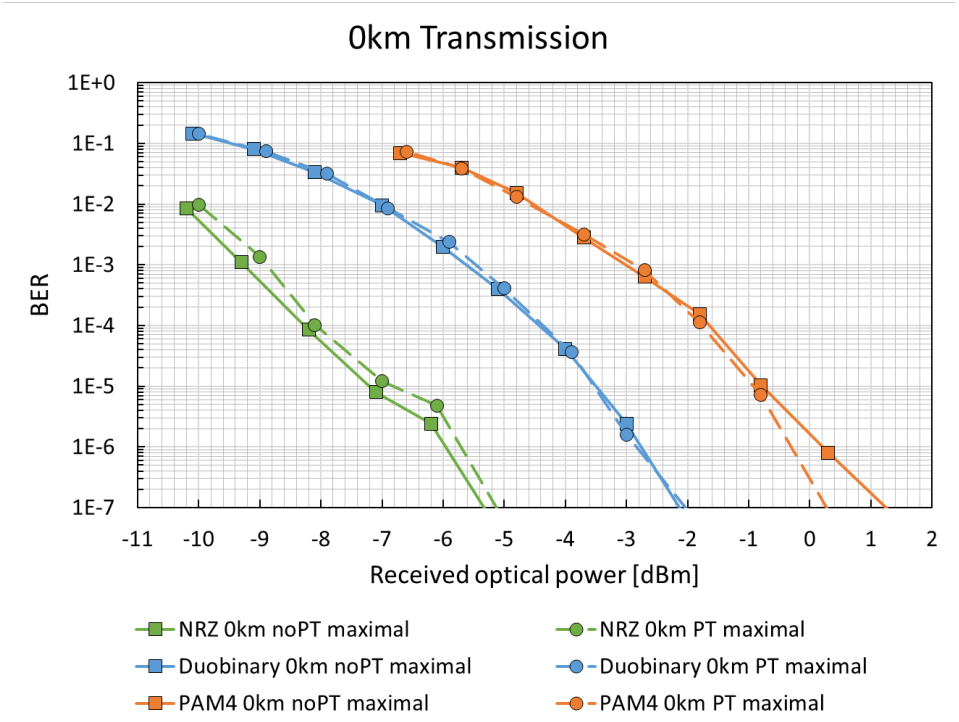

Figure 5.9: Resulting BER from transmitting NRZ, duobinary, with and without PT in the B2B case using the maximal dynamic receiver DSP.

The results from using the maximal receiver to demodulate the B2B traces are seen in Figure 5.9. Is it clear from the duobinary and PAM4 BER curves, that the dynamic receiver is eliminating some small amount of impairment from the traces. A similar performance is obtained for both duobinary and PAM4 with and without PT. A difference is still observed between the two NRZ curves. The performance for NRZ with and without PT is approximately 0.5 dBm better with the standard non-dynamic receiver DSP than the maximal dynamic one. Compared to the minimal receiver DSP performance, the maximal receiver performs better for duobinary and similar for PAM4. Reaching a BER of $1.6 \cdot 10^{-6}$ for duobinary and $8 \cdot 10^{-7}$ for PAM4 at a received power of -3 dBm and 0.5 dBm respectively. This corresponds to a 1 dB improvement for duobinary. For NRZ, the maximal receiver reaches roughly the same BER as the minimal receiver ($2.4 \cdot 10^{-6}$), but at the cost of 1 dB received power penalty.

5.3.2.2 20 km Transmission Results

The BER curves for NRZ, duobinary, and PAM4 when transmitted over 20 km, can be seen from Figure 5.10, 5.11.

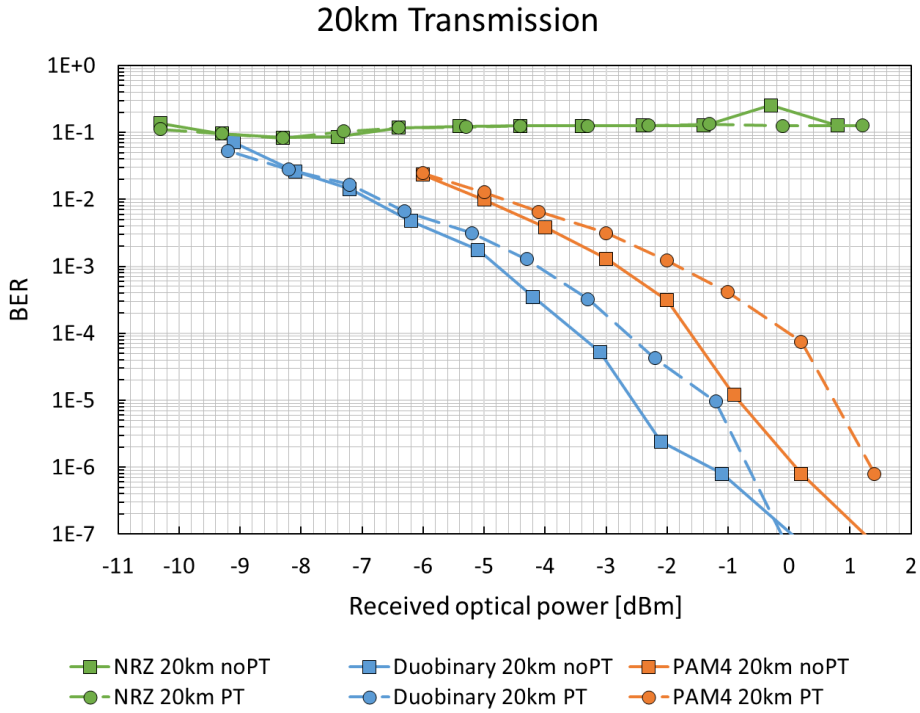

Figure 5.10: Resulting BER from transmitting NRZ, duobinary, PAM4 with and without PT over 20 km SSMF, using a standard receiver DSP.

The resulting BER curves from demodulating the stored 20 km transmission traces with the non-dynamic receiver DSP are shown in Figure 5.10. The first thing to notice is that NRZ at 25 Gbit/s over 20 km of SSMF is not receivable. The effects of fiber dispersion are too large for reliable transmission. In the case of duobinary and PAM4 the difference between with and without PT is much more distinct when transmitting over 20 km of SSMF. This is clearly shown by the penalty effect ot transmission with the PT, which maximizes to almost 2 dB for PAM4 at a BER of $7.5 \cdot 10^{-5}$ approximately. This is in agreement with the theory in subsubsection 5.2.2.4 where it was shown that modulation formats with more intensity levels preforms worse for a given SNR. As described in subsection 5.2.1 the PT modulation can be viewed as extra added noise. Therefore it should have a greater effect on modulation formats with a high number of intensity levels. The penalty to received optical power from transmitting over 20 km of SSMF seems quite low. This is because the optical input power to the PD was maximized with the VOA in Figure 5.6.

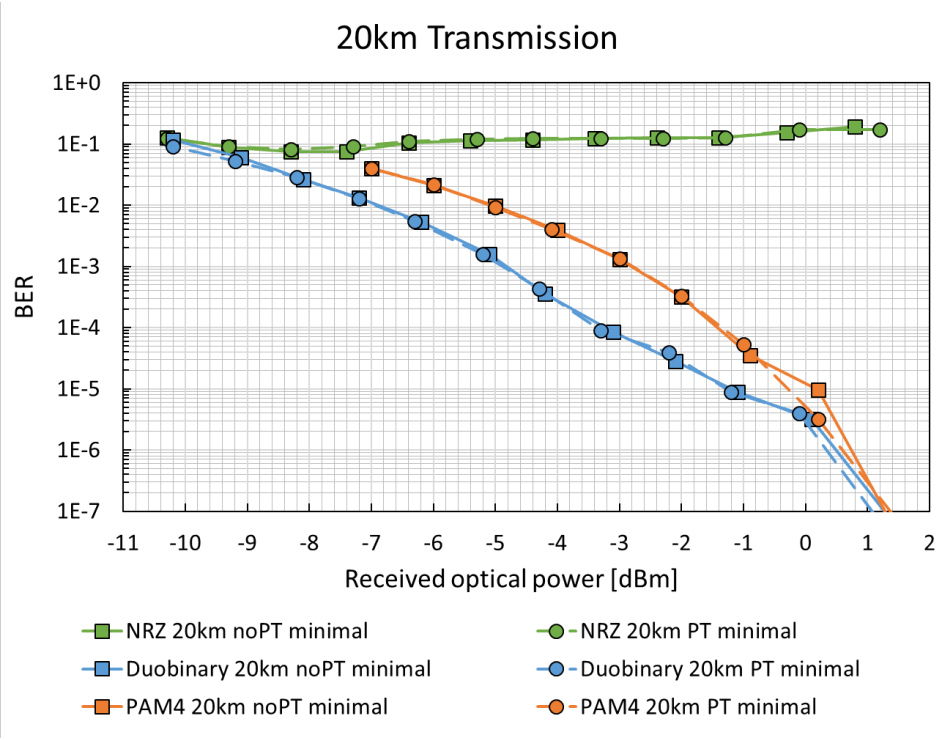

Figure 5.11: Resulting BER from transmitting NRZ, duobinary, PAM4 with and without PT over 20 km SSMF, using a minimal dynamic receiver.

The results from demodulating the 20 km transmission traces, using the minimal dynamic receiver DSP, is seen from the BER curves in Figure 5.11. As in the B2B scenario, the effects of the PT are removed by the dynamic receiver, and the performance with and without PT are now similar. When compared to demodulation with the standard receiver DSP, performance is now a little mixed. For duobinary, the BER curves of the minimal receiver, follows that of the standard non-dynamic duobinary BER curve with PT in Figure 5.10. This performance is worse than the standard non-dynamic receiver without the PT. This was not the expected result, as the results from the B2B case showed better performance when the demodulation was done with the minimal receiver. For PAM4, the BER curve resulting from demodulation with the minimal receiver DSP, lies some what between the BER curves for PAM4 when demodulated with the non-dynamic standard receiver DSP. Some of the PT modulation penalty effects have been removed from the trace, but performance is best when no PT modulation is transmitted and the receiver DSP is non-dynamic.

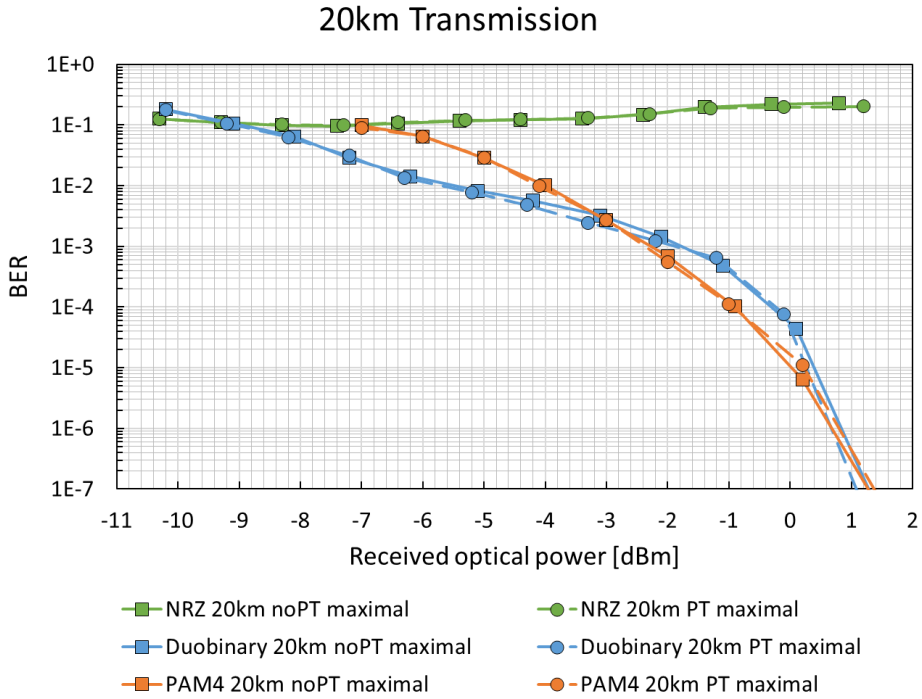

Figure 5.12: Resulting BER from transmitting NRZ, duobinary, PAM4 with and without PT over 20 km SSMF, using a maximal dynamic receiver.

The resulting BER curves from the maximal dynamic receiver DSP demodulation is seen from Figure 5.12. The difference between with and without PT is once again eliminated by the dynamic receiver DSP, and the performance is similar. From the BER curves of duobinary modulation it can be seen that the demodulation is unstable. The curve almost flat-lines between a BER of 10^{-2}and10^{-3}. Staying at this BER level for -6 dBm to -2 dBm of received optical power, before starting to drop below a BER of 10^{-6} at a received power of 0.5 dBm. In the range between -2 dBm to 0.5 dBm of received optical power, the performance of duobinary is worse than PAM4, which is not in agreement with the theory of subsection 5.2.1, thus the instability. The curve for PAM4 shows a similar or better performance than duobinary modulation for BER values from 10^{-3} to 10^{-6}. Worse performance is observed, when comparing the PAM4 maximal demodulation performance to that of the demodulation with the minimal dynamic receiver. The maximal dynamic receiver, reaches a BER of 10^{-4} at -1 dBm of received optical power. Where the minimal dynamic receiver, reaches a BER of approximately $5.5 \cdot 10^{-5}$, Which is a better performance. This is the general trend for all measurement points on the PAM4 curve.

5.4 Discussion

The initial work on the next generation PON networks, shows a clear need for moving past NRZ modulation in IM/DD systems transmitting further than 20 km, as this was never successfully achieved. Duobinary and PAM4 transmission holds much greater promise of being the next generation of modulation formats in systems with port agnostics. The penalty effects of the PT modulation seems enhanced when other signal penalties are present, such as fiber loss and dispersion. This is verified both theoretically and experimentally.
Since the penalty effects of multiplicative PT modulation are not easily filterable, a DSP based dynamic receiver was tested. The two different dynamic receivers proves that the penalty effects from the PT modulation can be removed in this way, but the overall performance of the DSP needs improvement. Splitting the traces into too many smaller parts, results in instability for certain measurement points. On the other hand, too few parts, results in an lower performance for the dynamic receiver. More work on the dynamic receiver is needed for optimal performance. Current results shows a mixture of best performance between the maximal and minimal dynamics, depending on fiber length and modulation format. Port agnostics in PON networks, is an interesting topic with many things to consider. The development of a standard similar to G.698.4 with increased transmission speed, poses a renewed focus on valuable engineering problems to solve for future IM/DD networks. As alternative implementations, coherent technologies are continuously developed, and reaching cheaper solutions with better performance. At some point they will merge into the PON networks [49]. This could happen before the problems evolving around port agnostics will be fully solved for IM/DD systems, forcing PON research that favor IM/DD to shift focus to coherent.
The theory developed for multilevel signals combined with PT modulation could use more work. Both through experimental verification, and further development of the additive PT BER estimation, such that the N_0 noise term can be evaluated even better. Also a mathematical expression for the Gaussian mean shift could be developed. This would help to get rid of the overestimation of the theoretical BER model.

CHAPTER 6

Conclusion and outlook

This chapter presents the concluding remarks and discusses the future perspective of partial response modulation formats.

6.1 Summary

Partial response modulation has been implemented and tested in various systems throughout the work of this thesis. It was stated in chapter 2 that duobinary was fairly easy to implement, and this was proven through analog filtering in chapter 3 and later through digital coding in chapter 4 and 5.
The experiments in chapter 3 showed that the traditional 10G PONs, with a transmission over 20 km of SMF fiber, could benefit a lot from duobinary in terms of BW utilization. Even for similar applications that uses PAM4, duobinary excels as an intermediate capacity upgrade. The experiments showed that, if performance close to the FEC limit is acceptable, duobinary can easily be combined with PAM4 to further improve the system. It was shown chapter 4 that duobinary could effectively be used to bridge the capacity gab, that older data center interconnections will face in the future.
The experiments in chapter 4 showed that a 400 km DWDM system based on IM/DD technology could adopt duobinary. Although more investigations in channel interference may be needed to figure out the appropriate WDM grid to be used. 60 Gbaud duobinary transmitted over 320 km performs below the 25% OH FEC limit at a minimum OSNR of 26.5 dB. This stands in contrast to 32 Gbaud PAM4 transmitted over the same physical transport system. For PAM4 the 11% OH FEC limit can be reached at a minimum OSNR of 31.2 dB. Duobinary shows a better sensitivity, but PAM4 has a higher net bit rate. In chapter 5 it was shown that the traditional NRZ, that most PONs are using today, cannot be continued in future PONs, running 25 Gbit/s or faster. Duobinary works well in this scenario and the performance is slightly better then PAM4 for most results.
The experiments in chapter 5 shows that the effects of a low modulation depth PT on duobinary and PAM4, is most evident when other noise sources decreases the overall system SNR. Secondly, at the sacrifice of sensitivity, the PT effects can be negated by using a DSP based dynamic receiver.

Duobinary modulation is a strong contender to PAM4, and from all the results shown in the work of this thesis, apart from the unstable maximal dynamic receiver results

in chapter 5. Duobinary outperforms PAM4 solely because the three levels compared to the four levels. This allows for a better noise tolerance in duobinary transmission. The analog nature of IM/DD technologies and previous system requirements, have made PAM4 the favorite modulation format for future IM/DD systems. This is due to the demodulation process, which is somewhat simpler for PAM4 and have been implemented by analog means. Partial response on the other hand, needs to handle the introduced ISI in the demodulation process. This is most easily done with a modulo operation enabled by DSP. Which is why duobinary is being considered this day of age, where DSP is getting more and more influence in IM/DD systems.

6.2 Outlook

There is no doubt about what the future holds for metro and access, along with data center interconnections. Coherent optics, moves closer and closer to short reach networks. The constrains are lowered and so are the price of components. At some point in the near future, the price of IM/DD optics and coherent optics will be the same. Then it is just a matter of market readiness before the swap from one technology norm to the other happens.
While waiting for coherent optics, the increased amount of DSP, already in optical systems, eases the implementation of partial response modulation. With that state, there will never be a commercial optical system with partial response modulation as the main format. The ease of combining partial response with other modulation formats, will make partial response part of the modulation, but never the end to end format [50], [51]. Partial response will be used as a vendor trick to stall current technology while the market gets ready for the newly developed one.

APPENDIX A

Full Theoretical BER Calculation

BER theory for NRZ:

From Agrawal, Optical Communication Systems, fourth edition p. 162-163:

A sampled signal value I fluctuates from symbol to symbol around two average values for s_1 and s_0 denoted I_1 and I_0. The decision threshold value I_{th} is compared to the sampled value I, if $I > I_{th}$ then s_1 is detected and if $I < I_{th}$ then s_0 is detected. An error occurs if a s_1 is detected for $I < I_{th}$, and if s_0 is detected for $I > I_{th}$.

The error probability can be written as:

$$BER = p(s_1)P(s_0|s_1) + p(s_0)P(s_1|s_0)$$

Where $p(s_1)$ and $p(s_0)$ are the probabilities of receiving s_1 and s_0. $P(s_0|s_1)$ is the probability of deciding s_0 when s_1 is received and $P(s_1|s_0)$ is vice versa. Since s_1 and s_0 is equally likely to occur then $p(s_0) = p(s_1) = \frac{1}{2}$, the error probability becomes:

$$BER = \frac{1}{2}[P(s_0|s_1) + P(s_1|s_0)]$$

It is assumed that the noise affecting I has a Gaussian probability density function with the variance:

$$\sigma^2 = {\sigma_s}^2 + {\sigma_T}^2$$

Where ${\sigma_s}^2$ is the shot noise contribution and ${\sigma_T}^2$ is the thermal noise contribution defined as:

$${\sigma_s}^2 = 2q(I_p + I_d)\Delta f$$

$${\sigma_T}^2 = \left(\frac{4k_B T}{R_L}\right) F_n \Delta f$$

Where F_n represents a factor by which the thermal noise is enhanced by different amplifier in the system via their internal resistors. k_B is the Boltzmann constant. T is the absolute temperature (kelvin). Δf is the effective noise bandwidth of the receiver. q is the electron charge of a photon (constant). I_d is the dark current of the photo diode. I_p is the average current denoted as:

$$I_p = R_d P_{in}$$

Where R_d is the responsivity of the photo diode. P_{in} is incident optical power.

Both the average and variance σ^2 is different for s_0 and s_1, therefor the probabilities $P(s_0|s_1)$ and $P(s_1|s_0)$ are given by:

$$P(s_0|s_1) = \frac{1}{\sigma_1\sqrt{2\pi}}\int_{-\infty}^{I_{th}} \exp\left(-\frac{(I-I_1)^2}{2\sigma_1^2}\right)dI = \frac{1}{2}erfc\left(\frac{I_1 - I_{th}}{\sigma_1\sqrt{2}}\right)$$

$$P(s_1|s_0) = \frac{1}{\sigma_0\sqrt{2\pi}}\int_{I_{th}}^{\infty} \exp\left(-\frac{(I-I_0)^2}{2\sigma_0^2}\right)dI = \frac{1}{2}erfc\left(\frac{I_{th} - I_0}{\sigma_0\sqrt{2}}\right)$$

By substituting the BER becomes:

$$BER = \frac{1}{2}\left[\frac{1}{2}erfc\left(\frac{I_1 - I_{th}}{\sigma_1\sqrt{2}}\right) + \frac{1}{2}erfc\left(\frac{I_{th} - I_0}{\sigma_0\sqrt{2}}\right)\right] = \frac{1}{4}\left[erfc\left(\frac{I_1 - I_{th}}{\sigma_1\sqrt{2}}\right) + erfc\left(\frac{I_{th} - I_0}{\sigma_0\sqrt{2}}\right)\right]$$

BER theory for Duobinary

Duobinary is a 3-level partial response modulation format transmitting the symbols s_0, s_1 and s_2. When encoding the precoded data bits, the current symbol is based on adding the previous precoded bit to the bit to be encoded, hence the partial response.

If 0 is to be encoded and previous precoded bit was 0, then current symbol is s_0=0. $(0 + 0 = 0 = s_0)$
if 0 is to be encoded and previous precoded bit was 1, then current symbol is s_1=1. $(0 + 1 = 1 = s_1)$
if 1 is to be encoded and previous precoded bit was 0, then current symbol is s_1=1. $(1 + 0 = 1 = s_1)$
if 1 is to be encoded and previous precoded bit was 1, then current symbol is s_2=2. $(1 + 1 = 2 = s_2)$

The precoding is done to avoid error propagation by XOR-ing the current data bit with the previous precoded bit, initialized with a 1 bit.

If 0 is to be precoded and previous precoded bit was 0, then the resulting precoded bit is 0. $(0\ XOR\ 0 = 0)$
If 0 is to be precoded and previous precoded bit was 1, then the resulting precoded bit is 1. $(0\ XOR\ 1 = 1)$
If 1 is to be precoded and previous precoded bit was 0, then the resulting precoded bit is 1. $(1\ XOR\ 0 = 0)$
If 1 is to be precoded and previous precoded bit was 1, then the resulting precoded bit is 0. $(1\ XOR\ 1 = 1)$

At the receiver demodulation is done by a simple modulo 2 operation.

If s_2 is received, the data bit is 0. $(s_2 = 2\ mod\ 2 = 0)$
If s_1 is received, the data bit is 1. $(s_1 = 1\ mod\ 2 = 1)$
if s_0 is received, the data bit is 0. $(s_0 = 0\ mod\ 2 = 0)$

From the above operations, we can conclude that at the receiver will always demodulate one bit per symbol. Also, an error in a symbol will only effect one bit, therefor we can evaluate the BER based on the symbol levels, even though there are some intermediate steps in the precoding and encoding.

Working with the average signal levels I_0, I_1 and I_2 for symbols s_0, s_1 and s_2 respectively, and the thresholds I_{1th} and I_{2th}. We have a s_0 if $I < I_{1th}$, a s_1 if $I_{1th} < I < I_{2th}$ and a s_2 if $I > I_{2th}$. An error occurs if s_1 is detected for $I < I_{1th}$ or $I > I_{2th}$ and if s_0 is detected for $I_{1th} < I < I_{2th}$.

For the error probability we have the following:

$$BER = p(s_2)P(s_1|s_2) + p(s_1)P(s_0|s_1) + p(s_1)P(s_2|s_1) + p(s_0)P(s_1|s_0)$$

From the duobinary encoding we have that the $p(s_0) = p(s_2) = \frac{1}{4}$ and $p(s_1) = \frac{1}{2}$.

From this we have the error probability:

$$BER = \frac{1}{4}P(s_1|s_2) + \frac{1}{2}P(s_0|s_1) + \frac{1}{2}P(s_2|s_1) + \frac{1}{4}P(s_1|s_0)$$

the probabilities are given by:

$$P(s_0|s_1) = \frac{1}{\sigma_1\sqrt{2\pi}}\int_{-\infty}^{I_{1th}} \exp\left(-\frac{(I-I_1)^2}{2\sigma_1^2}\right)dI = \frac{1}{2}erfc\left(\frac{I_1 - I_{1th}}{\sigma_1\sqrt{2}}\right)$$

$$\begin{aligned} P(s_1|s_0) &= \frac{1}{\sigma_0\sqrt{2\pi}}\int_{I_{1th}}^{I_{2th}} \exp\left(-\frac{(I-I_0)^2}{2\sigma_0^2}\right)dI \\ &= \frac{1}{\sigma_0\sqrt{2\pi}}\left[\int_{I_{1th}}^{\infty} \exp\left(-\frac{(I-I_0)^2}{2\sigma_0^2}\right)dI - \int_{I_{2th}}^{\infty} \exp\left(-\frac{(I-I_0)^2}{2\sigma_0^2}\right)dI\right] \\ &= \frac{1}{2}\left[erfc\left(\frac{I_{1th} - I_0}{\sigma_0\sqrt{2}}\right) - erfc\left(\frac{I_{2th} - I_0}{\sigma_0\sqrt{2}}\right)\right] \end{aligned}$$

$$\begin{aligned} P(s_1|s_2) &= \frac{1}{\sigma_2\sqrt{2\pi}}\int_{I_{1th}}^{I_{2th}} \exp\left(-\frac{(I-I_2)^2}{2\sigma_2^2}\right)dI \\ &= \frac{1}{\sigma_2\sqrt{2\pi}}\left[\int_{-\infty}^{I_{2th}} \exp\left(-\frac{(I-I_2)^2}{2\sigma_2^2}\right)dI - \int_{-\infty}^{I_{1th}} \exp\left(-\frac{(I-I_2)^2}{2\sigma_2^2}\right)dI\right] \\ &= \frac{1}{2}\left[erfc\left(\frac{I_2 - I_{2th}}{\sigma_2\sqrt{2}}\right) - erfc\left(\frac{I_2 - I_{1th}}{\sigma_2\sqrt{2}}\right)\right] \end{aligned}$$

$$P(s_2|s_1) = \frac{1}{\sigma_1\sqrt{2\pi}}\int_{I_{2th}}^{\infty} \exp\left(-\frac{(I-I_1)^2}{2\sigma_1^2}\right)dI = \frac{1}{2}erfc\left(\frac{I_{2th} - I_1}{\sigma_1\sqrt{2}}\right)$$

We can now substitute into the error probability:

$$\begin{aligned} BER = \frac{1}{8}\left[erfc\left(\frac{I_2 - I_{2th}}{\sigma_2\sqrt{2}}\right) - erfc\left(\frac{I_2 - I_{1th}}{\sigma_2\sqrt{2}}\right)\right] + \frac{1}{4}erfc\left(\frac{I_1 - I_{1th}}{\sigma_1\sqrt{2}}\right) + \frac{1}{4}erfc\left(\frac{I_{2th} - I_1}{\sigma_1\sqrt{2}}\right) \\ + \frac{1}{8}\left[erfc\left(\frac{I_{1th} - I_0}{\sigma_0\sqrt{2}}\right) - erfc\left(\frac{I_{2th} - I_0}{\sigma_0\sqrt{2}}\right)\right] \end{aligned}$$

$$= \frac{1}{4}\left[erfc\left(\frac{I_1 - I_{1th}}{\sigma_1\sqrt{2}}\right) + erfc\left(\frac{I_{2th} - I_1}{\sigma_1\sqrt{2}}\right)\right] + \frac{1}{8}\left[erfc\left(\frac{I_{1th} - I_0}{\sigma_0\sqrt{2}}\right) + erfc\left(\frac{I_2 - I_{2th}}{\sigma_2\sqrt{2}}\right) - erfc\left(\frac{I_{2th} - I_0}{\sigma_0\sqrt{2}}\right) - erfc\left(\frac{I_2 - I_{1th}}{\sigma_2\sqrt{2}}\right)\right]$$

BER theory for PAM4

The BER differs from the SER in that one symbol error might in fact be generating two bit errors. Therefor the BER probabilities are different from the SER in that a division based on bits are done. Assuming gray code encoding as follows.

Data bit 00 is encoded to symbol s_0
Data bit 01 is encoded to symbol s_1
Data bit 11 is encoded to symbol s_2
Data bit 10 is encoded to symbol s_3

We still have 4 symbol levels thus 4 average signal levels I_0, I_1, I_2 and I_3 for symbols s_0, s_1, s_2 and s_3 respectively, and the thresholds I_{1th}, I_{2th} and I_{3th}. We have s_0 if $I < I_{1th}$, s_1 if $I_{1th} < I < I_{2th}$, s_2 if $I_{2th} < I < I_{3th}$, and s_3 if $I > I_{3th}$. An error occurs on the first bit if s_2 or s_3 is detected for $I < I_{1th}$ and if s_2 or s_3 is detected for $I_{1th} < I < I_{2th}$ and if s_0 or s_1 is detected for $I_{2th} < I < I_{3th}$, and finally if s_0 or s_1 for $I > I_{3th}$. We call these class 1 errors. Class 2 errors are errors on the second bits of the symbols, that is; an error occurs on the second bit if s_1 or s_2 is detected for $I < I_{1th}$ and if s_0 or s_3 is detected for $I_{1th} < I < I_{2th}$ and if s_0 or s_3 is detected for $I_{2th} < I < I_{3th}$, and finally if s_1 or s_2 for $I > I_{3th}$. We can now describe the probabilities in terms of symbols while still referring to the BER and not the SER.

$$BER = p(s_0)[P(s_2, s_3|s_0) + P(s_1, s_2|s_0)] + p(s_1)[P(s_2, s_3|s_0) + P(s_0, s_3|s_1)] + p(s_2)[P(s_0, s_1|s_2) + P(s_0, s_3|s_2)] + p(s_3)[P(s_0, s_1|s_3) + P(s_1, s_2|s_3)]$$

From the PAM4 encoding we have the symbol probability $p(s_0) = p(s_1) = p(s_2) = p(s_3) = \frac{1}{4}$ which is still valid but because each symbol has a probability of consisting or either 1 bits or 0 bits or a combination. The total probability is time with 1/2. So $\frac{1}{2} * [p(s_0) = p(s_1) = p(s_2) = p(s_3)] = \frac{1}{4} * \frac{1}{2} = \frac{1}{8}$

$$BER = \frac{1}{8}[P(s_2, s_3|s_0) + P(s_1, s_2|s_0)] + \frac{1}{8}[P(s_2, s_3|s_1) + P(s_0, s_3|s_1)] + \frac{1}{8}[P(s_0, s_1|s_2) + P(s_0, s_3|s_2)] + \frac{1}{8}[P(s_0, s_1|s_3) + P(s_1, s_2|s_3)]$$

Now the probabilities are found by combining the symbol spaces:

$$P(s_2, s_3|s_0) = \frac{1}{\sigma_0\sqrt{2\pi}}\int_{I_{2th}}^{\infty} \exp\left(-\frac{(I - I_0)^2}{2\sigma_0^2}\right) dI = \frac{1}{2} erfc\left(\frac{I_0 - I_{2th}}{\sigma_0\sqrt{2}}\right)$$

$$P(s_1,s_2|s_0)=\frac{1}{\sigma_0\sqrt{2\pi}}\int_{I_{1th}}^{I_{3th}}\exp\left(-\frac{(I-I_0)^2}{2\sigma_0^2}\right)dI=$$
$$=\frac{1}{\sigma_0\sqrt{2\pi}}\left[\int_{I_{1th}}^{I_{\infty}}\exp\left(-\frac{(I-I_0)^2}{2\sigma_0^2}\right)dI-\int_{I_{3th}}^{\infty}\exp\left(-\frac{(I-I_0)^2}{2\sigma_0^2}\right)dI\right]$$
$$=\frac{1}{2}\left[erfc\left(\frac{I_0-I_{1th}}{\sigma_0\sqrt{2}}\right)-erfc\left(\frac{I_0-I_{3th}}{\sigma_0\sqrt{2}}\right)\right]$$
$$P(s_0,s_3|s_1)=\frac{1}{\sigma_0\sqrt{2\pi}}\left[\int_{-\infty}^{I_{1th}}\exp\left(-\frac{(I-I_1)^2}{2\sigma_1^2}\right)dI+\int_{I_{3th}}^{\infty}\exp\left(-\frac{(I-I_1)^2}{2\sigma_1^2}\right)dI\right]$$
$$=\frac{1}{2}\left[erfc\left(\frac{I_{1th}-I_1}{\sigma_1\sqrt{2}}\right)+erfc\left(\frac{I_1-I_{3th}}{\sigma_1\sqrt{2}}\right)\right]$$
$$P(s_2,s_3|s_1)=\frac{1}{\sigma_1\sqrt{2\pi}}\int_{I_{2th}}^{\infty}\exp\left(-\frac{(I-I_1)^2}{2\sigma_1^2}\right)dI=\frac{1}{2}erfc\left(\frac{I_1-I_{2th}}{\sigma_1\sqrt{2}}\right)$$
$$P(s_0,s_1|s_2)=\frac{1}{\sigma_2\sqrt{2\pi}}\int_{-\infty}^{I_{2th}}\exp\left(-\frac{(I-I_2)^2}{2\sigma_2^2}\right)dI=\frac{1}{2}erfc\left(\frac{I_{2th}-I_2}{\sigma_2\sqrt{2}}\right)$$
$$P(s_0,s_3|s_2)=\frac{1}{\sigma_0\sqrt{2\pi}}\left[\int_{-\infty}^{I_{1th}}\exp\left(-\frac{(I-I_2)^2}{2\sigma_2^2}\right)dI+\int_{I_{3th}}^{\infty}\exp\left(-\frac{(I-I_2)^2}{2\sigma_2^2}\right)dI\right]$$
$$=\frac{1}{2}\left[erfc\left(\frac{I_{1th}-I_2}{\sigma_2\sqrt{2}}\right)+erfc\left(\frac{I_2-I_{3th}}{\sigma_2\sqrt{2}}\right)\right]$$
$$P(s_0,s_1|s_3)=\frac{1}{\sigma_3\sqrt{2\pi}}\int_{-\infty}^{I_{2th}}\exp\left(-\frac{(I-I_3)^2}{2\sigma_3^2}\right)dI=\frac{1}{2}erfc\left(\frac{I_{2th}-I_3}{\sigma_3\sqrt{2}}\right)$$
$$P(s_1,s_2|s_3)=\frac{1}{\sigma_3\sqrt{2\pi}}\int_{I_{1th}}^{I_{3th}}\exp\left(-\frac{(I-I_3)^2}{2\sigma_3^2}\right)dI=$$
$$=\frac{1}{\sigma_3\sqrt{2\pi}}\left[\int_{-\infty}^{I_{3th}}\exp\left(-\frac{(I-I_3)^2}{2\sigma_3^2}\right)dI-\int_{-\infty}^{I_{1th}}\exp\left(-\frac{(I-I_3)^2}{2\sigma_3^2}\right)dI\right]$$
$$=\frac{1}{2}\left[erfc\left(\frac{I_{3th}-I_3}{\sigma_3\sqrt{2}}\right)-erfc\left(\frac{I_{1th}-I_3}{\sigma_3\sqrt{2}}\right)\right]$$

We can now substitute the probabilities into the BER formula:

$$BER=\frac{1}{16}erfc\left(\frac{I_0-I_{2th}}{\sigma_0\sqrt{2}}\right)+\frac{1}{16}\left[erfc\left(\frac{I_0-I_{1th}}{\sigma_0\sqrt{2}}\right)-erfc\left(\frac{I_0-I_{3th}}{\sigma_0\sqrt{2}}\right)\right]+\frac{1}{16}erfc\left(\frac{I_1-I_{2th}}{\sigma_1\sqrt{2}}\right)$$
$$+\frac{1}{16}\left[erfc\left(\frac{I_{1th}-I_1}{\sigma_1\sqrt{2}}\right)+erfc\left(\frac{I_1-I_{3th}}{\sigma_1\sqrt{2}}\right)\right]+\frac{1}{16}erfc\left(\frac{I_{2th}-I_2}{\sigma_2\sqrt{2}}\right)$$
$$+\frac{1}{16}\left[erfc\left(\frac{I_{1th}-I_2}{\sigma_2\sqrt{2}}\right)+erfc\left(\frac{I_2-I_{3th}}{\sigma_2\sqrt{2}}\right)\right]+\frac{1}{16}erfc\left(\frac{I_{2th}-I_3}{\sigma_3\sqrt{2}}\right)$$
$$+\frac{1}{16}\left[erfc\left(\frac{I_{3th}-I_3}{\sigma_3\sqrt{2}}\right)-erfc\left(\frac{I_{1th}-I_3}{\sigma_3\sqrt{2}}\right)\right]$$

$$= \frac{1}{16}\left[erfc\left(\frac{I_0 - I_{2th}}{\sigma_0\sqrt{2}}\right) + erfc\left(\frac{I_0 - I_{1th}}{\sigma_0\sqrt{2}}\right) - erfc\left(\frac{I_0 - I_{3th}}{\sigma_0\sqrt{2}}\right) + erfc\left(\frac{I_1 - I_{2th}}{\sigma_1\sqrt{2}}\right) + erfc\left(\frac{I_{1th} - I_1}{\sigma_1\sqrt{2}}\right)\right.$$
$$+ erfc\left(\frac{I_1 - I_{3th}}{\sigma_1\sqrt{2}}\right) + erfc\left(\frac{I_{2th} - I_2}{\sigma_2\sqrt{2}}\right) + erfc\left(\frac{I_{1th} - I_2}{\sigma_2\sqrt{2}}\right) + erfc\left(\frac{I_2 - I_{3th}}{\sigma_2\sqrt{2}}\right)$$
$$\left. + erfc\left(\frac{I_{2th} - I_3}{\sigma_3\sqrt{2}}\right) + erfc\left(\frac{I_{3th} - I_3}{\sigma_3\sqrt{2}}\right) - erfc\left(\frac{I_{1th} - I_3}{\sigma_3\sqrt{2}}\right)\right]$$

Sanity check:

Sanity check NRZ:

Calculating the energy per bit, lets us check the resulting BER up against other theoretical papers.

Applying the hamming distances d in the following manner:

$$I_0 = -d$$

$$I_1 = d$$

$$I_{1th} = 0$$

We assume the signal has symmetry around 0 such that:

$$\int_{-\infty}^{a} \exp(-u^2)\, du = \int_{a}^{\infty} \exp(-u^2)\, du$$

Once we have the hamming distances, we can describe the distance d via the energy per bit E_b by the following:

$$d = \sqrt{\frac{3 \cdot log_2(M) \cdot E_b}{(M^2 - 1)}} = a\sqrt{E_b}$$

Where a is a constant for the level of PAM-M modulation in this case 4.

If we assume that the noise has the same variance for all signal levels, then we have:

$$2\sigma_0^2 = 2\sigma_1^2 = 2\sigma_2^2 = 2\sigma_3^2 = N_0$$

In the combination of the hamming distance as function of energy per bit and the assumption on the noise, we get the following BER probability for NRZ:

$$BER = \frac{1}{4}\left[erfc\left(\frac{I_1 - I_{th}}{\sigma_1\sqrt{2}}\right) + erfc\left(\frac{I_{th} - I_0}{\sigma_0\sqrt{2}}\right)\right] = \frac{1}{4}\left[erfc\left(\frac{d - 0}{\sqrt{N_0}}\right) + erfc\left(\frac{0 - (-d)}{\sqrt{N_0}}\right)\right] = \frac{1}{2}erfc\left(\frac{d}{\sqrt{N_0}}\right)$$

Sanity check Duobinary:

We apply the following hamming distance:

$$I_0 = -2d$$

$$I_1 = 0$$

$$I_2 = 2d$$

$$I_{1th} = -d$$

$$I_{2th} = d$$

Substituting into the error probability for Duobinary and using the same assumptions as in the NRZ case:

$$BER = \frac{1}{4}\left[erfc\left(\frac{0-(-d)}{\sqrt{N_0}}\right) + erfc\left(\frac{d-0}{\sqrt{N_0}}\right)\right] + \frac{1}{8}\left[erfc\left(\frac{-d-(-2d)}{\sqrt{N_0}}\right) + erfc\left(\frac{2d-d}{\sqrt{N_0}}\right) - erfc\left(\frac{d-(-2d)}{\sqrt{N_0}}\right) - erfc\left(\frac{2d-(-d)}{\sqrt{N_0}}\right)\right]$$

$$= \frac{1}{4}\left[erfc\left(\frac{d}{\sqrt{N_0}}\right) + erfc\left(\frac{d}{\sqrt{N_0}}\right)\right] + \frac{1}{8}\left[erfc\left(\frac{d}{\sqrt{N_0}}\right) + erfc\left(\frac{d}{\sqrt{N_0}}\right) - erfc\left(\frac{3d}{\sqrt{N_0}}\right) - erfc\left(\frac{3d}{\sqrt{N_0}}\right)\right]$$

$$= \frac{3}{4}erfc\left(\frac{d}{\sqrt{N_0}}\right) - \frac{1}{4}erfc\left(\frac{3d}{\sqrt{N_0}}\right)$$

Sanity check PAM4:

We apply the hamming distances:

$$I_0 = -3d$$

$$I_1 = -d$$

$$I_2 = d$$

$$I_3 = 3d$$

$$I_{1th} = -2d$$

$$I_{2th} = 0$$

$$I_{3th} = 2d$$

Substituting into the error probability PAM4 in the same manner as with NRZ and duobinary we get:

$$BER = \frac{1}{16}\left[erfc\left(\frac{I_0 - I_{2th}}{\sqrt{N_0}}\right) + erfc\left(\frac{I_0 - I_{1th}}{\sqrt{N_0}}\right) - erfc\left(\frac{I_0 - I_{3th}}{\sqrt{N_0}}\right) + erfc\left(\frac{I_1 - I_{2th}}{\sqrt{N_0}}\right) + erfc\left(\frac{I_{1th} - I_1}{\sqrt{N_0}}\right)\right.$$
$$+ erfc\left(\frac{I_1 - I_{3th}}{\sqrt{N_0}}\right) + erfc\left(\frac{I_{2th} - I_2}{\sqrt{N_0}}\right) + erfc\left(\frac{I_{1th} - I_2}{\sqrt{N_0}}\right) + erfc\left(\frac{I_2 - I_{3th}}{\sqrt{N_0}}\right)$$
$$\left. + erfc\left(\frac{I_{2th} - I_3}{\sqrt{N_0}}\right) + erfc\left(\frac{I_{3th} - I_3}{\sqrt{N_0}}\right) - erfc\left(\frac{I_{1th} - I_3}{\sqrt{N_0}}\right)\right]$$
$$= \frac{1}{16}\left[erfc\left(\frac{-3d - 0}{\sqrt{N_0}}\right) + erfc\left(\frac{-3d - (-2d)}{\sqrt{N_0}}\right) - erfc\left(\frac{-3d - 2d}{\sqrt{N_0}}\right) + erfc\left(\frac{-d - 0}{\sqrt{N_0}}\right)\right.$$
$$+ erfc\left(\frac{(-2d) - (-d)}{\sqrt{N_0}}\right) + erfc\left(\frac{-d - 2d}{\sqrt{N_0}}\right) + erfc\left(\frac{0 - d}{\sqrt{N_0}}\right) + erfc\left(\frac{(-2d) - d}{\sqrt{N_0}}\right)$$
$$\left. + erfc\left(\frac{d - 2d}{\sqrt{N_0}}\right) + erfc\left(\frac{0 - 3d}{\sqrt{N_0}}\right) + erfc\left(\frac{2d - 3d}{\sqrt{N_0}}\right) - erfc\left(\frac{(-2d) - 3d}{\sqrt{N_0}}\right)\right]$$
$$= \frac{1}{16}\left[erfc\left(\frac{-3d}{\sqrt{N_0}}\right) + erfc\left(\frac{-d}{\sqrt{N_0}}\right) - erfc\left(\frac{-5d}{\sqrt{N_0}}\right) + erfc\left(\frac{-d}{\sqrt{N_0}}\right) + erfc\left(\frac{-d}{\sqrt{N_0}}\right) + erfc\left(\frac{-3d}{\sqrt{N_0}}\right)\right.$$
$$\left. + erfc\left(\frac{-d}{\sqrt{N_0}}\right) + erfc\left(\frac{-3d}{\sqrt{N_0}}\right) + erfc\left(\frac{-d}{\sqrt{N_0}}\right) + erfc\left(\frac{-3d}{\sqrt{N_0}}\right) + erfc\left(\frac{-d}{\sqrt{N_0}}\right) - erfc\left(\frac{-5d}{\sqrt{N_0}}\right)\right]$$
$$= \frac{1}{4}erfc\left(\frac{-3d}{\sqrt{N_0}}\right) + \frac{3}{8}erfc\left(\frac{-d}{\sqrt{N_0}}\right) - \frac{1}{8}erfc\left(\frac{-5d}{\sqrt{N_0}}\right)$$

Distances cannot be negative! Easy fix is to change signs.

SNR per bit:

We can now Express the error probabilities as function of SNR per bit, using the formula for energy per bit and hamming distance:

$$n\frac{d}{\sqrt{N_0}} = n\frac{a(M)\sqrt{E_b}}{\sqrt{N_0}} = na(M)\sqrt{SNR}$$

This now becomes our argument for the complementary error function, where $M \in \{2,3,4\}$ and $n \in \{1,3,5\}$

$$a(M) = \sqrt{\frac{3 \cdot log_2(M)}{(M^2 - 1)}}$$

SNR per bit for NRZ:

$$BER_{NRZ} = \frac{1}{2}erfc\left(a(2)\sqrt{SNR}\right)$$

SNR per bit for Duobinary:

$$BER_{duobinary} = \frac{3}{4}erfc\left(a(3)\sqrt{SNR}\right) - \frac{1}{4}erfc\left(3 * a(3)\sqrt{SNR}\right)$$

SNR per bit for PAM4:

$$BER_{PAM4} = \frac{1}{4}erfc\left(a(4)\sqrt{SNR}\right) + \frac{3}{8} * erfc\left(3 * a(4)\sqrt{SNR}\right) - \frac{1}{8}erfc\left(5 * a(4)\sqrt{SNR}\right)$$

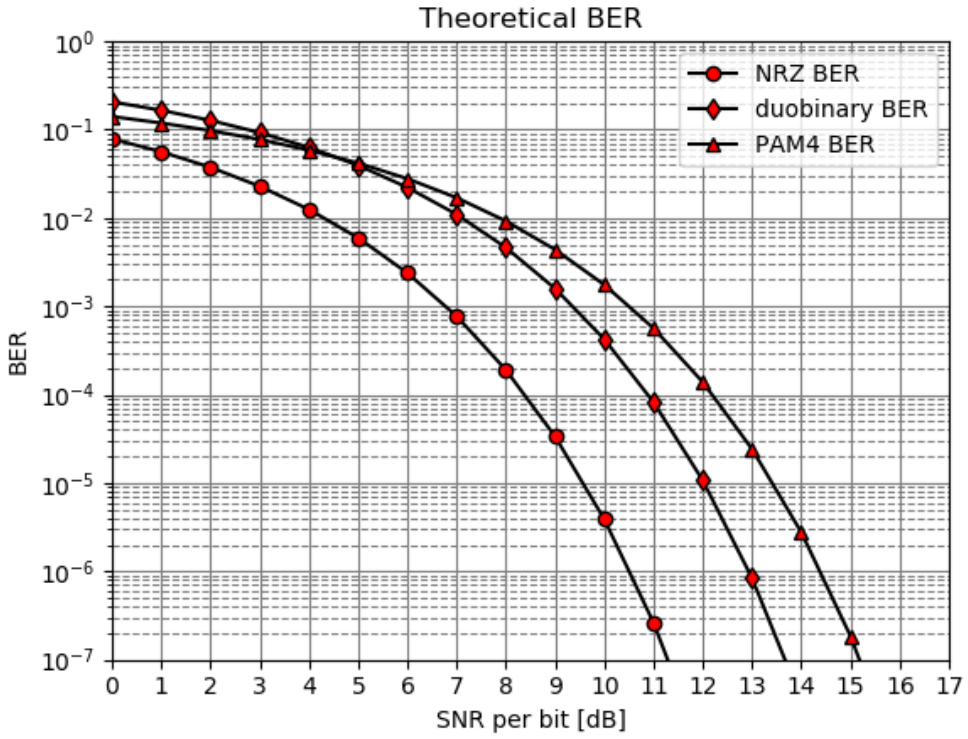

PT modulation influence:

The Pilot Tone (PT) can be modulated onto a signal with two different methods leading to either additive or multiplicative modulation.

$$P_{Add}(t) = \hat{P}\left[d(t) + m * \cos\left(2\pi f_t(t)\right)\right]$$

$$P_{Mul}(t) = \hat{P}\left[1 + m * \cos\left(2\pi f_t(t)\right)\right] * d(t)$$

Where $\hat{P}$ is the unmodulated laser power, $d(t)$ is the optically modulated data signal, m is the modulation depth of the PT in percent, finally $f_t(t)$ is the PT frequency in Hz.

To give an analytic BER expression for a signal influenced by a given PT modulation, the time dependency of $P_M(t)$ and $P_A(t)$ needs to be taken care of.

According to an analysis of subcarrier overmodulation, done by Makoto Murakami, Takamasa Imai, and Masaharu Aoyama in the paper "A Remote Supervisory System Based on Subcarrier Overmodulation for Submarine Optical Amplifier Systems", the error probability for the combined effects of the sinusoidal and the transmitted signal is found by convolving the Gaussian approximated probability distribution, for a given signal symbol, with the probability distribution for the sinusoidal. This results in a complex expression which can be simplified by applying stationary values for the sinusoids maximum and minimum value, whichever is closest to the threshold.

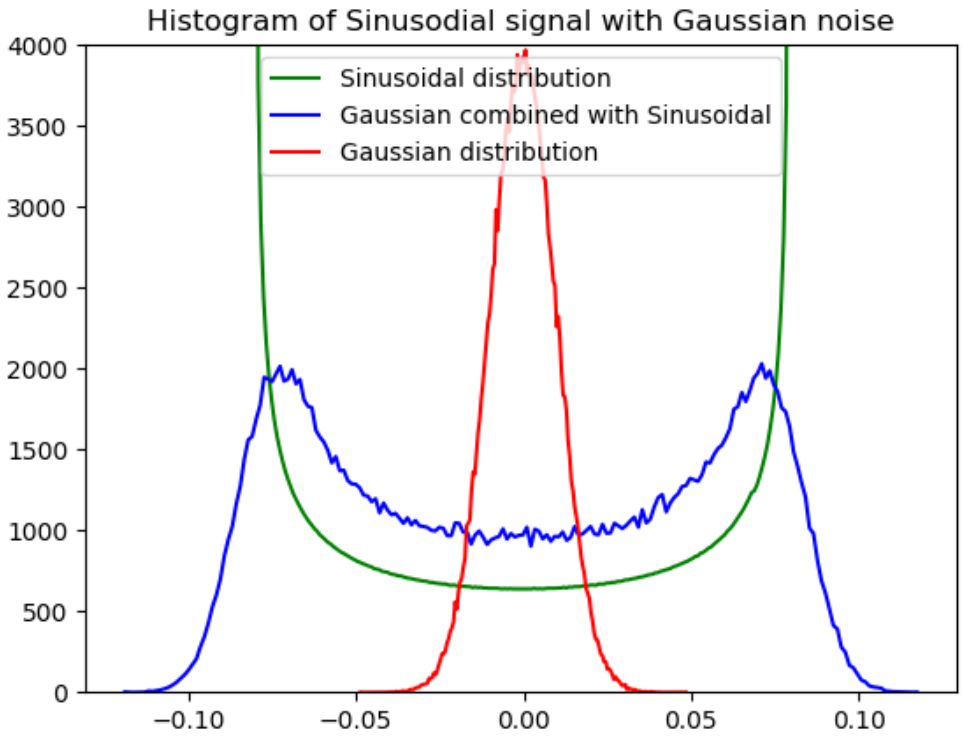

Based on this, we can simplify our expression by evaluate at worst case scenario. As stated $d(t)$ is the optically modulated signal, as such it can be substituted for the average signal value for a given symbol (I_{s_n}). $\hat{P}$ is evaluated equal to 1 to ease the calculations. The $\cos(2\pi f_t(t))$ expression takes a minimum value of -1 and a maximum value of 1. Choosing the minimum value for the cosine let us evaluate the worst-case scenario for when the signal levels.

We now get the following:

$$P_{Add} = I_{s_n} - m$$

$$P_{Mul} = I_{s_n} - m * I_{s_n}$$

We can now substitute P_{Add} and P_{Mul} into the error probabilities found earlier.

NRZ

$$BER_{Add} = \frac{1}{4}\left[erfc\left(\frac{(I_1 - m) - I_{th}}{\sigma_1\sqrt{2}}\right) + erfc\left(\frac{I_{th} - (I_0 - m)}{\sigma_0\sqrt{2}}\right)\right]$$

$$BER_{Mul} = \frac{1}{4}\left[erfc\left(\frac{(I_1 - m * I_1) - I_{th}}{\sigma_1\sqrt{2}}\right) + erfc\left(\frac{I_{th} - (I_0 - m * I_0)}{\sigma_0\sqrt{2}}\right)\right]$$

Duobinary

$$\begin{aligned} BER_{Add} = {} & \frac{1}{4}\left[erfc\left(\frac{(I_1 - m) - I_{1th}}{\sigma_1\sqrt{2}}\right) + erfc\left(\frac{I_{2th} - (I_1 - m)}{\sigma_1\sqrt{2}}\right)\right] \\ & + \frac{1}{8}\left[erfc\left(\frac{I_{1th} - (I_0 - m)}{\sigma_0\sqrt{2}}\right) + erfc\left(\frac{(I_2 - m) - I_{2th}}{\sigma_2\sqrt{2}}\right) - erfc\left(\frac{I_{2th} - (I_0 - m)}{\sigma_0\sqrt{2}}\right)\right. \\ & \left. - erfc\left(\frac{(I_2 - m) - I_{1th}}{\sigma_2\sqrt{2}}\right)\right] \end{aligned}$$

$$\begin{aligned} BER_{Mul} = {} & \frac{1}{4}\left[erfc\left(\frac{(I_1 - m * I_1) - I_{1th}}{\sigma_1\sqrt{2}}\right) + erfc\left(\frac{I_{2th} - (I_1 - m * I_1)}{\sigma_1\sqrt{2}}\right)\right] \\ & + \frac{1}{8}\left[erfc\left(\frac{I_{1th} - (I_0 - m * I_0)}{\sigma_0\sqrt{2}}\right) + erfc\left(\frac{(I_2 - m * I_2) - I_{2th}}{\sigma_2\sqrt{2}}\right)\right. \\ & \left. - erfc\left(\frac{I_{2th} - (I_0 - m * I_0)}{\sigma_0\sqrt{2}}\right) - erfc\left(\frac{(I_2 - m * I_2) - I_{1th}}{\sigma_2\sqrt{2}}\right)\right] \end{aligned}$$

PAM4

$$\begin{aligned} BER_{Add} = {} & \frac{1}{16}\left[erfc\left(\frac{(I_0 - m) - I_{2th}}{\sqrt{N_0}}\right) + erfc\left(\frac{(I_0 - m) - I_{1th}}{\sqrt{N_0}}\right) - erfc\left(\frac{(I_0 - m) - I_{3th}}{\sqrt{N_0}}\right)\right. \\ & + erfc\left(\frac{(I_1 - m) - I_{2th}}{\sqrt{N_0}}\right) + erfc\left(\frac{I_{1th} - (I_1 - m)}{\sqrt{N_0}}\right) + erfc\left(\frac{(I_1 - m\ ) - I_{3th}}{\sqrt{N_0}}\right) \\ & + erfc\left(\frac{I_{2th} - (I_2 - m)}{\sqrt{N_0}}\right) + erfc\left(\frac{I_{1th} - (I_2 - m)}{\sqrt{N_0}}\right) + erfc\left(\frac{(I_2 - m) - I_{3th}}{\sqrt{N_0}}\right) \\ & \left. + erfc\left(\frac{I_{2th} - (I_3 - m)}{\sqrt{N_0}}\right) + erfc\left(\frac{I_{3th} - (I_3 - m)}{\sqrt{N_0}}\right) - erfc\left(\frac{I_{1th} - (I_3 - m)}{\sqrt{N_0}}\right)\right] \end{aligned}$$

$$BER_{Mul} = \frac{1}{16}\left[erfc\left(\frac{(I_0 - m*I_0) - I_{2th}}{\sqrt{N_0}}\right) + erfc\left(\frac{(I_0 - m*I_0) - I_{1th}}{\sqrt{N_0}}\right) - erfc\left(\frac{(I_0 - m*I_0) - I_{3th}}{\sqrt{N_0}}\right)\right.$$
$$+ erfc\left(\frac{(I_1 - m*I_1) - I_{2th}}{\sqrt{N_0}}\right) + erfc\left(\frac{I_{1th} - (I_1 - m*I_1)}{\sqrt{N_0}}\right) + erfc\left(\frac{(I_1 - m*I_1) - I_{3th}}{\sqrt{N_0}}\right)$$
$$+ erfc\left(\frac{I_{2th} - (I_2 - m*I_2)}{\sqrt{N_0}}\right) + erfc\left(\frac{I_{1th} - (I_2 - m*I_2)}{\sqrt{N_0}}\right) + erfc\left(\frac{(I_2 - m*I_2) - I_{3th}}{\sqrt{N_0}}\right)$$
$$\left. + erfc\left(\frac{I_{2th} - (I_3 - m*I_3)}{\sqrt{N_0}}\right) + erfc\left(\frac{I_{3th} - (I_3 - m*I_3)}{\sqrt{N_0}}\right) - erfc\left(\frac{I_{1th} - (I_3 - m*I_3)}{\sqrt{N_0}}\right)\right]$$

Sanity check

We can now calculate the BER as function of SNR per bit by substituting the hamming distances and using the same noise assumption into the expressions above.

NRZ

$$BER_{Add} = \frac{1}{4}\left[erfc\left(\frac{(d-m)-0}{\sqrt{N_0}}\right) + erfc\left(\frac{0-(-d-m)}{\sqrt{N_0}}\right)\right]$$
$$= \frac{1}{4}\left[erfc\left(\frac{d-m}{\sqrt{N_0}}\right) + erfc\left(\frac{d+m)}{\sqrt{N_0}}\right)\right]$$

$$BER_{Mul} = \frac{1}{4}\left[erfc\left(\frac{(d - m*d) - 0}{\sqrt{N_0}}\right) + erfc\left(\frac{0-(-d - m*(-d))}{\sqrt{N_0}}\right)\right]$$
$$= \frac{1}{2}erfc\left(\frac{d - m*d}{\sqrt{N_0}}\right)$$

Duobinary

$$BER_{Add} = \frac{1}{4}\left[erfc\left(\frac{(0-m)-(-d)}{\sqrt{N_0}}\right) + erfc\left(\frac{d-(0-m)}{\sqrt{N_0}}\right)\right]$$
$$+ \frac{1}{8}\left[erfc\left(\frac{-d-(-2d-m)}{\sqrt{N_0}}\right) + erfc\left(\frac{(2d-m)-d}{\sqrt{N_0}}\right) - erfc\left(\frac{d-(-2d-m)}{\sqrt{N_0}}\right)\right.$$
$$\left. - erfc\left(\frac{(2d-m)-(-d)}{\sqrt{N_0}}\right)\right]$$

$$= \frac{3}{8}\left[erfc\left(\frac{d-m}{\sqrt{N_0}}\right) + erfc\left(\frac{d+m}{\sqrt{N_0}}\right)\right] + \frac{1}{8}\left[-erfc\left(\frac{3d+m}{\sqrt{N_0}}\right) - erfc\left(\frac{3d-m}{\sqrt{N_0}}\right)\right]$$

$$BER_{Mul} = \frac{1}{4}\left[erfc\left(\frac{(0 - m*0) - (-d)}{\sqrt{N_0}}\right) + erfc\left(\frac{d - (0 - m*0)}{\sqrt{N_0}}\right)\right]$$
$$+ \frac{1}{8}\left[erfc\left(\frac{-d - (-2d - m*(-2d))}{\sqrt{N_0}}\right) + erfc\left(\frac{(2d - m*2d) - d}{\sqrt{N_0}}\right)\right.$$
$$\left. - erfc\left(\frac{d - (-2d - m*(-2d))}{\sqrt{N_0}}\right) - erfc\left(\frac{(2d - m*2d) - (-d)}{\sqrt{N_0}}\right)\right]$$
$$= \frac{1}{2}erfc\left(\frac{d}{\sqrt{N_0}}\right) + \frac{1}{4}\left[erfc\left(\frac{d - 2d*m}{\sqrt{N_0}}\right) - erfc\left(\frac{3d - 2d*m}{\sqrt{N_0}}\right)\right]$$

PAM4

$$BER_{Add} = \frac{1}{16}\left[erfc\left(\frac{(-3d - m) - 0}{\sqrt{N_0}}\right) + erfc\left(\frac{(-3d - m) - (-2d)}{\sqrt{N_0}}\right) - erfc\left(\frac{(-3d - m) - 2d}{\sqrt{N_0}}\right)\right.$$
$$+ erfc\left(\frac{((-d) - m) - 0}{\sqrt{N_0}}\right) + erfc\left(\frac{(-2d) - ((-d) - m)}{\sqrt{N_0}}\right) + erfc\left(\frac{((-d) - m) - 2d}{\sqrt{N_0}}\right)$$
$$+ erfc\left(\frac{0 - (d - m)}{\sqrt{N_0}}\right) + erfc\left(\frac{(-2d) - (d - m)}{\sqrt{N_0}}\right) + erfc\left(\frac{(d - m) - 2d}{\sqrt{N_0}}\right)$$
$$\left. + erfc\left(\frac{0 - (3d - m)}{\sqrt{N_0}}\right) + erfc\left(\frac{2d - (3d - m)}{\sqrt{N_0}}\right) - erfc\left(\frac{(-2d) - (3d - m)}{\sqrt{N_0}}\right)\right]$$
$$= \frac{1}{8}\left[erfc\left(\frac{-3d - m}{\sqrt{N_0}}\right) + erfc\left(\frac{m - 3d}{\sqrt{N_0}}\right)\right] + \frac{3}{16}\left[erfc\left(\frac{-d - m}{\sqrt{N_0}}\right) + erfc\left(\frac{m - d}{\sqrt{N_0}}\right)\right]$$
$$- \frac{1}{16}\left[erfc\left(\frac{-5d - m}{\sqrt{N_0}}\right) + erfc\left(\frac{m - 5d}{\sqrt{N_0}}\right)\right]$$

$$BER_{Mul} = \frac{1}{16}\left[erfc\left(\frac{(-3d - m*-3d) - 0}{\sqrt{N_0}}\right) + erfc\left(\frac{(-3d - m*-3d) - (-2d)}{\sqrt{N_0}}\right)\right.$$
$$- erfc\left(\frac{(-3d - m*-3d) - 2d}{\sqrt{N_0}}\right) + erfc\left(\frac{((-d) - m*(-d)) - 0}{\sqrt{N_0}}\right)$$
$$+ erfc\left(\frac{(-2d) - (d - m*(-d))}{\sqrt{N_0}}\right) + erfc\left(\frac{((-d) - m*(-d)) - 2d}{\sqrt{N_0}}\right)$$
$$+ erfc\left(\frac{0 - (d - m*d)}{\sqrt{N_0}}\right) + erfc\left(\frac{(-2d) - (d - m*d)}{\sqrt{N_0}}\right) + erfc\left(\frac{(d - m*d) - 2d}{\sqrt{N_0}}\right)$$
$$+ erfc\left(\frac{0 - (3d - m*3d)}{\sqrt{N_0}}\right) + erfc\left(\frac{2d - (3d - m*3d)}{\sqrt{N_0}}\right)$$
$$\left. - erfc\left(\frac{(-2d) - (3d - m*3d)}{\sqrt{N_0}}\right)\right]$$

$$= \frac{1}{8}\left[erfc\left(\frac{3d*m-3d}{\sqrt{N_0}}\right) + erfc\left(\frac{3d*m-d}{\sqrt{N_0}}\right) - erfc\left(\frac{3d*m-5d}{\sqrt{N_0}}\right) + erfc\left(\frac{d*m-d}{\sqrt{N_0}}\right) + erfc\left(\frac{d*m-3d}{\sqrt{N_0}}\right)\right] + \frac{1}{16}\left[erfc\left(\frac{-m*d-3d}{\sqrt{N_0}}\right) + erfc\left(\frac{-m*d-d}{\sqrt{N_0}}\right)\right]$$

SNR per bit

We now relate the hamming distance and energy per bit through the SNR per bit:

$$n\frac{d}{\sqrt{N_0}} = n\frac{a(M)\sqrt{E_b}}{\sqrt{N_0}} = na(M)\sqrt{SNR}$$

$$a(M) = \sqrt{\frac{3\cdot log_2(M)}{(M^2-1)}}$$

NRZ

We get the following for NRZ:

$$BER_{Add} = \frac{1}{4}\left[erfc\left(a(2)\sqrt{SNR} - \frac{m}{\sqrt{N_0}}\right) + erfc\left(a(2)\sqrt{SNR} + \frac{m}{\sqrt{N_0}}\right)\right]$$

$$BER_{Mul} = \frac{1}{2}erfc\left(a(2)\sqrt{SNR} - m\,a(2)\sqrt{SNR}\right)$$

Duobinary

We can now do the same for duobinary:

$$BER_{Add} = \frac{3}{8}\left[erfc\left(a(3)\sqrt{SNR} - \frac{m}{\sqrt{N_0}}\right) + erfc\left(a(3)\sqrt{SNR} + \frac{m}{\sqrt{N_0}}\right)\right] + \frac{1}{8}\left[-erfc\left(3*a(3)\sqrt{SNR} + \frac{m}{\sqrt{N_0}}\right) - erfc\left(3*a(3)\sqrt{SNR} - \frac{m}{\sqrt{N_0}}\right)\right]$$

$$BER_{Mul} = \frac{1}{2}erfc\left(a(3)\sqrt{SNR}\right) + \frac{1}{4}\left[erfc\left(a(3)\sqrt{SNR} - 2*a(3)\sqrt{SNR}*m\right) - erfc\left(3*a(3)\sqrt{SNR} - 2*a(3)\sqrt{SNR}*m\right)\right]$$

PAM4

For PAM4 we get the following:

$$BER_{Add} = \frac{1}{8}\left[erfc\left(-3 * a(4)\sqrt{SNR} - \frac{m}{\sqrt{N_0}}\right) + erfc\left(\frac{m}{\sqrt{N_0}} - 3 * a(4)\sqrt{SNR}\right)\right] + \frac{3}{16}\left[erfc\left(-a(4)\sqrt{SNR} - \frac{m}{\sqrt{N_0}}\right) + erfc\left(\frac{m}{\sqrt{N_0}} - a(4)\sqrt{SNR}\right)\right] - \frac{1}{16}\left[erfc\left(-5 * a(4)\sqrt{SNR} - \frac{m}{\sqrt{N_0}}\right) + erfc\left(\frac{m}{\sqrt{N_0}} - 5 * a(4)\sqrt{SNR}\right)\right]$$

$$BER_{Mul} = \frac{1}{8}\left[erfc\left(3 * a(4)\sqrt{SNR} * m - 3 * a(4)\sqrt{SNR}\right) + erfc\left(3 * a(4)\sqrt{SNR} * m - a(4)\sqrt{SNR}\right) - erfc\left(3 * a(4)\sqrt{SNR} * m - 5 * a(4)\sqrt{SNR}\right) + erfc\left(a(4)\sqrt{SNR} * m - a(4)\sqrt{SNR}\right) + erfc\left(a(4)\sqrt{SNR} * m - 3 * a(4)\sqrt{SNR}\right)\right] + \frac{1}{16}\left[erfc\left(-m * a(4)\sqrt{SNR} - 3 * a(4)\sqrt{SNR}\right) + erfc\left(-m * a(4)\sqrt{SNR} - a(4)\sqrt{SNR}\right)\right]$$

note that distances cannot be negative:

$$BER_{Add} = \frac{1}{8}\left[erfc\left(3 * a(4)\sqrt{SNR} + \frac{m}{\sqrt{N_0}}\right) + erfc\left(3 * a(4)\sqrt{SNR} - \frac{m}{\sqrt{N_0}}\right)\right] + \frac{3}{16}\left[erfc\left(a(4)\sqrt{SNR} + \frac{m}{\sqrt{N_0}}\right) + erfc\left(a(4)\sqrt{SNR} - \frac{m}{\sqrt{N_0}}\right)\right] - \frac{1}{16}\left[erfc\left(5 * a(4)\sqrt{SNR} + \frac{m}{\sqrt{N_0}}\right) + erfc\left(5 * a(4)\sqrt{SNR} - \frac{m}{\sqrt{N_0}}\right)\right]$$

$$BER_{Mul} = \frac{1}{8}\left[erfc\left(-3 * a(4)\sqrt{SNR} * m + 3 * a(4)\sqrt{SNR}\right) + erfc\left(-3 * a(4)\sqrt{SNR} * m + a(4)\sqrt{SNR}\right) - erfc\left(-3 * a(4)\sqrt{SNR} * m + 5 * a(4)\sqrt{SNR}\right) + erfc\left(-a(4)\sqrt{SNR} * m + a(4)\sqrt{SNR}\right) + erfc\left(-a(4)\sqrt{SNR} * m + 3 * a(4)\sqrt{SNR}\right)\right] + \frac{1}{16}\left[erfc\left(m * a(4)\sqrt{SNR} + 3 * a(4)\sqrt{SNR}\right) + erfc\left(m * a(4)\sqrt{SNR} + a(4)\sqrt{SNR}\right)\right]$$

Bibliography

[1] *The Zettabyte Era: Trends and Analysis*. Technical report. 2017. URL: https://www.cisco.com/c/en/us/solutions/collateral/service-provider/visual-networking-index-vni/vni-hyperconnectivity-wp.pdf.

[2] Sandvine. *The 2018 Global Internet Phenomena report*. October 2018. URL: https://www.sandvine.com/press-releases/sandvine-releases-2018-global-internet-phenomena-report.

[3] *Cisco Global Cloud Index: Forecast and Methodology, 2016–2021 White Paper*. Technical report. 2018. URL: https://www.cisco.com/c/en/us/solutions/collateral/service-provider/global-cloud-index-gci/white-paper-c11-738085.html.

[4] T.s Rokkas, I. Neokosmidis, B. Shariati, et al. "Techno-Economic Evaluations of 400G Optical Interconnect Implementations for Datacenter Networks". In: *Optical Fiber Communication Conference*. Optical Society of America, 2018, M1A.1.

[5] T. Rokkas, I. Neokosmidis, B. Shariati, et al. "Techno-Economic Evaluations of 400G Optical Interconnect Implementations for Datacenter Networks". In: *2018 Optical Fiber Communications Conference and Exposition (OFC)*. April 2018, pages 1–3.

[6] K. Zhong, X. Zhou, C. Yu, et al. "DSP for high speed short reach transmission systems". In: *2016 Progress in Electromagnetic Research Symposium (PIERS)*. August 2016, pages 4874–4874.

[7] J. Wei. "DSP-based multi-band schemes for high speed next generation optical access networks". In: *2017 Optical Fiber Communications Conference and Exhibition (OFC)*. March 2017, pages 1–3.

[8] C. Cole. "Beyond 100G client optics". In: *IEEE Communications Magazine* 50.2 (February 2012), pages 58–66.

[9] E. P. da Silva, F. Klejs, M. Lillieholm, et al. "Experimental Characterization of 10 × 8 GBd DP-1024QAM Transmission with 8-bit DACs and Intradyne Detection". In: *Proc. European Conference on Optical Communication (ECOC2018, Rome)* Th1D (2018).

[10] T. Kupfer, A. Bisplinghof, T. Duthel, et al. "Optimizing power consumption of a coherent DSP for metro and data center interconnects". In: (March 2017), pages 1–3.

[11] K. Ishii, Y. Akiyama, T. Yoshida, et al. “Low-power consumption DSP circuit design for IFDMA-based PON systems”. In: (July 2011), pages 770–771.

[12] G. C. Gupta, M. Kashima, H. Iwamura, et al. “Hybrid WDM-CDM-PON for Ultra Long Reach Access Network”. In: *2006 European Conference on Optical Communications*. September 2006, pages 1–2.

[13] D. Mahgerefteh and C. Thompson. “Techno-economic comparison of Silicon Photonics and multimode VCSELs”. In: *2015 Optical Fiber Communications Conference and Exhibition (OFC)*. March 2015, pages 1–3.

[14] Y. Ma and Zhensheng J.Ma. *Evolution and Trends of Broadband Access Technologies and Fiber-Wireless Systems. Fiber-Wireless Convergence in Next-Generation Communication Networks*. Springer International Publishing, 2017, pages 43–75.

[15] X. Li, J. L. Wei, N. Bamiedakis, et al. “Avalanche photodiode enhanced PAM-32 5 Gb/s LED-POF link”. In: *2014 The European Conference on Optical Communication (ECOC)*. September 2014, pages 1–3.

[16] A. Lender. “The duobinary technique for high-speed data transmission”. In: *Transactions of the American Institute of Electrical Engineers, Part I: Communication and Electronics* 82.2 (May 1963), pages 214–218.

[17] P. J. Winzer and R. Essiambre. “Advanced Modulation Formats for High-Capacity Optical Transport Networks”. In: *Journal of Lightwave Technology* 24.12 (December 2006), pages 4711–4728.

[18] L. F. Suhr, J.J. Vegas Olmos, and I. Tafur Monroy. “10-Gbps duobinary-4-PAM for High-Performance Access Networks”. In: *Asia Communications and Photonics Conference 2014*. Optical Society of America, 2014, ATh3A.161.

[19] K. Wu and K. Feher. “Multilevel PRS/QPRS Above the Nyquist Rate”. In: *IEEE Transactions on Communications* 33.7 (July 1985), pages 735–739.

[20] S. Walklin and J. Conradi. “Multilevel signaling for increasing the reach of 10 Gb/s lightwave systems”. In: *Journal of Lightwave Technology* 17.11 (November 1999), pages 2235–2248.

[21] M. Eiselt K. Grobe. *Wavelength Division Multiplexing. A Pratical Engineering Guide*. Wiley, 2013, pages 224–226.

[22] G. P. Agrawal. *Fiber-Optic Communication Systems. Fourth Edition*. Wiley, 2011, pages 162–163.

[23] I. A. Stegun Eds. M. Abramowitz. *Handbook of Mathematical Functions. With Formulas, Graphs, and Mathematical Tables*. National Bureau of Stnadards, 1972, page 296.

[24] D. Yoon K. Cho. “On the general BER expression of one- and two-dimensional amplitude modulations”. In: *IEEE Transactions on Communications* 50.7 (July 2002), pages 1074–1080.

[25] ITU-T. *Recommendation ITU-T G.987. 10-Gigabit-capable passive optical network (XG-PON) systems: Definitions, abbreviations and acronyms*. ITU-T. 2012.

[26] *Visual Networking Index: Forecast and Methodology, 2014-2019 White Paper*. Technical report. 2015. URL: www.cisco.com.

[27] D. Qian, N. Cvijetic, J. Hu, et al. "Optical OFDM Transmission in Metro/Access Networks". In: *Optical Fiber Communication Conference and National Fiber Optic Engineers Conference* (2009), OMV1.

[28] D. van Veen, V. Houtsma, P. Winzer, et al. "26-Gbps PON transmission over 40-km using duobinary detection with a low cost 7-GHz APD-based receiver". In: (September 2012), pages 1–3.

[29] N. Eiselt, D. Muench, A. Dochhan, et al. "Performance Comparison of 112-Gb/s DMT, Nyquist PAM4, and Partial-Response PAM4 for Future 5G Ethernet-Based Fronthaul Architecture". In: *Journal of Lightwave Technology* 36.10 (May 2018), pages 1807–1814.

[30] B. Li, K. J. Larsen, J. J. Vegas Olmos, et al. "Application of Beyond Bound Decoding for High Speed Optical Communications". In: *Asia Communications and Photonics Conference 2013* (2013), AF4C.6.

[31] T. Mizuochi. "Forward error correction in next generation optical communication systems". In: (June 2009), pages 1–2.

[32] Y. Takita, T. Hashiguchi, K. Tajima, et al. "Towards seamless service migration in network re-optimization for optically interconnected datacenters". In: *Optical Switching and Networking* 23 (2017). SDN Optical DCNs, pages 241–249. ISSN: 1573-4277.

[33] J. Theodoras. *Terabit for Data Centers*. January 2017. URL: https://www.lightwaveonline.com/articles/2017/01/terabit-for-data-centers.html.

[34] A. Larsson, J. S. Gustavsson, P. Westbergh, et al. "VCSEL design and integration for high-capacity optical interconnects". In: *Proc.SPIE* 10109 (2017).

[35] "The homepage of IEEE P802.3bs 400 Gb/s Ethernet Task Force". In: (January 2018). URL: http://www.ieee802.org/3/bs/.

[36] ITU-T. "Recommendation ITU-T G.975.1. Forward error correction for high bit-rate DWDM submarine systems". In: (2004).

[37] R. G. Priest and T. G. Giallorenzi. "Dispersion compensation in coherent fiber-optic communications". In: *Opt. Lett.* 12.8 (August 1987), pages 622–624.

[38] T. Xu, G. Jacobsen, S. Popov, et al. "Chromatic dispersion compensation in coherent transmission system using digital filters". In: *Opt. Express* 18.15 (July 2010), pages 16243–16257.

[39] J. P. Elbers, N. Eiselt, A. Dochhan, et al. "PAM4 vs Coherent for DCI Applications". In: *Advanced Photonics 2017 (IPR, NOMA, Sensors, Networks, SPPCom, PS)* (2017), SpTh2D.1.

[40] ITU-T. "Recommendation ITU-T G.698.4. Multichannel bi-directional DWDM applications with port agnostic single-channel optical interfaces". In: (2018).

[41] J. H. Lee, H. H. Yoon, M. Y. Park, et al. “Novel Wavelength Initialization of the Bragg-grating based tunable External Cavity Laser for WDM-PON”. In: (September 2007), pages 1–2.

[42] S. Pachnicke, J. Zhu, M. Lawin, et al. “Novel WDM-PON System with Shared Wavelength Locking and Full C-Band Tunability”. In: (May 2014), pages 1–5.

[43] S. Pachnicke, J. Zhu, M. Lawin, et al. “Tunable WDM-PON System With Centralized Wavelength Control”. In: *Journal of Lightwave Technology* 34.2 (January 2016), pages 812–818.

[44] D. de Felipe, M. Kresse, H. Conradi, et al. “Ultra-Wide Band Tunable Lasers on the PolyBoard Polymer Waveguide Based Photonic Integration Platform”. In: *Proc. European Conference on Optical Communication (ECOC2018, Rome)* We3C (2018).

[45] H. Elfaiki, K. Hassan, G. Duan, et al. “Ultra Wide Hybrid III-V On Silicon Tunable Laser”. In: *Proc. European Conference on Optical Communication (ECOC2018, Rome)* We4C (2018).

[46] C. Wagner, M. H. Eiselt, M. Lawin, et al. “Impairment Analysis of WDM-PON Based on Low-Cost Tunable Lasers”. In: *Journal of Lightwave Technology* 34.22 (November 2016), pages 5300–5307.

[47] M. Murakami, T. Imai, and M. Aoyama. “A remote supervisory system based on subcarrier overmodulation for submarine optical amplifier systems”. In: *Journal of Lightwave Technology* 14.5 (May 1996), pages 671–677.

[48] C. Wagner, M. Eiselt, S. Zou, et al. “Wavelength-agnostic WDM-PON system”. In: *2016 18th International Conference on Transparent Optical Networks (ICTON)*. July 2016, pages 1–4.

[49] D. van Veen and V. Houtsma. “50 Gbps Low Complex Burst Mode Coherent Detection for Time-Division Multiplexed Passive Optical Networks”. In: *Proc. European Conference on Optical Communication (ECOC2018, Rome)* Tu1B (2018).

[50] O. Ozolins, J. M. Estaran, A. Udalcovs, et al. “140 Gbaud On-Off Keying Links in C-Band for Short-Reach Optical Interconnects”. In: *Proc. European Conference on Optical Communication (ECOC2018, Rome)* Mo3I (2018).

[51] Q. Hu, K. Schuh, M. Chagnon, et al. “Up to 94 GBd THP PAM-4 Transmission with 33 GHz Bandwidth Limitation”. In: *Proc. European Conference on Optical Communication (ECOC2018, Rome)* pdp (2018).